THE REGULATION AND FUNCTION OF HU-LI TAI SHAO (HTS) AT THE DROSOPHILA NEUROMUSCULAR JUNCTION

by

Vincent Sing Yip Chui
B. Sc. (First Class Honors), Simon Fraser University, 2004

THESIS
SUBMITTED IN PARTIAL FULFILLMENT OF
THE REQUIREMENTS FOR THE DEGREE OF

MASTER OF SCIENCE

In the
Department of Molecular Biology and Biochemistry

SIMON FRASER UNIVERSITY

Spring 2011

Approval

Name: **Vincent Sing Yip Chui**

Degree: **Master of Science**

Title of Thesis: **The regulation and function of Hu-li tai shao (Hts) at the *Drosophila* neuromuscular junction**

Examining Committee:

Chair: **Dr. Christopher Beh**
Associate Professor, Department of Molecular Biology and Biochemistry

_____

Dr. Charles Krieger
Senior Supervisor
Associate Professor, Department of Biomedical Physiology and Kinesiology

_____

Dr. Nicholas Harden
Committee Member
Associate Professor, Department of Molecular Biology and Biochemistry

_____

Dr. Esther Verheyen
Committee Member
Professor, Department of Molecular Biology and Biochemistry

_____

Dr. Nancy Hawkins
Internal Examiner
Associate Professor, Department of Molecular Biology and Biochemistry

Date Defended/Approved: 15 April 2011

Declaration of
Partial Copyright Licence

Abstract

Hu-li tai shao (Hts) is the Drosophila homolog of mammalian adducin, a cytoskeletal protein that regulates the submembranous actin-spectrin network. Potential upstream regulatory proteins that alter the distribution or function of Hts at the neuromuscular junction (NMJ) were evaluated, along with putative interacting proteins and phosphoinositides. Muscle-specific RNAi knockdown of the regulatory PKA subunit or conventional PKC altered immunoreactivity against phosphorylated Hts at the NMJ, suggesting that these kinases are involved in Hts phosphorylation. Hts was required for proper assembly of the spectrin cytoskeleton at the NMJ, as changes in hts expression levels strongly disrupted alpha-Spectrin organization. Hts immunoreactivity colocalized with a GFP reporter for phosphatidylinositol-(4,5)-bisphosphate, which Hts could potentially interact with via its conserved MARCKS-homology domain. The transmembrane engulfment receptor draper genetically interacted with hts. These results highlight many avenues by which Hts may be exerting its influence on NMJ development, and open up worthwhile possibilities for future studies.

Keywords: Hu-li tai shao; Hts; MARCKS-homology domain; spectrin cytoskeleton; phosphoinositides; neuromuscular junction; synaptic plasticity

Dedication

To all my friends and family who kept supporting me all these years and encouraging me to reach my full potential.

And most of all to Lesley – none of this would be possible without you.

Acknowledgements

I would like to thank my senior supervisor Dr. Charles Krieger for giving me this opportunity, and especially for helping me 'see the bigger picture' of how this project fits in with other research going on in this area. I would like to thank my committee members (and previous employers) Dr. Nick Harden and Dr. Esther Verheyen for all their support and mentorship throughout these years. Their advice and insights have helped shape my professional identity, and will continue to be a guiding light as I further advance my career.

Special thanks to Bari Zahedi for suggesting not to start graduate school until I was sure it was what I wanted, as I'm sure the experience would have been very different had I begun graduate studies without having some work experience first. Thanks go out to the Hardenites - Justina Sanny, Ryan Conder, Stephanie Vlachos, Simon Wang, Xi Chen, Michael Chou, David Cheng and Kevin Dong; the Verheyenites - Maryam Rahnama, Wendy Lee, Lorena Braid, Sharan Swarup, Joanna Chen; Amy Tsai from the Krieger lab; Lesley Chen and Phanh (Thi Phuong Anh) Nguyen from the Leroux Lab; and Gritta Tettweiler from the Lasko lab at McGill University. All your technical help and camaraderie have made my graduate student life a very fun and rewarding experience. Thanks to my undergrads who helped with dissections and stainings - Melanie Wilson, Lindsay Wainwright, Christine Barr, Karly Doehring, Sandy Lou. Finally, thanks to Ziwei Ding from the Molecular Biology Service Centre for help with some difficult subcloning, and technical help from Tim Heslip, Duncan Napier and Apollos Kim.

Table of Contents

Approval ii
Abstract iii
Dedication iv
Acknowledgements v
Table of Contents vi
List of Figures viii
Glossary ix

1: Introduction 1
1.1 Development and function of the *Drosophila* neuromuscular junction 2
1.1.1 Establishment of the neuromuscular system during embryogenesis 2
1.1.2 Structure and organization of the neuromuscular junction 6
1.1.3 Synaptic plasticity and experience-dependent growth 9
1.1.4 The actin-spectrin cytoskeleton as a key component of the NMJ 10
1.2 Adducin is an important regulator of the actin-spectrin cytoskeleton 14
1.2.1 Structure and function of mammalian adducin 14
1.2.2 Adducin regulation by phosphorylation and calmodulin binding 17
1.2.3 Adducin may interact with phosphatidylinositol-(4,5)-bisphosphate through polybasic residues at its MHD 18
1.2.4 Disruption of adducin expression or function leads to disease 19
1.3 Hu-li tai shao at the *Drosophila* NMJ 21
1.3.1 Structure and function of Hts 21
1.3.2 Hts regulates larval NMJ development through interactions with synaptic proteins 26
1.4 Specific objectives of this study 30
1.4.1 Rationale, research goals and overview of approach 30
1.4.2 Strength of *Drosophila* NMJ as a model synapse 30

2: Materials and Methods 32
2.1 *Drosophila* strains and crosses 32
2.2 Site-directed mutagenesis, PCR and subcloning 32
2.2.1 Creating wildtype and non-phosphorylable UAS transgenes of *hts* 32
2.2.2 Creating doubly non-phosphorylable UAS transgene of *dlg* 33
2.3 Generation of transgenic stocks 33
2.3.1 *UAS-hts*^{S705S} and *UAS-hts*^{S705A} 33
2.3.2 *UAS-eGFP-dlg*^{S48A,S797A} 34
2.4 Larval body wall preparations 34
2.4.1 Platform slides for mounting 34

2.4.2 Larval dissections 34
2.4.3 Body wall fixation 35
2.5 Immunohistochemistry 35
2.5.1 Antibodies used 35
2.5.2 Immunostaining 35
2.5.3 Phalloidin staining 36
2.5.4 Mounting of samples onto platform slides 36
2.6 Visualization and Quantification 36
2.6.1 Fluorescence microscopy 36
2.6.2 Data processing and quantification 37

3: Results 40

3.1 Muscle-specific RNAi knockdown of candidate proteins that may interact with Hts 40
3.2 PKC and PKA regulate Hts phosphorylation levels 41
3.3 Hts is required for organization of the postsynaptic spectrin cytoskeleton 46
3.4 *hts* null mutant NMJ exhibit decreased levels of the active zone marker Bruchpilot 52
3.5 GFP reporter complication in $hts^{GS13858}$ 57
3.6 Generation of *hts* & *dlg1* transgenic lines 57
3.6.1 *UAS-*hts^{S705S} and *UAS-*hts^{S705A} 57
3.6.2 *UAS-eGFP-*$dlg1^{S48A,S797A}$ 58
3.7 The phospholipid PI(4,5)P_2 is detected at the NMJ 59
3.8 The transmembrane engulfment receptor gene *draper* interacts with *hts* 65

4: Discussion 73

4.1 A note on variability in NMJ development 73
4.2 Regulation of Hts by phosphorylation 73
4.3 Hts regulates postsynaptic spectrin organization 77
4.4 Hts regulates active zone stability 78
4.5 Hts may have a role in the sequestration of PI(4,5)P_2 80
4.6 Interaction between *hts* and *drpr* 83
4.7 Calpain as a speculative regulator of synaptic protein levels at the NMJ 85

5: Concluding remarks 88

Appendices 90

Appendix A: Primers used for mutagenesis, PCR and sequencing 90
Appendix B: Transgenic stocks received from BestGene Inc 91
Appendix C: Summary of results for RNAi knockdown studies 92

Reference List 93

List of Figures

Figure 1.1 Anatomy of the *Drosophila* larval neuromuscular system 5

Figure 1.2 Structure and organization of the *Drosophila* larval NMJ 8

Figure 1.3 Structure and organization of the actin-spectrin cytoskeleton 13

Figure 1.4 Adducin structure, regulation and protein interactions 16

Figure 1.5 Domain structure and relative sizes of Hts protein isoforms 25

Figure 1.6 Current model of Hts function at the *Drosophila* larval NMJ 29

Figure 2.1 Semi-automated method for object identification and quantification in Volocity software 39

Figure 3.1 RNAi knockdown of *Pkc53E* expression reduces pAdd immunoreactivity at the NMJ 43

Figure 3.2 RNAi knockdown of *Pka-R2* expression increases pAdd immunoreactivity at the NMJ 45

Figure 3.3 Changes in Hts levels disrupt α-spectrin localization 49

Figure 3.4 FITC-conjugated phalloidin staining of a muscle 12/13 NMJ 51

Figure 3.5 *hts* null mutant NMJ exhibit fewer and smaller Brp puncta 54

Figure 3.6 Overexpression of Hts in muscle does not affect Brp immunoreactivity 56

Figure 3.7 Anti-PI(4,5)P_2 antibody detects PI(4,5)P_2 at the presynaptic NMJ, and *Sac1*^{EY02269} mutant NMJ exhibit lower presynaptic PI(4,5)P_2 immunoreactivity 62

Figure 3.8 PI(4,5)P_2 immunoreactive puncta interdigitates with gaps in HRP immunoreactivity at the NMJ 63

Figure 3.9 GFP-tagged *in vivo* PI(4,5)P_2 reporter localizes to the NMJ and colocalizes with HRP and Hts immunoreactivity 64

Figure 3.10 *drpr* mutant NMJ show mildly decreased Hts immunoreactivity 69

Figure 3.11 *drpr* mutant NMJ show moderate decrease in pAdd immunoreactivity 71

Figure 4.1 Proposed model of Hts regulation and function at the *Drosophila* larval NMJ 76

Figure 4.2 Speculative Model: Hts inhibits Calpain activation by sequestering PI(4,5)P_2 87

Glossary

ALS Amyotrophic lateral sclerosis, also known as Lou Gehrig's Disease. A late-onset, progressive neurodegenerative disease.

Brp Bruchpilot, a presynaptic active zone T-bar/ribbon component

CAM Cell adhesion molecule, mediates cell-cell and cell-matrix adhesion

Dlg Discs-large, *Drosophila* homolog of mammalian PSD-95, a postsynaptic scaffolding protein

Drpr Draper, *Drosophila* homolog of nematode engulfment receptor CED-1

Fas2 Fasciclin 2, *Drosophila* homolog of N-CAM, a homophilic cell adhesion molecule

Hts Hu-li tai shao, *Drosophila* homolog of mammalian adducin

MHD MARCKS-homology domain, a conserved sequence homologous to the effector domain of mammalian MARCKS protein. Contains many basic residues, a binding site for Ca^{2+}/calmodulin, and conserved serine residue that is a phosphorylation target of PKC/PKA.

NMJ Neuromuscular junction, a specialized axonal terminal connecting a motoneuron to muscle

pAdd Phosphorylated adducin, refers to an antibody that specifically recognizes mammalian γ-adducin phosphorylated at Ser662, and cross-reacts with Hts phosphorylated at the MARCKS-homology domain

PKA cAMP-dependent kinase, also known as protein kinase A

PKC Protein kinase C

RNAi RNA interference, a technique to silence gene expression by the production of siRNA molecules that result in destruction of target mRNA

SSR Subsynaptic reticulum, a specialized postsynaptic membrane structure containing intricate membrane involutions

1: Introduction

The past two decades have presented both technological and methodological advancements that have revolutionized the field of neuronal cell biology. These include genome sequencing and online databases, recombinant DNA, primary culture techniques, fluorophore-tagging and real-time imaging. This has enabled the detailed examination of the activity and behaviour of cultured neurons. However, despite these advances, the challenge of unraveling the complex neuronal connections that mediate higher order mental tasks remains a tremendously daunting task.

Model organisms serve as a means of simplifying the process by reducing the relative complexity of the study subject. The *Drosophila* genome encodes about 13,600 predicted genes on four chromosomes (Adams *et al.*, 2000) compared to about 25,000 genes on 23 chromosomes for humans (International Human Genome Sequencing Consortium, 2004). The *Drosophila* larval neuromuscular system in particular has emerged as an increasingly popular model for the *in vivo* study of axonal guidance, synaptic development, synapse structure and physiology, and synaptic plasticity. This is owing in part to the ease of access to neuromuscular junctions for analysis, and the wide range of genetic and molecular tools available for use in this system.

Many studies in recent years have used the *Drosophila* neuromuscular junction as a model to study human neurological conditions, including associative learning defects, spinal muscular atrophy, Friedreich ataxia and other neurodegenerative diseases (Knight *et al.*, 2007; Chang *et al.*, 2008; Shidara and Hollenbeck, 2010; Bayat

et al., 2011). In the case of amyotrophic lateral sclerosis, a progressive motor neuron disease, analysis of spinal cord samples from human patients and animal models have found hyperphosphorylation of adducin protein (Hu *et al.*, 2003; Shan *et al.*, 2005); however, how this change relates to the etiology of disease symptoms is not known. To better understand how adducin may affect neuromuscular junction stability, the present study focuses on the *Drosophila* adducin homolog Hu-li tai shao, and its role in the development of the larval neuromuscular junction.

1.1 Development and function of the *Drosophila* neuromuscular junction

1.1.1 Establishment of the neuromuscular system during embryogenesis

In *Drosophila*, motoneurons are derived from neuroblasts along the ventral nerve cord (Schmid *et al.*, 1999). During embryonic development, motoneurons extend axons along the ventral nerve cord, splitting into one of three major nerve trunks, and finally branching off towards their corresponding muscle area. Each motoneuron then further separates to innervate its specific target muscle(s) (Figure 1.1a; Johansen *et al.*, 1989b). Each branching event in this process is guided by specific netrins, semaphorins and membrane receptors (Keleman and Dickson, 2001; Kolodkin *et al.*, 1993; Winberg *et al.*, 1998), as well as cell adhesion molecules (CAMs) expressed by various cell types in the developing embryo (Chiba *et al.*, 1995; Rose *et al.*, 1997). Recognition between each motoneuron and its specific target is thus thought to be mediated by a balance between attractive and repellent cues, and interaction between cell-specific membrane proteins (Landgraf *et al.*, 1999). The specification of motoneuronal subclasses is tightly regulated through transcriptional control of determinant genes, whereas unique cellular

identity may involve temporal differences in expression or post-translational modifications (Landgraf and Thor, 2006).

The abdominal musculature of the third-instar larval body wall in *Drosophila* is arranged as a series of segmentally repeated arrays, each containing a highly organized pattern of 30 muscles per hemisegment (Figure 1.1b,c). Each individual muscle is a syncytium initially formed from the fusion of a single founder cell with one or more fusion-capable myoblasts (Bate, 1990). A specific expression profile of transcription factors determines each muscle's unique identity, which is characterized by its shape, size, axial orientation, and sites of muscle attachment (Frasch, 1999). Once identity is established, each muscle expresses a set combination of genes, which aids its corresponding axon to correctly find its target and form a neuromuscular junction (NMJ; Tixier *et al.*, 2010; Landgraf *et al.*, 1999).

Muscle innervation begins at about embryonic stage 15, approximately 13 hours after egg laying, when the growth cone of a motoneuron makes contact with membrane processes called myopodia from its target muscle (Ritzenthaler *et al.*, 2000). Once contact is established, the homophilic CAM Fasciclin 2 (Fas2) clusters around the contact site where it stabilizes this interaction, and initiates the synapse assembly process by recruiting the scaffolding protein Discs large (Dlg; Kohsaka *et al.*, 2007). Dlg is the *Drosophila* homolog of the mammalian postsynaptic density-95 protein (PSD-95), and mediates many protein-protein interactions via its three Class I PDZ repeats and SH3 domain (Woods and Bryant, 1991). Dlg is required for the localization of Shaker K^+ channels and facilitates stable Fas2 accumulation at the nascent synapse (Tejedor *et al.*, 1997; Thomas *et al.*, 1997; Zito *et al.*, 1997). Glutamate receptors dispersed throughout the muscle membrane congregate at the nascent synapse in response to spontaneous

releases of glutamate by the immature presynaptic terminal (Broadie and Bate, 1993a). Glutamate receptors will also preferentially localize to sites of highest glutamate concentration (Marrus and DiAntonio, 2004), and this process may be mediated by the *Drosophila* 4.1 protein Coracle, filamentous actin and Dlg (Chen *et al.*, 2005; Chen and Featherstone, 2005). By embryonic stage 17, about 18 hours after egg laying, all major morphological and functional features of a mature synapse will have developed (Broadie and Bate, 1993b; Schuster *et al.*, 1996a).

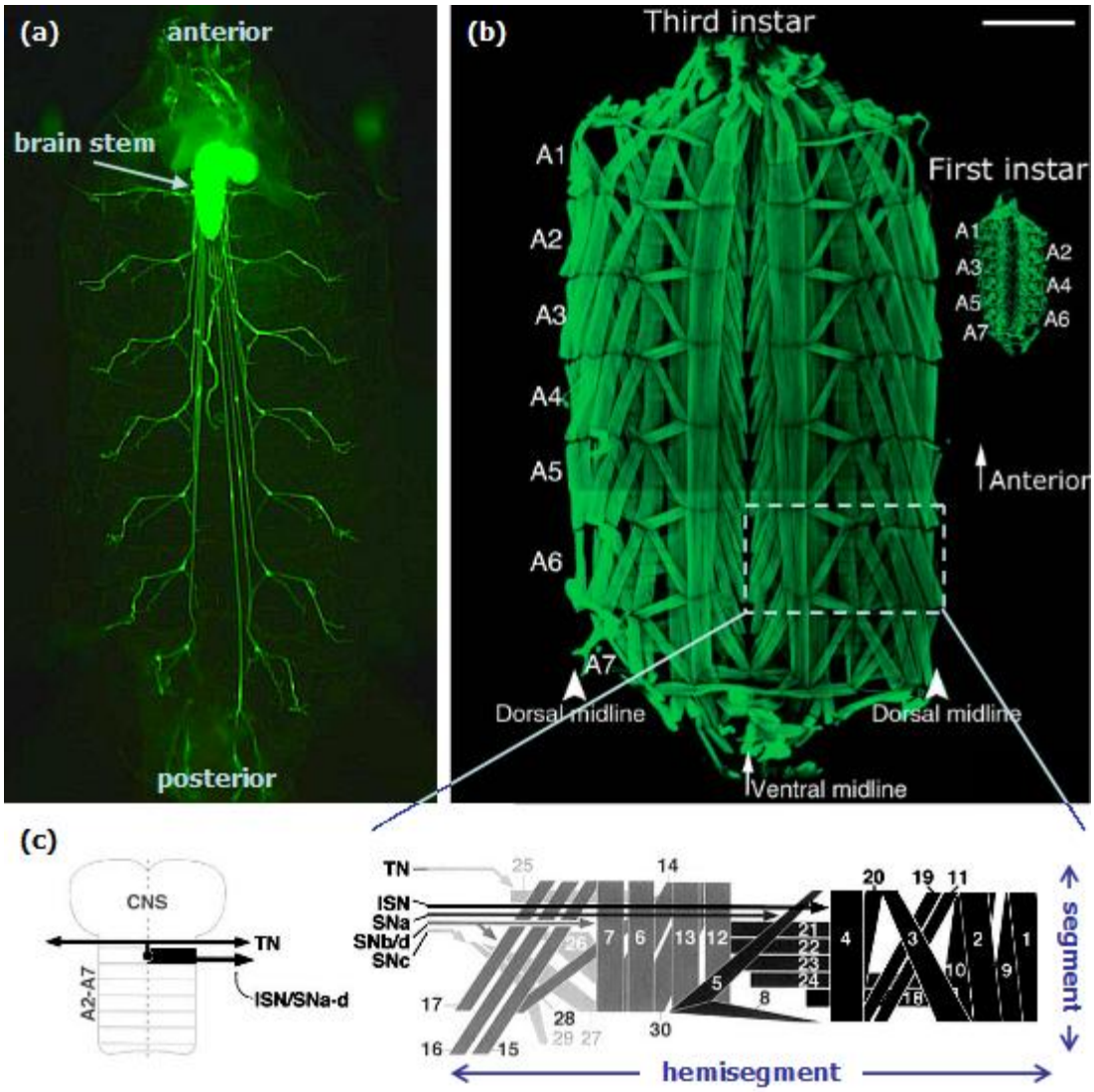

Figure 1.1 Anatomy of the *Drosophila* larval neuromuscular system

(a) Dissected larvae with neuronal expression of GFP, showing major nerve trunks branching off from the brain stem toward abdominal muscle segments.
(b) Dissected late third instar and first instar larvae, stained with FITC-phalloidin, showing musculature of abdominal muscle segments A1-A7. (a) and (b) shown at same orientation and approximately same scale for comparison. Scale bar, 0.5 mm.
(c) Schematic of motoneurons from corresponding areas in the brain stem extending axons toward specific target muscles in a hemisegment. CNS: central nervous system, TN: transverse nerve, ISN: intersegmental nerve, SN: segmental nerve.
(Images modified from Hoy, 2006; Gorczyca and Budnik, 2006; Hoang and Chiba, 2001, respectively.)

1.1.2 Structure and organization of the neuromuscular junction

The entire structure where the motoneuron axon forms a connection with the muscle is referred to as a synaptic terminal. The synaptic terminal consists of branched chains of boutons, which are roughly spherical structures that imbed into the surface of the muscle tissue but remain interconnected by the axonal tract (Keshishian and Chiba, 1993). Each bouton houses many active zones, where synaptic vesicle fusion and neurotransmitter release occurs, allowing communication across the individual synapses (Figure 1.2c; Atwood *et al.*, 1993). Directly apposing the active zone at each synapse are the neurotransmitter receptor clusters located in the muscle (Petersen *et al.*, 1997).

The size and arrangement of boutons depends on their motoneuron class. The length and degree of branching of the synaptic terminals also depend on motoneuron class and varies with different muscle sets. There are three classes of motoneuron in *Drosophila*, Types I, II and III (Figure 1.2a,b). The largest class is Type I, which is further subdivided based into the 'big' and 'small' categories, Type Ib and Type Is. Type I motoneurons are purely glutamatergic, whereas Type II and III are also capable of providing octopaminergic and peptidergic signals, respectively (Johansen *et al.*, 1989a; Jan and Jan, 1976; Monastirioti *et al.*, 1995; Cantera and Nassel, 1992; Gorczyca *et al.*, 1993). Most muscles will be innervated by three motoneurons: a specific stimulatory Type Ib motoneuron, a common stimulatory Type Is motoneuron, and a common neuromodulatory Type II motoneuron. Type III motoneurons are only found on muscle pair 12 but its function is not well understood (Hoang and Chiba, 2001).

After embryogenesis is complete, the plasma membrane of the muscle that surrounds the receptor clusters begins to develop a specialized structure referred to as the subsynaptic reticulum (SSR; Figure 1.2c). The SSR is an elaborate network of

membrane invaginations that remains open to extrasynaptic space, and the localization of Dlg and the cytoskeletal protein Spectrin are required for its proper formation (Lahey *et al.*, 1994; Guan *et al.*, 1996; Pielage *et al.*, 2006). Type Ib boutons are surrounded by a larger SSR than Type Is boutons, whereas Type II and Type III boutons are not surrounded by SSR at all (Jia *et al.*, 1993). Unlike the postsynaptic junctional folds at vertebrate NMJ, which contain acetylcholine receptors and contribute to signalling (Rinholm *et al.*, 2007), the specific function of the SSR is unclear.

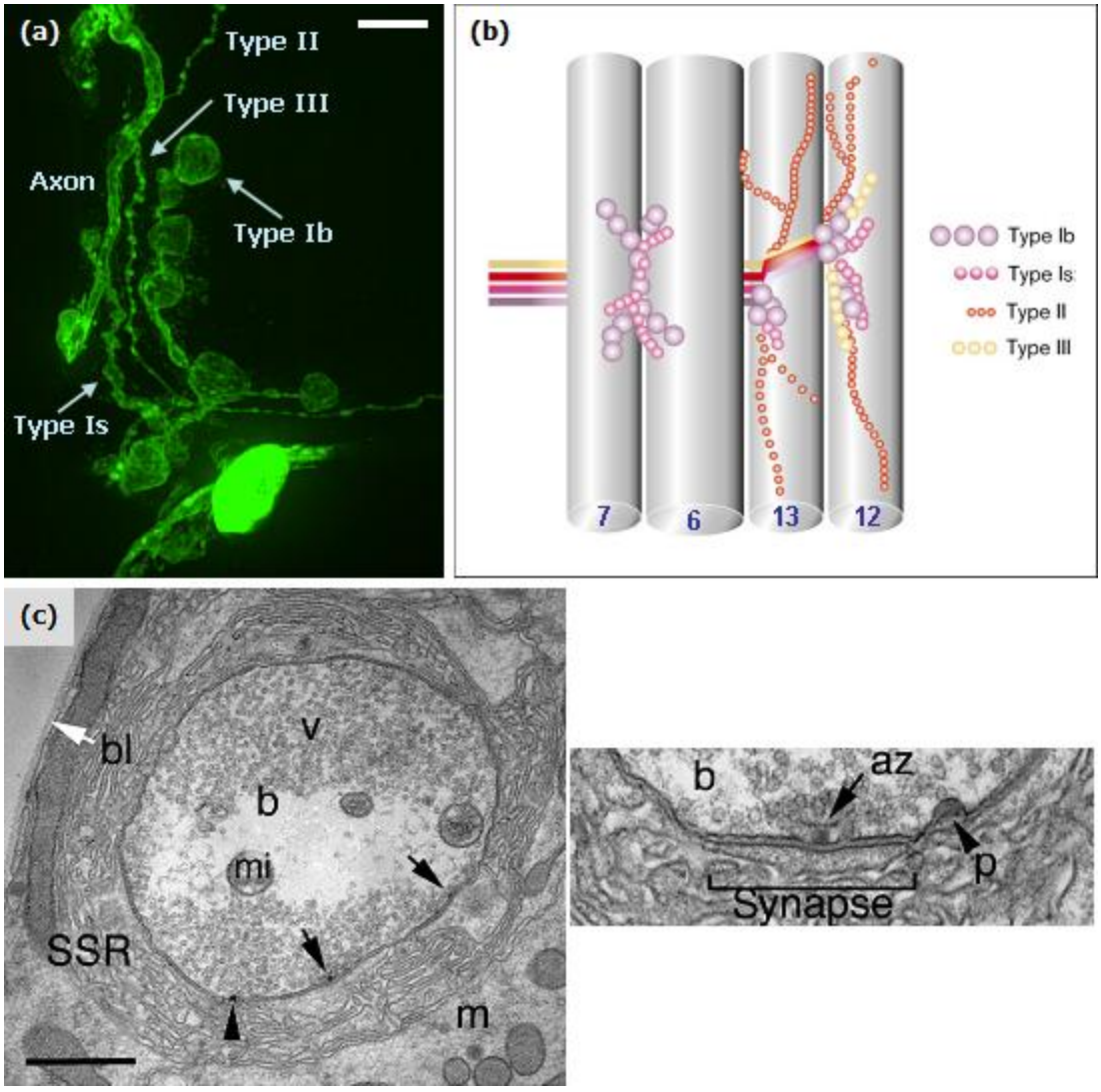

Figure 1.2 Structure and organization of the *Drosophila* larval NMJ

(a) Wildtype muscle 12 NMJ, immunostained against a neuronal marker, showing the major bouton types. Scale bar, 10μm.
(b) Schematic of innervation patterns for muscle pairs 7/6 and 13/12.
(c) EM images of a Type Ib bouton in muscle 12. Right panel shows an electron-dense region surrounding the active zone, indicating a synapse (bracketed).
b: bouton, v: synaptic vesicles, mi: mitochondrion, SSR: subsynaptic reticulum, m: muscle, bl (white arrow): basal lamina, p (arrowheads): coated pit, az (arrows): T-bar/active zone. Calibration bar, 0.8μm in left panel, 0.3μm in right panel.
(Panels b and c modified from Guan *et al.*, 1996; Gorczyca and Budnik, 2006, respectively)

1.1.3 Synaptic plasticity and experience-dependent growth

Throughout the life of an animal, many processes such as developing memory and adaptive learning, or even just simply the growth of an organism, require continuous reworking and expansion of the neural networks. Synaptic plasticity is an intricate balance between stability of the existing synaptic structure and its ability to adapt to signalling cues that may require changes in structure or transmission characteristics. Despite the tightly controlled layout and pairing of the motoneurons with their target muscles in *Drosophila*, individual NMJ are in fact highly dynamic connections capable of expansion, retraction, strengthening and weakening, in response to the changing demands of the growing animal.

During the growth of *Drosophila* larvae from hatching to late third-instar stage, their muscles undergo an increase upwards of 150 times in volume (Guan *et al.*, 1996) (Figure 1.1b). Concurrent with this massive muscle growth, the NMJ must also expand in size to provide appropriate levels of synaptic transmission, ensuring proper postsynaptic potential and muscle contraction response (Budnik, 1996). This enhanced signal is mediated by an increase in the number of synaptic boutons, as well as an increase in the number and density of active zones (Gorczyca *et al.*, 1993). Studies have shown that both anterograde and retrograde feedback signals between the motoneuron and muscle are necessary to regulate the degree of presynaptic growth and levels of neurotransmitter release (Davis and Goodman, 1998; Keshishian and Kim, 2004; Marques, 2005). This allows the demand and supply of synaptic stimuli to reach an effective equilibrium that retains the functionality of the neuromuscular system throughout the larval stages.

In addition to the growth-driven developmental plasticity, *Drosophila* NMJ also exhibit what is referred to as experience-dependent plasticity, induced by changes in larval behaviour such as increased neuronal and muscle activity. This type of plasticity can be broken down into several phases based on the characteristics of NMJ electrophysiology and morphology (Schuster, 2006). The first phase involves potentiation of the existing NMJ architecture and begins after about 30 minutes of increased activity, when an increase in the cycling of large synaptic vesicles elicit stronger depolarization in the muscle (Steinert *et al.*, 2006). The potentiation reaches a plateau at the second phase, and by the third phase, about 2 hours after the initial increase in activity, there is an increase in local postsynaptic protein synthesis and recruitment of glutamate receptors (Sigrist *et al.*, 2000). At the fourth and final phase, more than 4 hours since the start, bouton enlargement and new bouton growth is induced by downregulation of Fas2 (Zito *et al.*, 1999; Sigrist *et al.*, 2003; Schuster *et al.*, 1996b). The Notch signalling pathway has been found to be required for this process, however it is not yet known in which phases it is involved (de Bivort *et al.*, 2009). This experience-dependent process enables a situation-appropriate expansion of the neuromuscular system, allowing the larvae to adapt to increased foraging and mobility demands in response to environmental changes and stresses.

1.1.4 The actin-spectrin cytoskeleton as a key component of the NMJ

In addition to the CAMs mediating trans-synaptic adhesion, certain intracellular structures implicated in maintaining NMJ stability include protein complexes, the submembranous spectrin-based cytoskeleton, and the core microtubule-based cytoskeleton.

Actin and spectrin form a cytoskeletal network that lies beneath the plasma membrane, and the molecular framework they establish is important in maintaining NMJ organization and stability in both vertebrates and *Drosophila* (Kordeli, 2000; Pielage *et al.*, 2005). The two types of spectrins, α- and β-spectrin, form antiparallel dimers that then join head-to-head to form tetramers. These act as crosslinkers for short actin filaments, and also tether the network to the plasma membrane (Figure 1.3a; Bennett and Baines, 2001). This crosslinking has been observed to form intricate lattices of pentagonal and hexagonal patterns in human erythrocyte membranes (Figure 1.3b; Byers and Branton, 1985; Liu *et al.*, 1987).

The actin-spectrin cytoskeleton thus acts as a scaffold for protein complexes. Attachment of proteins to the cytoskeleton results in lower lateral diffusion rates (Bennett and Gilligan, 1993), making it possible for the actin-spectrin network to establish defined domains of protein accumulation, and it has been proposed to act as a physical constraint for the specification of active zone size at *Drosophila* NMJ (Pielage *et al.*, 2006). Null mutations or RNAi knockdown of either form of spectrin in muscle leads to an expansion of postsynaptic Dlg immunoreactivity, and also has a negative impact on synaptic growth, resulting in a net decrease in the number of boutons (Pielage *et al.*, 2006).

Given its important role as a scaffold at the NMJ, it is clear that stringent regulation of actin-spectrin cytoskeletal dynamics is necessary to ensure proper NMJ development and plasticity. α-spectrin has a C-terminal calcium-binding EF-hand domain, while β-spectrin has an N-terminal actin-binding domain and a C-terminal Pleckstrin-homology domain. In mammals, these binding sites allow interactions with a range of cellular targets, among which are ankyrin, 4.1 protein, adducin and membrane

phospholipids (Figure 1.3c; Bennett and Baines, 2001). In the following section, the role that adducin plays in regulation of the actin-spectrin cytoskeleton at the NMJ will be examined in detail.

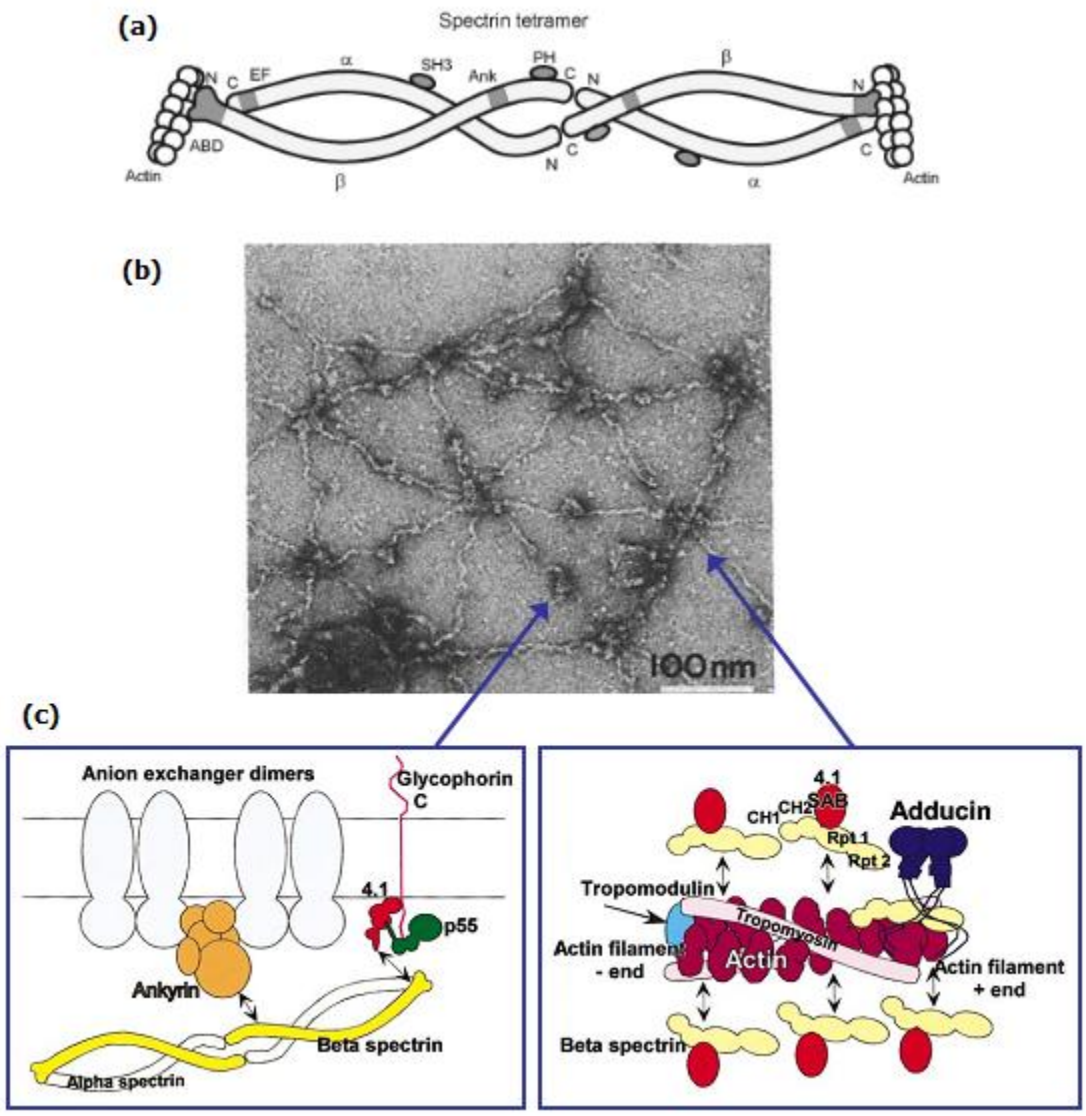

Figure 1.3 Structure and organization of the actin-spectrin cytoskeleton

(a) Arrangement of spectrin tetramers, and interaction with actin filaments through the N-terminal actin-binding domain (ABD) of β-spectrin. PH: pleckstrin homology domain, SH3: sarc homology domain, EF: calcium-binding EF-hand domain. Ank: ankyrin binding domain.
(b) EM image of freeze-etched erythrocyte membrane actin-spectrin cytoskeleton, forming pentagonal and hexagonal networks.
(c) Left panel, tethering of actin-spectrin network to the membrane through interaction with ankyrin and 4.1 proteins. Right panel, recruitment of spectrin to actin fast-growing ends by adducin.
(Images modified from Baines and Pinder, 2005; Liu *et al.*, 1987; Bennett and Baines, 2001, respectively)

1.2 Adducin is an important regulator of the actin-spectrin cytoskeleton

1.2.1 Structure and function of mammalian adducin

Adducin is a ubiquitously expressed membrane-associated cytoskeletal protein. Humans have three closely related genes that encode adducin subunits, α-, β- and γ-adducin, which share over 60% sequence similarity (Joshi *et al.*, 1991; Dong *et al.*, 1995). Adducin functions as a heterotetramer composed of either α/β or α/γ dimers. α- and γ-adducin are widely expressed in most cell types, whereas β-adducin is mainly found in the CNS and in erythrocytes (Matsuoka *et al.*, 2000). Structurally, each subunit contains a globular 39-kDa N-terminal head domain, a short 9-kDa neck domain, and a 33-kDa C-terminal tail domain (Figure 1.4a; Joshi *et al.*, 1991). The head and neck domains mediate oligomerization, while the tail domain contains a highly basic sequence of 22-residues called the MARCKS-homology domain (MHD) (Li *et al.*, 1998). This is named after a similar sequence in the effector domain of myristoylated alanine-rich C kinase substrate (MARCKS) protein (Figure 1.4b).

The MHD houses key residues and binding sequences that are critical to many adducin interactions. Serine-726 in α-adducin, serine-713 in β-adducin and serine-660 in γ-adducin are conserved phosphorylation residues for protein kinases A and C. (Matsuoka *et al.*, 2000; Fowler *et al.*, 1998). The MHD also contains a sequence for Ca^{2+}-dependent calmodulin binding (Gardner and Bennett, 1987), and many lysine residues of unknown function. In the vicinity of the neck domain are also several phosphorylation sites for protein kinase A and Rho-kinase (Matsuoka *et al.*, 1996; Kimura *et al.*, 1998).

Adducin is one of several proteins involved in the establishment and maintenance of the actin-spectrin cytoskeleton. Adducin recruits spectrin to sites of growing actin filaments, and also functions to cap the fast growing end of actin (Figure 1.4c; Gardner and Bennett, 1987; Bennett *et al.*, 1988). This stabilizes a network of short actin filaments linked together by spectrin tetramers, which forms the basis for the actin-spectrin cytoskeleton. The specific binding sites for these interactions are not known, but the neck domain contributes to binding, while the MHD is necessary but not sufficient for binding (Li *et al.*, 1998). Both α- and β- adducin have recently been shown to tether the actin-spectrin cytoskeleton to the erythrocyte membrane via direct binding to the integral membrane protein band 3 (Anong *et al.*, 2009).

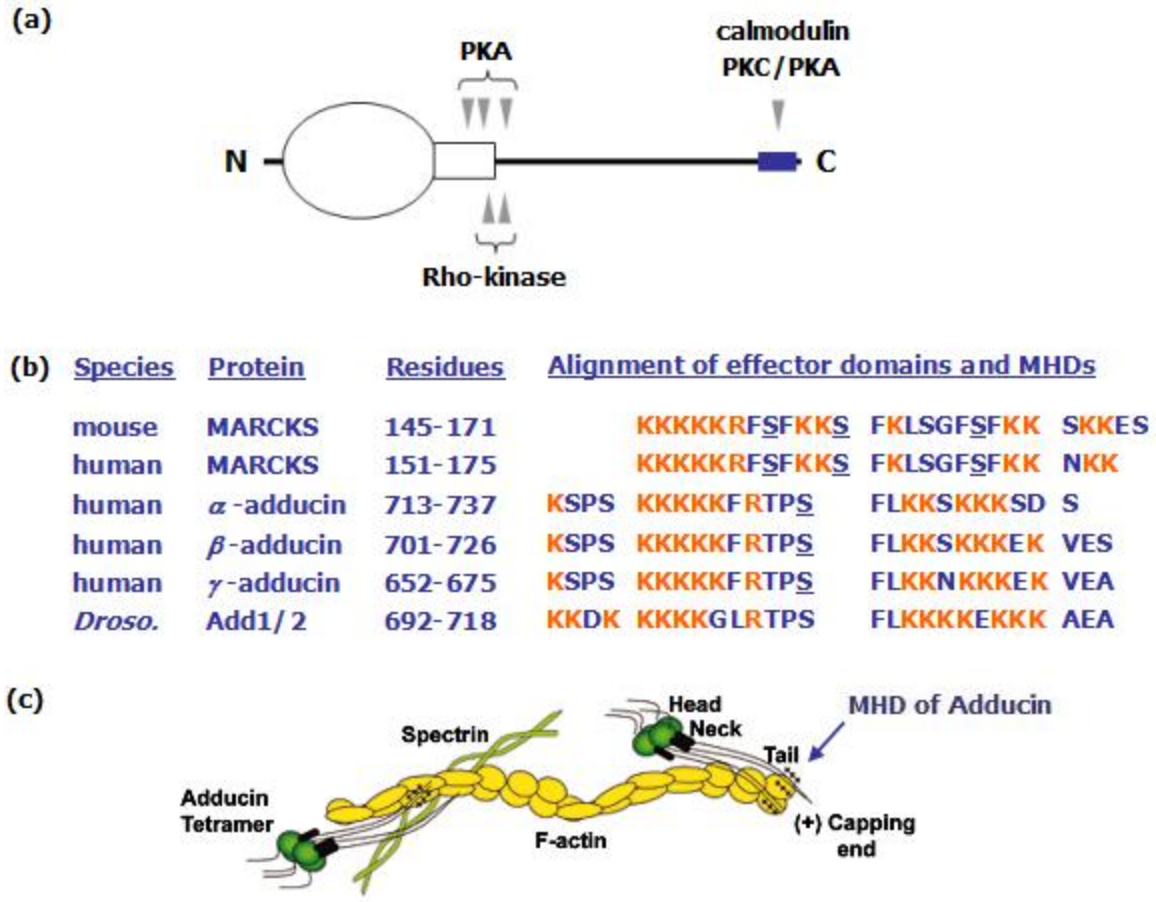

Figure 1.4 Adducin structure, regulation and protein interactions

(a) Adducin is composed of an N-terminal globular head domain, a neck domain and a C-terminal tail containing a MARCKS-homology domain (blue) that can bind to Ca^{2+}-calmodulin. Known phosphorylation sites are marked with arrowheads.
(b) Alignment of the effector domains of mammalian MARCKS proteins, and the MARCKS-homology domains from human adducins and Add1/2 isoforms of *Drosophila* Hts. Numerous basic residues (orange) are conserved at this region. Confirmed target residues for PKC/PKA phosphorylation are underlined.
(c) Schematic of adducin interactions at the actin-spectrin cytoskeleton. Adducin forms tetramers through interactions at the head and neck domains. Adducin recruits spectrin to F-actin and caps fast-growing ends (+) of actin filaments through interactions at the neck and tail domains.
(Panel c modified from Pariser *et al.*, 2005. Amino acid sequences from Whittaker *et al.*, 1999; Rossi *et al.*, 1999; Harlan *et al.*, 1991)

1.2.2 Adducin regulation by phosphorylation and calmodulin binding

Adducin activity is in part regulated by phosphorylation of the conserved serine residue in its MHD. Phosphorylation by protein kinase C (PKC) has been shown *in vitro* and *in vivo*, whereas phosphorylation by cAMP-dependent protein kinase (PKA) has been demonstrated *in vitro*. In both cases, phosphorylation inhibits the ability of adducin to recruit spectrin molecules or to cap actin filaments (Matsuoka *et al.*, 1996). In human platelets, phosphorylated α- and γ-adducin has been shown to disassociate from the spectrin-actin network and translocate away from the membrane toward the cytosol (Gilligan *et al.*, 2002; Barkalow *et al.*, 2003).

PKA phosphorylates serines-408, -436, and -481 in the neck domain of α-adducin and has a similar effect of inhibiting adducin's binding capabilities (Figure 1.4a; Matsuoka *et al.*, 1996). Threonines-445 and -480, also in the neck domain of α-adducin, are targets for phosphorylation by Rho-kinase; contrary to the effects of PKC and PKA, this has been found to increase adducin's ability to bind to actin and recruit spectrin. Myosin phosphatase is the only known phosphatase for adducin, however, its activity has only been demonstrated with respect to the Rho-kinase target residues (Kimura *et al.*, 1998). Adducin activity is also regulated by binding of Ca^{2+}-calmodulin to its MHD. Like PKC/PKA phosphorylation, this interaction inhibits both the actin capping and spectrin recruiting functions of adducin (Gardner and Bennett, 1987; Kuhlman *et al.*, 1996).

It is of interest to note that the conserved PKC/PKA target residue and the Ca^{2+}-calmodulin binding site are both located at the MHD of adducin. The mammalian membrane-associated MARCKS protein contains an effector domain that shares these sequence features and regulatory mechanisms (Figure 1.4b; Herget *et al.*, 1995; Ulrich

et al., 2000). Studies have indicated that due to occlusion of the common target region, PKC phosphorylation and Ca^{2+}-calmodulin binding of MARCKS are mutually exclusive interactions (Blackshear, 1993; Porumb *et al.*, 1997). This has led to the suggestion that the regulation of MARCKS, and possibly other proteins containing MHDs, could act as a junction point for crosstalk between two antagonistic signalling pathways and offer a means of dynamic regulation of cell activities (Chakravarthy *et al.*, 1999). While this relationship has not been directly studied in adducin, the high degree of sequence conservation at the MHD suggests that it is a possibility.

1.2.3 Adducin may interact with phosphatidylinositol-(4,5)-bisphosphate through polybasic residues at its MHD

Phosphatidylinositol-(4,5)-bisphosphate, hereafter referred to as $PI(4,5)P_2$, is a membrane phospholipid that interacts with many proteins and is a source of secondary signals. $PI(4,5)P_2$ constitutes upwards of 1% of total lipid at the plasma membrane in eukaryotic cells, and is predominantly localized to the inner leaflet. $PI(4,5)P_2$ is cleaved by activated phospholipase C, in response to G protein-coupled receptor signalling, to produce two derivative second messengers: diacylglycerol (DAG) and inositol-(1,4,5)-trisphosphate (IP_3). The two secondary messengers in turn activate protein kinase C and trigger intracellular calcium release, respectively (Berridge and Irvine, 1984). Apart from producing second messengers, $PI(4,5)P_2$ itself is an important molecule that has been implicated in diverse cellular functions, including endo- and exocytosis, protein docking and activation, initiating actin polymerization and cytoskeletal attachment (Gaidarov and Keen, 1999; Loyet *et al.*, 1998; Huang and Huang, 1991; Hartwig *et al.*, 1995; Raucher *et al.*, 2000).

Given its broad range of cellular functions, tight regulation of $PI(4,5)P_2$ metabolism and bioavailability are of critical importance. In mammals, the membrane-associated MARCKS protein can reversibly bind to $PI(4,5)P_2$ through its effector domain, and in effect reduce the levels of free $PI(4,5)P_2$ available for interaction with other proteins (Glaser *et al.*, 1996). This binding is not sequence-specific, but is instead mediated by electrostatic interaction through the stretch of lysine residues located in the effector domain of MARCKS protein (Figure 1.4b). The positive charges from these basic amino acids bind to the negatively charged polar heads of $PI(4,5)P_2$, enabling MARCKS protein to sequester many $PI(4,5)P_2$ molecules at the plasma membrane (Wang *et al.*, 2002).

Given the nature of this interaction, other proteins with MHDs that also retain stretches of polybasic residues could potentially bind to $PI(4,5)P_2$ as well. Indeed, an *in vitro* study using 99:1 phosphatidylcholine:$PI(4,5)P_2$ vesicles has shown that polylysine and polyarginine peptides, as well as peptides corresponding to the MHDs from various proteins including α- and β-adducin, are capable of binding to $PI(4,5)P_2$. The strength of the interaction was also directly correlated to the net charge of the peptides (Wang *et al.*, 2002). While no studies have examined this *in vivo*, the possibility exists that adducin, which retains many conserved lysines at its MHD (Figure 1.4b), may interact with $PI(4,5)P_2$ at the cellular membrane.

1.2.4 Disruption of adducin expression or function leads to disease

The importance of adducin becomes apparent when considering the wide range of problems that arise from its misexpression or misregulation. The membrane linkage that adducin provides to the actin-spectrin cytoskeleton is vital to the integrity of the human erythrocyte membrane, and when this bridge is disrupted leads to membrane

destabilization and fragmentation (Anong *et al.*, 2009). Adducin has also been implicated in maintaining apical junction stability in human epithelial cells; when α- or γ-adducin expression is reduced by RNAi knockdown, the resulting decrease in junctional levels of spectrin and actin promotes junction disassembly (Naydenov and Ivanov, 2010). Several long-term epidemiological studies regarding a Gly460Trp polymorphism in α-adducin suggests that, when in combination with other factors, may be associated with increased risk of hypertension (Citterio *et al.*, 2010).

Another example of great clinical significance is adducin's association with amyotrophic lateral sclerosis (ALS), also known as Lou Gehrig's Disease in the US. ALS is a late-onset motor neuron disease characterized by retraction and degeneration of upper and lower motoneurons in the brain stem and spinal cord, progressive paralysis and muscle atrophy, eventually leading to death usually within one to five years of diagnosis (Boillee *et al.*, 2006). Previous work on spinal cord tissue obtained from human ALS patients has found elevated levels of adducin phosphorylation at its MHD, along with increases in PKA and PKCα/β, compared to samples from the control population (Hu *et al.*, 2003). Increased pAdd was also detected specifically in neurons, astrocytes and motoneurons of mice that were overexpressing a human Gly93Ala mutant of superoxide dismutase (mSOD), a murine model for ALS (Shan *et al.*, 2005). Adducin may also have additional roles in the nervous system, as β-adducin knockout mice exhibit impaired synaptic plasticity and defects in memory and learning (Rabenstein *et al.*, 2005; Porro *et al.*, 2010). The mechanism for these neurological defects, however, are currently unknown. In order to gain a better understanding of the roles that adducin plays in the neuronal system, studies of its *Drosophila* homolog, *hu-li*

tai shao, were conducted, taking advantage of the well-characterized neuromuscular system and vast genetic techniques available in *Drosophila*.

1.3 Hu-li tai shao at the *Drosophila* NMJ

The gene encoding the only *Drosophila* homolog of mammalian adducin is *hu-li tai shao (hts)*, as known as *adducin-like*. Meaning "too little nursing" in Chinese (护理太少), *hts* was originally named for its mutant phenotype of having an inadequate number of nurse cells in the developing egg chamber during oogenesis (Yue and Spradling, 1992). Extensive studies addressing the role of Hts in oogenesis has demonstrated distinct expression profiles and localization patterns for its various protein isoforms, and *hts* null mutants are female sterile due to defects in fusome formation, ring canal structure, cell division synchronization and oocyte specification (Yue and Spradling, 1992; Ding *et al.*, 1993; Robinson *et al.*, 1994; Lin *et al.*, 1994; Lin and Spradling, 1995). In comparison, very few studies have been carried out investigating the roles Hts may have beyond oogenesis. The following sections will explore the different protein isoforms of Hts and its various roles in the development of *Drosophila*.

1.3.1 Structure and function of Hts

Transcripts from the *hts* locus can be alternatively spliced to give four different protein products: ShAdd, Add1, Add2, and Ovhts. These four protein isoforms share a common head and neck domain, but contain distinct C-terminal regions (Figure 1.5). ShAdd is a 55kDa protein that lacks the common tail domain, but contains a novel string of 23 amino acids at its C-terminus (Petrella *et al.*, 2007). The 87kDa Add1 and 95kDa Add2 isoforms are the closest homologs to mammalian adducins, showing ~40% amino acid identity and ~60% similarity (Whittaker *et al.*, 1999). Add2 only differs from Add1

by having an extra exon of 23 residues, and both isoforms contain a conserved MARCKS-homology domain at their C-terminus (Petrella *et al.*, 2007). Ovhts is a 140kDa polyprotein that is only expressed in females but is not expressed in the adult head (Telonis-Scott *et al.*, 2009); when cleaved by proteolysis, Ovhts produces two functional derivative proteins, 80kDa Ovhts-fus and 60kDa Ovhts-RC. Ovhts-fus shares a truncated tail domain with Add1/2 but does not contain an MHD. Ovhts-RC is unique to *Drosophila* and does not show homology to mammalian adducins (Petrella *et al.*, 2007).

Data from oogenesis studies suggest that Hts associates with actin and spectrin molecules and is required for their proper localization at different cellular structures. Hts, α-spectrin, β-spectrin and protein 4.1 all localize to a specialized organelle called the fusome during the cell division phase of early germline cyst development. htsF immunoreactivity (recognizing Add1/2, Ovhts and Ovhts-fus) at the fusome is decreased in α-*spec*$^{-}$ cysts, whereas α-spectrin immunoreactivity is completely lost at the fusome in *hts*^{1} mutants (de Cuevas *et al.*, 1996; Lin *et al.*, 1994). Following cyst formation, fusomes disintegrate in concurrence with the formation of structures called ring canals. Ovhts-RC colocalizes with F-actin at ring canals, and Ovhts-RC expression is required for actin localization to this structure (Robinson *et al.*, 1994; Petrella *et al.*, 2007). Late in oogenesis, Add1, F-actin and spectrin all localize to the cortex of the developing oocyte; alterations to Add1 distribution or expression levels lead to severe disruptions of F-actin and spectrin organization in the early embryonic cytoskeleton (Zaccai and Lipshitz, 1996a; b). These studies suggest that Hts may have a conserved role as a regulator of actin-spectrin networks in a manner similar to mammalian adducins.

High throughput gene expression analysis has shown that *hts* is expressed throughout all developmental stages, and is expressed at moderate levels in the adult

brain, adult/larval CNS and adult/larval gut, and also at lower levels in many other tissues (Chintapalli *et al.*, 2007). A recent publication by Ohler *et al*. demonstrated for the first time, a role for Hts in the central nervous system of *Drosophila*. Golden goal (gogo) is a single-pass transmembrane receptor that has been implicated in axonal guidance of the R8 photoreceptors towards the optic ganglion in the brain during development of the *Drosophila* visual system (Tomasi *et al.*, 2008). Tagged ShAdd and Add1 were coimmunoprecipitated by Gogo in *Drosophila* Schneider cells, and this interaction was mediated by the head and neck domains common to the ShAdd/Add1/Add2/Ovhts-fus Hts isoforms. Eye-specific *hts* or *β-spec* mutant clones exhibited R8 photoreceptor axonal guidance defects, and rescue experiments showed that the presence and function of the tail domain in Add1/2 was required for proper R8 axonal guidance; however, the MHD was found to be unnecessary for this role. While the exact mechanism was not clear, the authors propose that Gogo regulates axonal guidance by the binding of external ligands that may be guidance cues, and subsequently steers the movement of the growth cone by modulating actin-spectrin dynamics through its interaction with Hts (Ohler *et al.*, 2011).

(a)

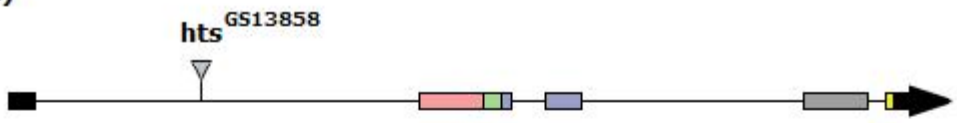

(b)

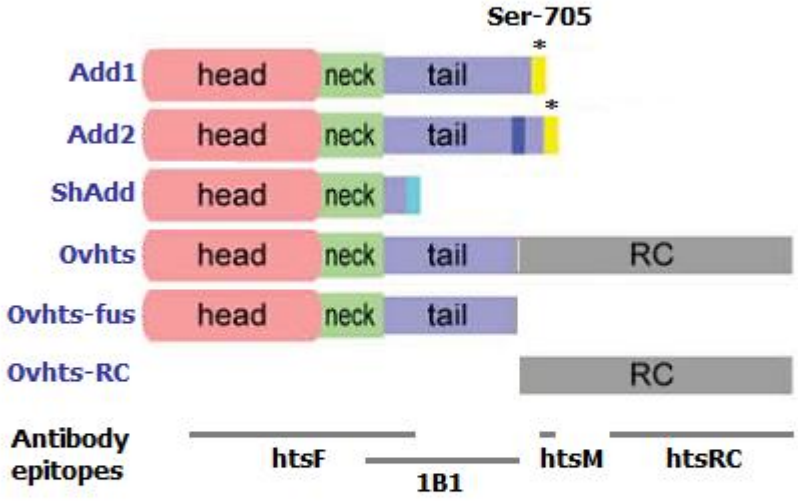

(c)

Hts isoform	Whittaker Transcript	Predicted Size (kDa)	Band Size (kDa)
Add1	R1	80	87 } doublet
Add2		80	95 } doublet
ShAdd	N32/ R2	55	
Ovhts	N4	128	140
├ Ovhts-fus			80
└ Ovhts-RC			60

Figure 1.5 Domain structure and relative sizes of Hts protein isoforms

(a) Schematic of known transcribed regions (wide bars) for the *hts* gene. Alternative splicing produces four different protein isoforms. Insertion location of the GSV6 vector for the $hts^{GS13858}$ allele is indicated. Cytological location of the P-element insertion in the hts^{01103} allele has not been mapped.
(b) Schematic of Hts protein isoforms and antibody epitopes. Add1 and Add2 are the only isoforms of Hts with a MARCKS-homology domain (yellow) in their tail domain, and display highest degree of homology to mammalian adducins. Add2 is identical to Add1 except for an extra exon of 23 amino acids (dark blue). ShAdd has a truncated tail domain with a novel stretch of 23 amino acids at the C-terminus (cyan). Ovhts contains an extended tail domain unique to *Drosophila*, which is cleaved to form two functional proteins, Ovhts-fus and Ovhts-RC. Asterisks indicate location of the conserved phosphorylation target residue, which is mutated in the phosphomimetic hts^{S705D} and non-phosphorylable hts^{S705A} transgenic lines for Add1. Regions corresponding to antibody epitopes are shown by bars. The htsF epitope spans residues 49-500, and has been shown by immunoblotting to recognize Add1/2 and Ovhts-fus. The 1B1 epitope spans residues 465-658 of Ovhts, and recognizes Add1/2, Ovhts and Ovhts-fus. The htsRC epitope spans residues 806-1156 of Ovhts, and recognizes Ovhts and Ovhts-RC. The htsM epitope spans 689-718 of Add1, and recognizes Add1/2.
(c) Hts protein isoforms and corresponding transcripts. Band sizes for each isoform are based on Western blotting data. There has yet to be any published studies with immunoblots showing a band corresponding to ShAdd.
(Panel b adapted from Ohler *et al.*, 2011. Epitope and immunoblotting data from Lin *et al.*, 1994; Zaccai and Lipshitz, 1996a; Robinson *et al.*, 1994; Petrella *et al.*, 2007. Data in table adapted from Whittaker *et al.*, 1999; Petrella *et al.*, 2007; Zaccai and Lipshitz, 1996b)

1.3.2 Hts regulates larval NMJ development through interactions with synaptic proteins

Apart from its involvement in oogenesis and R8 photoreceptor axonal guidance, Hts has also been found to be a key regulatory factor in the development of the Drosophila NMJ. Initial studies characterizing *hts* expression and function at the NMJ have revealed important roles for it in development of the NMJ. Two transgenic UAS lines were used for overexpression studies: $hts^{GS13858}$ has a GSV6 vector insertion that activates transcription of endogenous *hts*, whereas hts^{S705D} contains serine to aspartate mutation at the conserved phosphorylation target residue Ser-705 at the MHD of Add1 cDNA, which confers a negative charge mimicking phosphorylation (Figure 1.5a,b). Hts expression has a strong effect on the morphology of the NMJ, as *hts* null mutants exhibit underdeveloped synaptic terminals with a decrease in branch length and branch number. Muscle-specific overexpression of the endogenous *hts* gene or the phosphomimetic Add1 transgene hts^{S705D} leads to the opposite phenotype: overgrowth of synaptic terminals with an increase in bouton numbers, branch length and branch number. These data demonstrate that postsynaptic Hts contributes to synaptic growth at the NMJ (Yang, 2008).

Two antibodies were primarily used for immunohistochemistry: 1B1 that recognizes Add1/2, Ovhts and Ovhts-fus, as well as a polyclonal antibody directed against phosphorylated Ser660 at the MHD of mammalian γ-adducin (hereafter referred to as pAdd; Fowler *et al.*, 1998). Anti-pAdd cross-reacts with *Drosophila* phosphorylated Hts due to the high degree of conservation at the MHD. Bands corresponding to Add1/2 have been identified in Western blots of larval body wall lysates using 1B1 and anti-pAdd antibodies, but these bands were absent in *hts* null mutant samples, demonstrating the

specificity of these antibodies. In immunostained larval body wall preps, Hts immunoreactivity is observed predominantly at the postsynaptic NMJ surrounding the presynaptic terminals. pAdd immunoreactivity also localizes predominantly to the postsynaptic NMJ, albeit not always in colocalization with Hts immunoreactivity, and is also observed at low levels in the muscle. This suggests that at least part of the Hts found at the NMJ are of the Add1/2 isoforms since only they contain the MHD epitope recognized by the pAdd antibody (Yang, 2008).

Immunostainings show that Hts partially colocalizes with the trans-synaptic CAM Fas2 as well as the postsynaptic scaffolding protein Dlg. As described in above sections, Fas2 and Dlg have important roles during early development of the neuromuscular system, and Hts interaction with these two proteins could explain how it regulates synaptic growth. Muscle-specific overexpression of endogenous *hts* results in upregulated expression of Fas2 in muscle. Hts and Dlg are each able to coimmunoprecipitate the other, however, phosphorylated Hts was not able to coimmunoprecipitate Dlg, suggesting that phosphorylation at the MHD of Hts disrupts this interaction (Yang, 2008; Wang *et al.*, submitted) (Figure 1.6).

Dlg is regulated by phosphorylation at Ser48 and Ser797 by Ca^{2+}/calmodulin-dependent kinase II (CaMKII) and PAR-1 kinase, respectively. Overexpression of either kinase in muscle causes delocalization of Dlg away from the NMJ and impairs its scaffolding function (Koh *et al.*, 1999; Zhang *et al.*, 2007). A very similar phenotype is observed when endogenous *hts* or a phosphomimetic hts^{S705D} transgene is overexpressed in muscle. Muscle-specific overexpression of endogenous *hts* also increases both CaMKII and PAR-1 immunoreactivity at the postsynaptic NMJ. Finally, *hts* expression levels correlate with the levels of phosphorylated-Ser797 in Dlg at the NMJ,

suggesting that Hts may be regulating synaptic growth partially through modulation of Dlg phosphorylation via CaMKII and PAR-1 (Wang *et al.*, submitted) (Figure 1.6).

A recent publication by Pielage *et al.* has indicated a role for Hts at the presynaptic NMJ. *hts* null mutant NMJ exhibit signs of synaptic retraction that are very rarely observed in wildtype NMJ. Presynaptic silencing of *hts* expression by RNAi recapitulates this defect, and presynaptic overexpression of Add1 was able to fully rescue the defect in a *hts* null background. Furthermore, a premature truncation mutant of *hts* that lacks an MHD also exhibits synaptic retraction but at lower frequency and severity than in presynaptic *hts* knockdown or *hts* null NMJ, suggesting that the MHD in Add1/2 plays a role in maintaining NMJ stability (Pielage *et al.*, 2011).

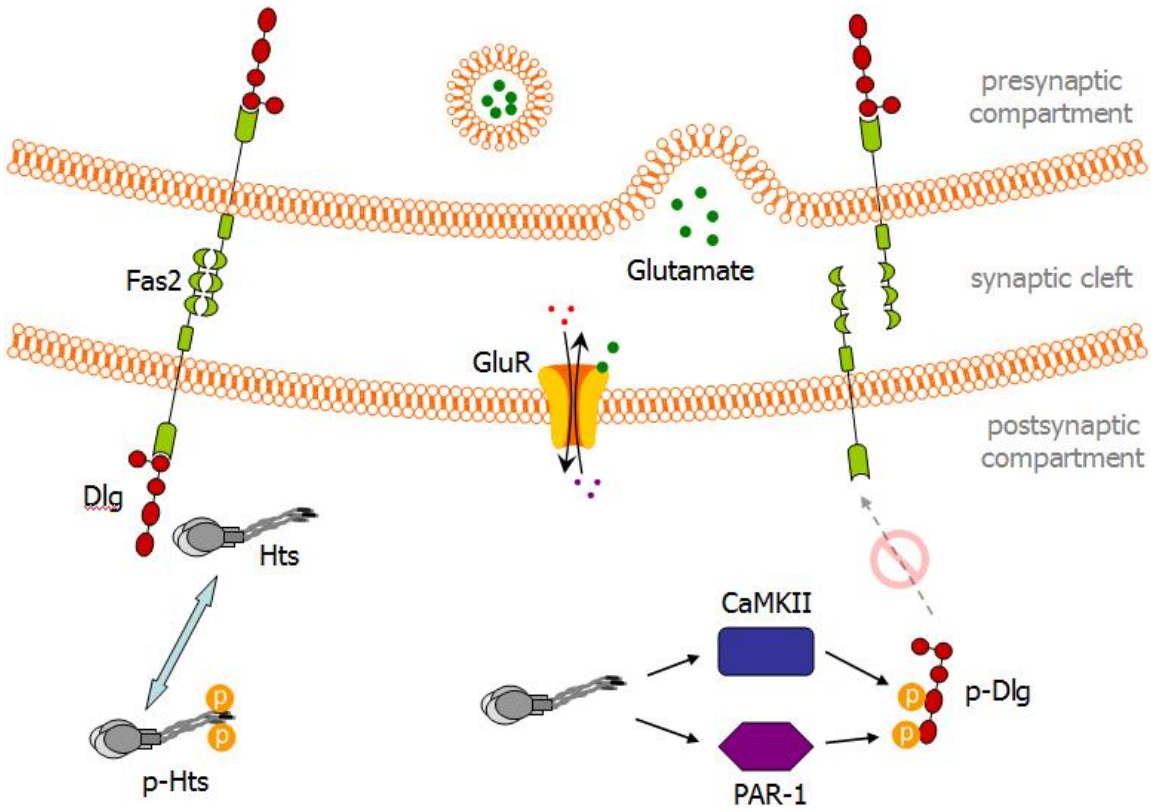

Figure 1.6 Current model of Hts function at the *Drosophila* larval NMJ

Hts associates with the scaffolding protein Dlg postsynaptically, however Hts that is phosphorylated at its MHD cannot. Dlg stabilizes intercellular adhesion mediated by the CAM Fas2. Hts increases protein levels of the kinases CaMKII and PAR-1 at the postsynaptic NMJ, each of which can phosphorylate Dlg. Phosphorylated Dlg can no longer associate with Fas2, leading to destabilization of the NMJ, which allows for morphological synaptic changes.

1.4 Specific objectives of this study

1.4.1 Rationale, research goals and overview of approach

Previous characterizations of Hts at the NMJ have established a role for it in development of the NMJ, but details regarding the mechanism(s) of its influence remain unclear. It should be noted that while overexpression of *hts* in muscle (which increases CaMKII and PAR-1 immunoreactivity) leads to NMJ overgrowth, previously published data indicate that overexpression of either CaMKII or PAR-1 in muscle leads to underdeveloped NMJ (Yang, 2008; Wang *et al.*, submitted; Koh *et al.*, 1999; Zhang *et al.*, 2007). This discrepancy suggests that beyond its involvement with Dlg phosphorylation, there are likely other interacting proteins present at the NMJ, through which Hts positively regulates synaptic growth.

The goals of this study are to identify potential upstream regulatory proteins that may affect Hts localization and function at the NMJ, and to investigate other signalling routes that Hts may be involved with during development of the NMJ. Briefly, these goals will be achieved using the following approaches: (a) identification of potential interacting partners of Hts based upon sequence homology to mammalian adducin and insights from current literature, (b) investigation of potential interacting partners by searching for interactions with *hts*, and (c) creation of new transgenic lines that will be useful in future research involving Hts function at the NMJ.

1.4.2 Strength of *Drosophila* NMJ as a model synapse

Drosophila larval body walls have abdominal muscles with a genetically predetermined layout, and the same is true for the arborisation pattern of the motor neurons that innervate them. Each segment at muscle pair 6/7 is innervated by a single

Type I synaptic terminal that is large and easily identified, allowing consistent and reliable comparisons between different animals, and electrophysiological studies are straightforward to conduct. Mutations that perturb NMJ morphology can be easily examined in immuno-labelled body wall samples that highlight the structural features of the NMJ. This allows for relatively easy screening of mutants and transgenic flies for changes in synaptic development or protein expression. Furthermore, a wide range of powerful tools for genetic manipulation is available in *Drosophila*, including stage- and tissue-specific induction or silencing of gene expression.

As mentioned before, Drosophila NMJ undergo substantial expansion in time with growth of the larvae, and also display activity-dependent growth, making it useful in the study of synaptic plasticity. Type I synapses are glutamatergic, as such some of the signalling mechanisms and molecular components are similar to the glutamatergic synapses found in the mammalian central nervous system, making it possible to draw parallels between the two systems. Thus, genetic and molecular analysis of factors and mechanisms that affect synaptic growth and plasticity at the *Drosophila* NMJ could help shed light on processes that involve changes in synaptic strength or connectivity in the mammalian CNS, such as learning and memory. These traits altogether make *Drosophila* NMJ a powerful model system for studying synaptic development and plasticity (Ruiz-Canada and Budnik, 2006).

2: Materials and Methods

2.1 *Drosophila* strains and crosses

mef2-GAL4, *D42-GAL4*, *elav-GAL4*, *Sac1*^{EY02269} and *hts*^{01103} were from Bloomington *Drosophila* Stock Center. *hts*^{GS13858} was from *Drosophila* Genetic Resource Center, Japan. *hts*$^{1889\text{-}1\text{-}2M}$ (referred to as *hts*^{S705D} in the text) was previously generated as described in Yang, 2008. *UAS-PH*$_{PLC\delta}$*-GFP* was from Julie Brill (Wong *et al.*, 2005). *drpr*$^{\Delta 5\text{-}rec8}$, *UAS-drpr* and *UAS-drpr*^{RNAi} were from Marc Freeman (Fuentes-Medel *et al.*, 2009). Additional RNAi stocks were obtained from the Vienna *Drosophila* RNAi Center (Dietzl *et al.*, 2007) and the NIG-Fly Stock Center in Japan (Appendix C).

Stocks were raised at 25°C on standard yeast-cornmeal-molasses media. Genetic crosses were performed at 25°C except for transgene overexpression and RNAi studies, which were carried out at 29°C.

2.2 Site-directed mutagenesis, PCR and subcloning

2.2.1 Creating wildtype and non-phosphorylable UAS transgenes of *hts*

A phosphomimetic *hts*^{S705D} transgene in pBluescript II SK(+) was previously generated by Tomas Kuca in the Harden lab (Yang, 2008), using *pUAST-HtsR1*^{S705D}. Site-directed mutagenesis of serine 705[†] was carried out with a QuikChange II Site-Directed

[†] The S705 designation in the original *hts* construct was based on the conserved MARCKS-homology domain phosphorylation target residue in the *hts-R1 (Add1)* transcriptional isoform (Whittaker *et al*. 1999). When designing primers, the corresponding serine residue was mislabeled as S835 based on its position in the *hts* cDNA in this construct. For all intents and purposes, both "S705" and "S835" refer to the same conserved serine residue located in the MARCKS-homology domain, and will be referred to as S705 in the remainder of the document.

Mutagenesis Kit (Stratagene/Agilent Technologies, Inc) according to manufacturer's protocol. Primer sets used were HtsR1-D835S-F/HtsR1-D835S-R to create *hts*^{S705S}, and HtsR1-D835A-F/HtsR1-D835A-R to create *hts*^{S705A} (see Appendix A for a full description of primers). Transformants for both mutations were confirmed by sequencing. The transgenes were then subcloned into *pUAST* using EcoRI/XhoI, and transformants were fully sequenced for verification.

2.2.2 Creating doubly non-phosphorylable UAS transgene of *dlg*

The *pUAST-eGFP-dlg1*^{S797A} construct was obtained from BingWei Lu (Zhang *et al.*, 2007). The transgene was subcloned into pBluescript KS(-) using PstI/XbaI. Site-directed mutagenesis was carried out as described above, using the primer set dlg1-S48A-F/dlg1-S48A-R (Appendix A). Transformants of the resulting construct *pBS.KS(-)-eGFP-dlg1*^{S48A,S797A} were fully sequenced and both residue substitutions were confirmed to be present. HindIII and XbaI restriction sites were added to the 5' and 3' ends of the insert, respectively, via PCR stitching (Appendix A) and then subcloned into a *pUAST.attB* vector (Bischof *et al.*, 2007) by Dr. Ziwei Ding at the SFU Molecular Biology Service Centre. The correct sequence and orientation of the final construct in the transformants were verified by sequencing.

2.3 Generation of transgenic stocks

2.3.1 *UAS-hts*^{S705S} and *UAS-hts*^{S705A}

The constructs isolated from confirmed transformants (A) *pUAST-hts*^{S705S} and (B) *pUAST-hts*^{S705A} were sent out to BestGene Inc for *Drosophila* embryo injection service, allowing random insertion of the constructs into the genome. 8 stable transformants

were returned for (A) *pUAST-hts*^{S705S} along with 9 stable transformants for (B) *pUAST-hts*^{S705A} (Appendix B).

2.3.2 *UAS-eGFP-dlg*^{S48A,S797A}

The construct isolated from confirmed transformant *pUAST.attB-eGFP-dlg1*^{S48A,S797A} was sent out to BestGene Inc for targeted genomic insertion utilizing ϕC31 recombinase-mediated cassette exchange (Bateman *et al.*, 2006; Bischof *et al.*, 2007). Target strains containing a known attP landing site were selected for each of chromosomes X, 2nd and 3rd (Appendix B).

2.4 Larval body wall preparations

Body wall preparations for immunostaining and visualization of the NMJ were performed using a modified protocol based on Bellen and Budnik, 2000. Procedures are briefly described below.

2.4.1 Platform slides for mounting

A pair of 22×22mm #1 coverslips was secured onto each glass slide with nail polish, leaving a 13mm gap in between. Slides were shielded from dust and left to air-dry overnight, then stored in a covered slide box.

2.4.2 Larval dissections

Wandering third-instar larvae were cleaned and dissected in phosphate-buffered saline, pH 7.4 (PBS) on a Pyrex spot plate (Corning). Briefly, 2-3 anterior-most segments were cut off, the dorsal surface of the larva was then cut open along the anterior-posterior axis. After discarding the innards, 2-3 posterior-most segments were removed.

Body walls were then pinned onto a platform made from Sylgard 184 silicone elastomer (Dow Corning Corporation; kit available through World Precision Instruments, Inc.).

2.4.3 Body wall fixation

Body walls were incubated at room temperature for 30 minutes in fixing solution (4% w/v para-formaldehyde in PBS), then rinsed thoroughly with PBT (0.1% w/v Triton in PBS). Cleaned body walls were unpinned, then transferred to Eppendorf tubes with PBT and stored at 4°C until ready for immunostaining.

2.5 Immunohistochemistry

2.5.1 Antibodies used

Mouse monoclonal antibodies against Hts (*1B1*, 1:5), Fas2 (*1D4*, 1:2), Dlg (*4F3*, 1:10), α-spectrin (*3A9*, 1:10) and Brp (*nc82*, 1:100) were from Developmental Studies Hybridoma Bank, goat anti-phosphoSer662-γ-adducin (sc-12614; 1:50) was from Santa Cruz Biotechnology Inc., rabbit and goat anti-HRP (1:500; 1:100) were from Jackson Immunolabs, mouse and rabbit anti-GFP (1:500; 1:200) were from Sigma, mouse anti-PI(4,5)P_2 (1:100) was from Echelon Biosciences Inc., Texas Red anti-goat (1:100) was from Santa Cruz Biotechnology Inc., and all other secondary antibodies (1:200) were from Vector Laboratories.

2.5.2 Immunostaining

Body wall samples were blocked at room temperature with rotation for one hour in blocking solution (1% w/v bovine serum albumin in PBT), followed by incubation in primary antibody solution (diluted in blocking solution) with rotation at 4°C overnight or at room temperature for two hours. After three 15-minute washes in PBT, samples were

incubated in secondary antibody solution (diluted in blocking solution) in foil-wrapped tubes with rotation at room temperature for two hours. After another three 15-minute washes in PBT, samples were left to equilibrate in three drops of Vectashield at room temperature for at least half an hour prior to mounting.

2.5.3 Phalloidin staining

After immunostaining, prior to adding in Vectashield, body wall samples were incubated in FITC-conjugated phalloidin (1:1000; Sigma-Aldritch Co.) for 30 minutes, followed by three 15-minute washes in PBS. Samples were left to equilibrate in three drops of Vectashield at room temperature for at least half an hour prior to mounting.

2.5.4 Mounting of samples onto platform slides

A portion of the Vectashield from the samples was pipetted onto the central gap of a platform slide. Immunostained body walls were then individually transferred to and aligned on the slide, ensuring that the inner surface of the body walls was facing up. A 22×40mm #1.5 coverslip was slowly lowered to cover the central chamber, and was secured in place with drops of nail polish at the corners. Vectashield was pipetted into the central chamber until completely filled, after which the edges of the chamber were sealed with nail polish to prolong the protective effect of Vectashield by preventing oxidation. Slides were stored in a slide box at -20°C until ready to be imaged.

2.6 Visualization and Quantification

2.6.1 Fluorescence microscopy

Larvae that required selection based on GFP markers were examined on a Zeiss Axioplan2 epifluorescence microscope. Immunostained samples were examined on a

Zeiss Observer.Z1 spinning disc confocal microscope with a 63× glycerol-immersion objective and Volocity software, or on a Nikon A1R laser scanning microscope with a 20× oil-immersion objective and Nikon NIS-Elements software. Confocal stacks of representative muscle 6/7 NMJ for samples and their respective controls were taken using identical exposure parameters.

Images were extracted from Volocity as maximum intensity projections of confocal stacks. Images were processed in Microsoft Paint or ImageJ software to add labels and arrange into figures.

2.6.2 Data processing and quantification

Quantitative analysis of immunoreactivity levels were performed by a semi-automated process using the Visualization and Quantitation modules in the Volocity software suite. Briefly, object identification parameters were set based on fluorescence intensity to differentiate between NMJ signal and background levels in the muscle, and further filtered based on size to remove objects less than $5\mu m^3$. After object identification, staining artifacts and erroneous objects that were not part of the NMJ were manually corrected by cropping the selection area or removing the specific objects (see Figure 2.1 for an example).

Areas included in the analysis were mainly high-intensity regions at the boutons and on the postsynaptic side immediately surrounding the boutons. Axons were excluded, as were background levels of immunoreactivity in the muscle unless otherwise specified in figure legends. For sample sets that required distinction between pre- and postsynaptic immunoreactivity levels, neuron-specific anti-HRP immunoreactivity was

used to define objects corresponding presynaptic domains, which were then subtracted from the overall NMJ region to define postsynaptic domains.

Quantitative data including raw intensity levels and NMJ volumes were exported to Microsoft Excel. Relative intensity of a given immunostain at each NMJ was standardized using either NMJ volume or intensity of a staining control (anti-HRP) before compiling and comparing between groups. Values were expressed as mean standardized intensity with standard error of the mean as the error bar. F-tests were used to check for equality of group variances and Student's *t*-tests were used to determine statistical significance. Significant differences are indicated above bar graphs by asterisks (* for $p<0.05$, ** for $p<0.01$ and *** for $p<0.001$).

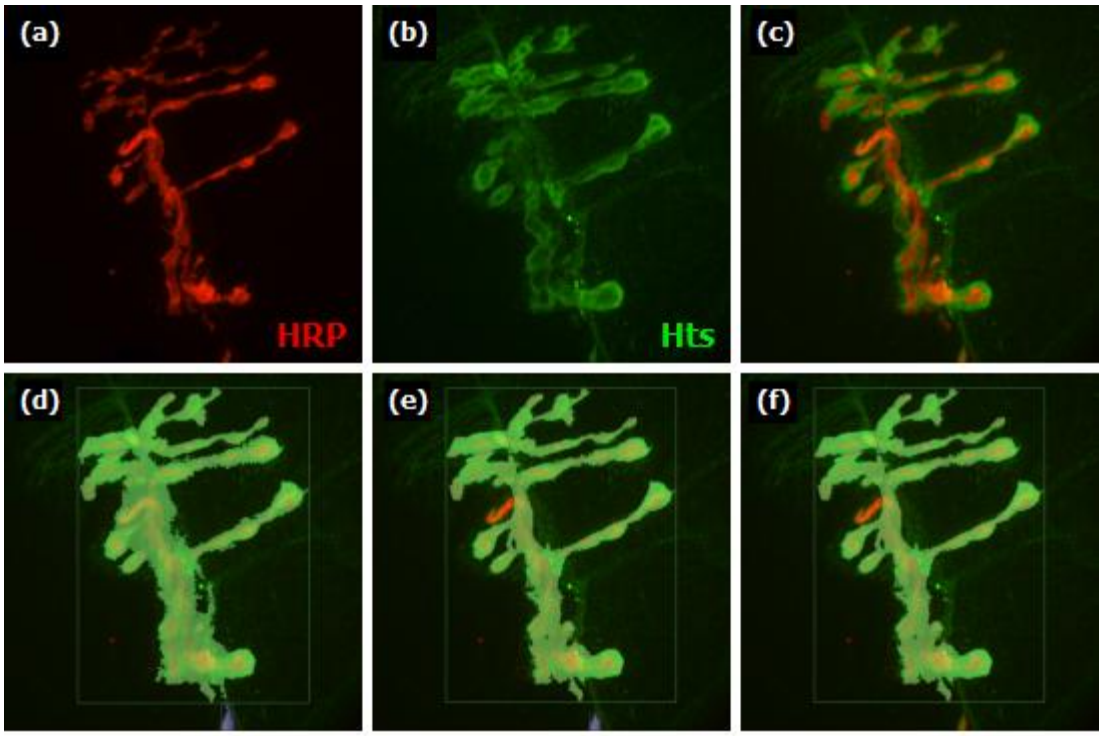

(g)

Name	ID	Volume (µm3)	Sum (RFP Confocal)	Sum (GFP Confocal)
ROI Object	2	2560.01194	5688499343	5444463601

Figure 2.1 Semi-automated method for object identification and quantification in Volocity software

(a-c) Maximum intensity projection from a confocal stack of a sample NMJ. HRP immunoreactivity (red) labels presynaptic terminals, while Hts immunoreactivity (green) is seen postsynaptically.
(d-f) Screen captures from the Volocity software showing (d) initial object identification with default parameters, (e) improved identification of NMJ regions by cropping and refining parameters, and (f) final object selection after removal of erroneous objects (blue object at bottom).
(g) Quantified data obtained from the sample NMJ. Raw intensity levels from multiple NMJ standardized using either NMJ volume or a reference immunostain (e.g. anti-HRP) and then averaged for each genotype before making comparisons between groups.

3: Results

As pointed out in the introduction, the details of how Hts regulates NMJ development are not entirely clear, and what is currently known about Hts interactions is insufficient to fully explain phenotypes observed at the NMJ in *hts* mutants. This study aims to broadly explore potential avenues through which Hts could be participating. To this end, the search for upstream regulatory proteins identified the involvement of two kinases, Pkc53E and PKA, in Hts phosphorylation at its MHD. Hts was found to play a role in the regulation of postsynaptic spectrin organization and presynaptic active zone stability. Hts could potentially interact with the membrane phospholipid $PI(4,5)P_2$ at the postsynaptic NMJ. Draper encodes a membrane receptor present at the NMJ, which could interact with and regulate *hts* expression.

3.1 Muscle-specific RNAi knockdown of candidate proteins that may interact with Hts

Since factors that regulate Hts activity and localization at the NMJ are not well understood, in order to identify potential interactions that may occur between Hts and other synaptic proteins, muscle-specific gene silencing for a selective group of candidates was carried out. RNAi stocks for these candidates genes were obtained from the NIG-Fly Stock Center in Japan and the Vienna *Drosophila* RNAi Center (Dietzl *et al.*, 2007). Candidates were selected on the basis that these proteins were presumed to interact with Hts and/or mammalian adducins at conserved binding sequences or phosphorylation target residues. Target genes examined include protein C kinases

(PKC), subunits of cAMP-dependent protein kinase (PKA), calmodulin, Rho-kinase, and PIP kinases (Appendix C). Overexpression of each *UAS-RNAi* construct was directed by the muscle-specific driver *mef2-GAL4* (myocyte-enhancing factor 2; Nguyen *et al.*, 1994). Body walls from the resulting larvae were immunostained against Hts and pAdd and examined for changes in immunoreactivity levels and distribution. Antibody staining directed against horseradish peroxidase (HRP), which cross-reacts with neuron-specific glycoproteins (Jan and Jan, 1982; Snow *et al.*, 1987), was used as a standard reference to label the presynaptic terminals.

Among the candidate genes examined, only two yielded significant results: *Pkc53E* and *Pka-R2* (described below). The remaining cases showed no signs of changes in Hts or pAdd levels or localization at the NMJ compared to wildtype (Appendix C). However, since *in situ* hybridization and immunoblotting were not conducted to verify decreases in mRNA and protein levels respectively, it cannot be concluded whether the reason why the other genes examined did not produce changes in Hts/pAdd immunoreactivity was due to a genuine lack of interaction with Hts or ineffective RNAi induction.

3.2 PKC and PKA regulate Hts phosphorylation levels

The activity of mammalian adducin is negatively regulated via phosphorylation at its MHD by PKC and PKA (Matsuoka *et al.*, 2000). Given the high degree of homology between the MHDs of mammalian adducin and *Drosophila* Hts, and in particular the conservation of the phosphorylation target residue (Figure 1.4b), it is plausible that Hts may be regulated in the same manner by PKC and PKA.

The *Drosophila* genome contains several PKC genes: conventional *Pkc53E* and *inaC*, novel *Pkc98E* and *Pkcδ*, and atypical *aPKC* (Shieh *et al.*, 2002). The *Pkc53E* gene encodes a calcium- and DAG-responsive serine/threonine kinase of the conventional PKC family, and shows sequence similarity to vertebrate PKCα and PKCβ (Rosenthal *et al.*, 1987). Pkc53E is strongly expressed in the adult fly CNS and male accessory gland, however it is also found at low levels during late embryogenesis and in larval CNS and body wall (Chintapalli *et al.*, 2007). Muscle-specific knockdown of *Pkc53E* by simultaneous expression of both *CG6622R-2* and *v27696* RNAi constructs in the same larvae caused a very strong decrease in pAdd immunoreactivity in about half the samples analyzed, to a point where the signal was barely detectable at the boutons (Figure 3.1a-f). While genotypically identical, about half the samples resembled wildtype and appeared to have little difference in pAdd immunoreactivity, possibly due to unsuccessful induction of RNA interference. Averaging the measurement of pAdd immunoreactivity at the NMJ for all the samples revealed a 54% (±22%, n=17, $p<0.001$) decrease in fluorescence at the NMJ compared to wildtype larvae (Figure 3.1g). This suggests a role for Pkc53E in the phosphorylation of Hts at its MHD. There was no statistically significant difference in Hts immunoreactivity at NMJ of larvae with muscle-specific RNAi knockdown of *Pkc53E* compared to wildtype NMJ. No differences in Hts and pAdd levels or localization were observed with muscle-specific RNAi knockdown of other *Drosophila* PKC genes, *Pkc98E, aPKC* and *inaC* (also called *Pkc53E(ey)* or *eye-PKC*) (Appendix C), when compared to wildtype NMJ. Note that no RNAi lines were available for *Pkcδ* and therefore it was not examined in this study.

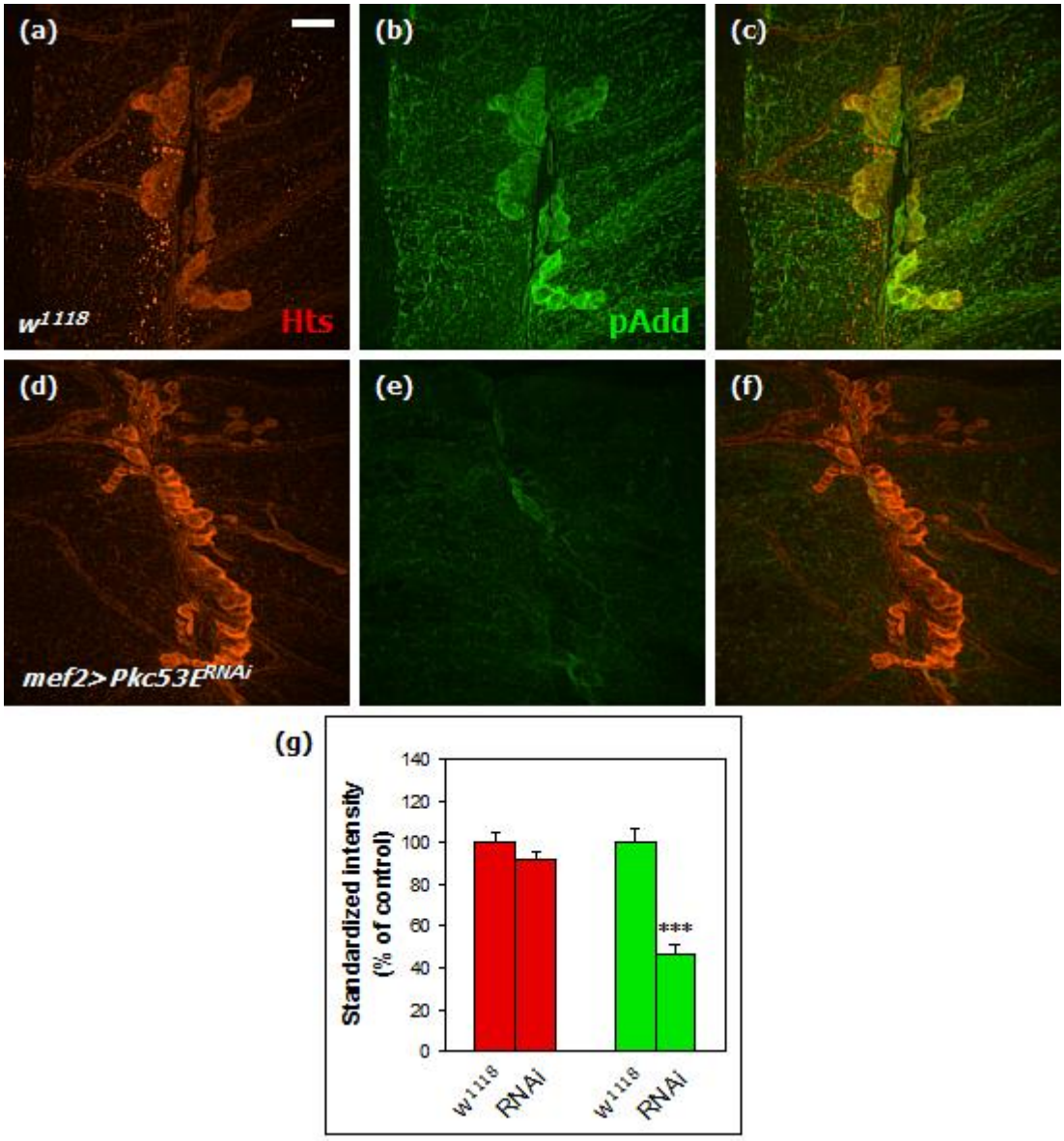

Figure 3.1 RNAi knockdown of *Pkc53E* expression reduces pAdd immunoreactivity at the NMJ

(a-c) Wildtype NMJ show colocalization of immunoreactivity against Hts and pAdd at the NMJ.
(d-f) Muscle-specific induction of RNAi constructs (*CG6622R-2; v27696*) against *Pkc53E* strongly reduces pAdd immunoreactivity but does not affect Hts immunoreactivity at the NMJ.
(g) Quantification of immunoreactivity shows no statistically significant changes in Hts immunoreactivity (red), while a 54% (±22%, n=17, $p<0.001$) decrease in overall pAdd immunoreactivity (green) was observed with RNAi knockdown compared to wildtype.
Scale bar, 10μm.

Another kinase that is known to phosphorylate mammalian adducins at its MHD is PKA, which is a tetrameric holoenzyme typically composed of two catalytic subunits and two negative regulatory subunits. Upon binding of cAMP to the regulatory subunits, the catalytic subunits dissociate and become active. In *Drosophila*, there are two regulatory subunit genes, *Pka-R1* and *Pka-R2*. *Pka-R1* is expressed from larval to early pupal stages, whereas *Pka-R2* is expressed throughout all developmental stages (Foster *et al.*, 1984). Tissue-specific expression data is unavailable for *Pka-R1*, but *Pka-R2* is moderately expressed in adult brain and ovaries, adult/larval gut and tracheal system as well as in the larval body wall (Chintapalli *et al.*, 2007). RNAi knockdown of either regulatory subunit gene is expected to relieve repression and therefore lead to an increase in PKA activity. Muscle-specific expression of the *v101763* RNAi construct against *Pka-R2* led to a 43% (±60%, n=22, $p<0.01$) increase in pAdd immunoreactivity at the NMJ compared to wildtype larvae (Figure 3.2), whereas there was no statistically significant difference in Hts immunoreactivity between these two groups. This suggests that PKA may contribute to Hts phosphorylation at its MHD. Note that no RNAi lines were available for *Pka-R1* and therefore it was not examined in this study.

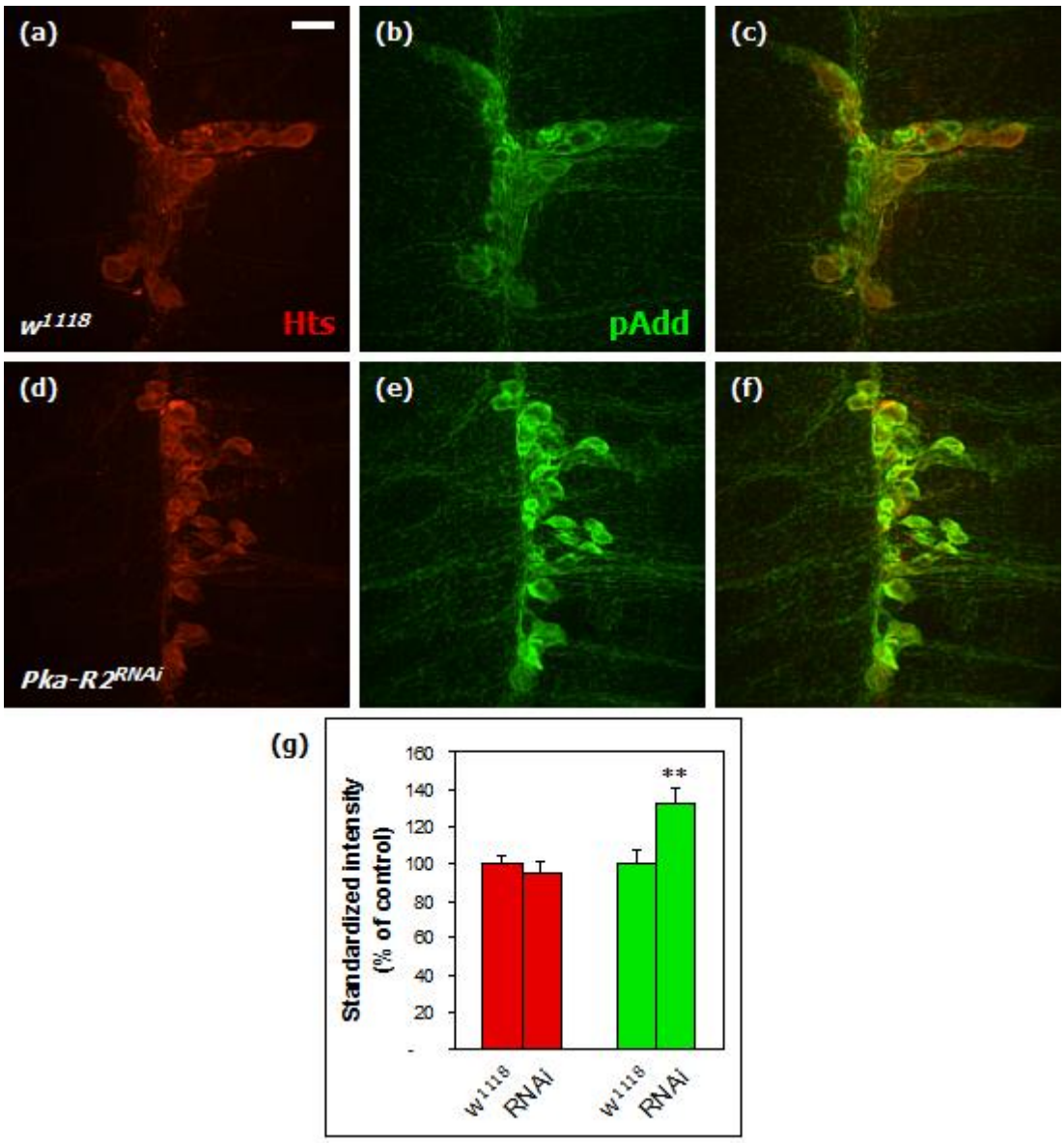

Figure 3.2 RNAi knockdown of *Pka-R2* expression increases pAdd immunoreactivity at the NMJ

(a-c) Wildtype NMJ show colocalization of immunoreactivity against Hts and pAdd at the NMJ.
(d-f) Muscle-specific induction of RNAi construct *v101763* against *Pka-R2* moderately increased pAdd immunoreactivity but does not affect Hts immunoreactivity at the NMJ.
(g) Quantification of immunoreactivity shows no statistically significant changes in Hts immunoreactivity (red), while a 43% (±60%, n=22, $p<0.01$) increase in pAdd immunoreactivity (green) was observed with RNAi knockdown compared to wildtype.
Scale bar, 10μm.

3.3 Hts is required for organization of the postsynaptic spectrin cytoskeleton

Another project goal was to examine whether *Drosophila* Hts has similar cellular functions as mammalian adducin, which has been shown to be one of the critical proteins that regulate the formation and maintenance of the actin-spectrin cytoskeleton (Matsuoka *et al.*, 2000). This submembranous cytoskeleton is an important structural scaffold for the organization of the NMJ in vertebrates and *Drosophila* (Kordeli, 2000; Pielage *et al.*, 2005). In order to determine whether Hts serves a similar function at the NMJ, larvae with altered expression levels of *hts* were examined for cytoskeletal changes near the NMJ.

A central component of the cytoskeletal network surrounding the postsynaptic NMJ is spectrin, which was examined by immunohistochemistry using an antibody directed against α-spectrin. In wildtype NMJ, α-spectrin immunoreactivity can be seen a clear bright band that surrounds the presynaptic marker HRP (Figure 3.3a-c). Note that α-spectrin does not directly abut HRP, and a small gap can be seen between the two, which is never observed with Hts immunostainings (compare Figure 3.3c and Figure 3.10c, page 69), suggesting that the spectrin cytoskeleton is situated apart from the postsynaptic membrane, perhaps just beyond the SSR. *hts* null mutant NMJs have decreased branch number and branch length as previously described (Yang, 2008). They have similar levels of HRP immunoreactivity as wildtype, but decreased amount of α-spectrin immunoreactivity, and in some cases α-spectrin immunoreactivity was barely detectable (Figure 3.3d-f). Overall, the *hts* null mutant NMJs exhibited a mean reduction in spectrin immunoreactivity of 34% (±19%, n=22, $p<0.001$) compared to wildtype (Figure 3.3m).

Larvae with muscle-specific overexpression of either phosphomimetic or non-phosphorylable mutant *hts* were also examined for changes in postsynaptic α-spectrin, which appeared less tightly associated with the boutons; instead of a clear narrow band surrounding the boutons as seen in wildtype NMJ, signals were generally spread out across a larger area. Quantification of the fluorescence intensity from these expanded postsynaptic domains for both genotypes showed lower α-spectrin immunoreactivity compared to wildtype, yielding a 26% (±15%, n=24, $p<0.01$) and 53% (±12%, n=20, $p<0.001$) decrease, respectively (Figure 3.3g-m). In addition to disorganization and decreased overall immunoreactivity levels, boutons were frequently seen only partially surrounded by α-Spectrin (Figure 3.3, arrows), and some without any α-Spectrin in the vicinity at all (Figure 3.3, arrowhead). Neither of these phenotypes are ever observed in wildtype NMJ. Overexpression of endogenous *hts* was also attempted, however, high levels of background GFP fluorescence in the muscle prevented objective analysis of postsynaptic α-Spectrin immunoreactivity (discussed in Section 3.5). These results suggest a role for Hts in regulating the organization of spectrin at the postsynaptic NMJ.

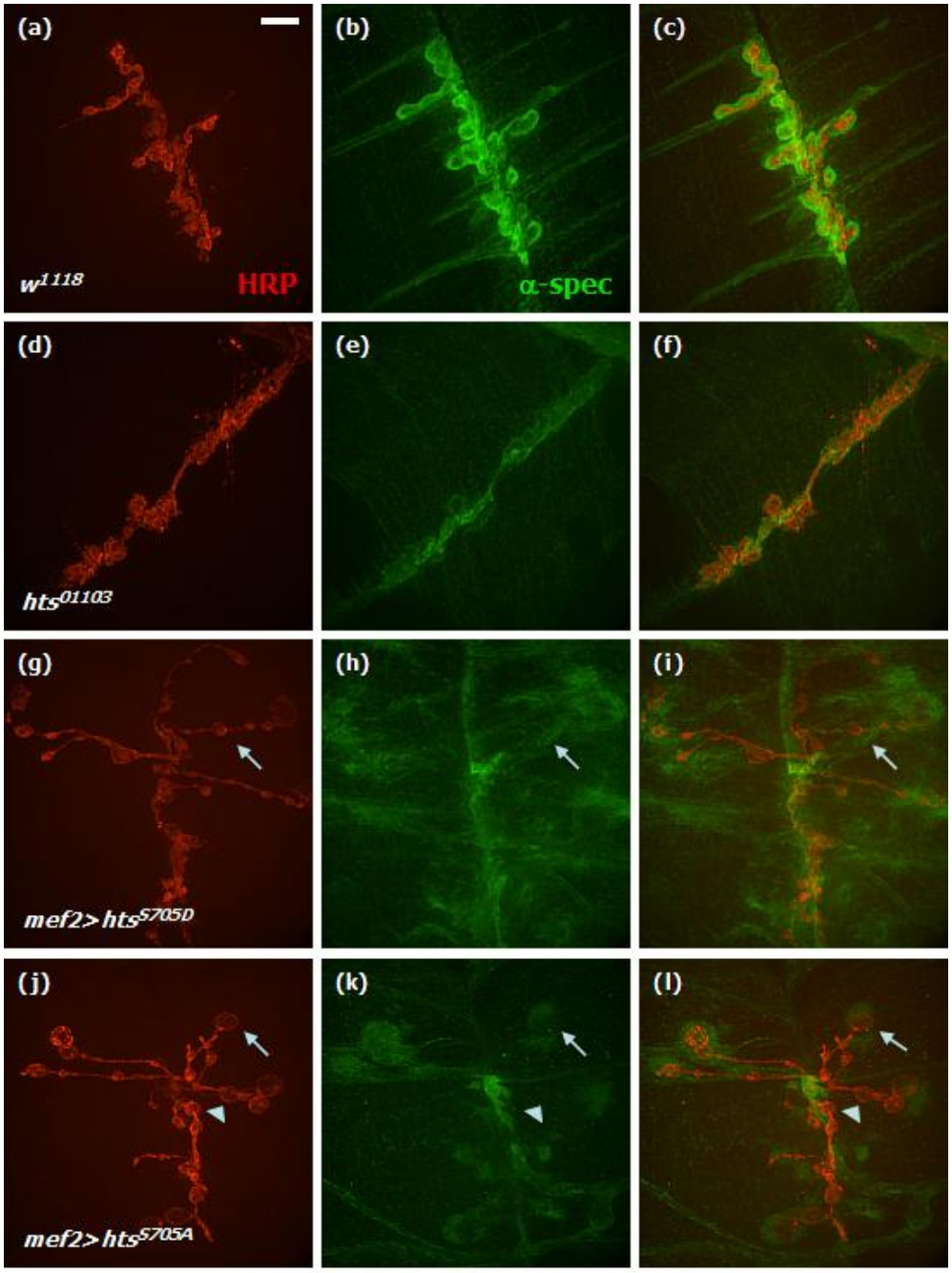
(a)
(b)
(c)
w1118
HRP
α-spec
(d)
(e)
(f)
hts01103
(g)
(h)
(i)
mef2>hts S705D
(j)
(k)
(l)
mef2>hts S705A
(m)
Standardized intensity (% of control)
120
100
80
60
40
20
0
***
**
***
w1118
hts01103
mef2>SD
mef2>SA

Figure 3.3 Changes in Hts levels disrupt α-spectrin localization

(a-c) Wildtype NMJ show strong α-spectrin immunoreactivity surrounding the presynaptic marker HRP. A narrow gap can be seen between the two signals, suggesting that the spectrin network does not directly abut the membrane.
(d-f) *hts* null mutants have underdeveloped NMJ as previously described (Yang, 2008), and show diminished levels of α-spectrin immunoreactivity.
(g-l) Overexpression of phosphomimetic or non-phosphorylable *hts* also leads to NMJ with diminished levels of α-spectrin immunoreactivity. Organization is disrupted and appears diffuse compared to wildtype NMJ. Some boutons are only partly surrounded by α-spectrin immunoreactivity (arrows), and some others are not surrounded at all (arrowhead).
(m) Quantification of α-spectrin immunoreactivity at the NMJ shows a mean decrease of 34% (±19%, n=22, $p<0.001$) in *hts* null mutant, 26% (±15%, n=24, $p<0.01$) with phosphomimetic *hts* overexpression, and 53% (±12%, n=20, $p<0.001$) with non-phosphorylable *hts* overexpression, when samples were compared to wildtype NMJ.
Scale bar, 10μm.

As postsynaptic spectrin is most likely to exist in a complex with actin, NMJ were also examined for F-actin localization. To visualize postsynaptic F-actin levels immediately adjacent to the NMJ, samples were stained using FITC-conjugated phalloidin by following a previously published protocol for muscle tissue (Ramachandran *et al.*, 2009). On rare occasions, single confocal slices showed fluorescence specifically surrounding boutons (Figure 3.4a-c) indicating the presence of postsynaptic F-actin localization, however, the overwhelming signal from the surrounding actomyosin fibres did not allow objective analysis (Figure 3.4d). For most samples examined, postsynaptic signal could not be distinguished from muscular actomyosin signals even in single confocal slices. To see if higher resolution microscopy could solve this problem, samples were examined under a two-photon microscope (courtesy of Dr. Saeid Kamal from the LASIR facility at 4D Labs). However, the lack of a mercury arc lamp for screening using the eyepiece greatly hampered progress and made it impossible to distinguish between muscle pairs and identify the target NMJ. After several attempts using different settings and fluorophores with no success, further experiments with F-actin staining were discontinued. Despite not being able to directly visualize postsynaptic actin, a recent publication demonstrated an actin-capping function of the Add1 isoform of Hts by *in vitro* actin depolymerization studies (Pielage *et al.*, 2011); together these results suggest that Hts may be able to interact with both actin and spectrin at the postsynaptic NMJ.

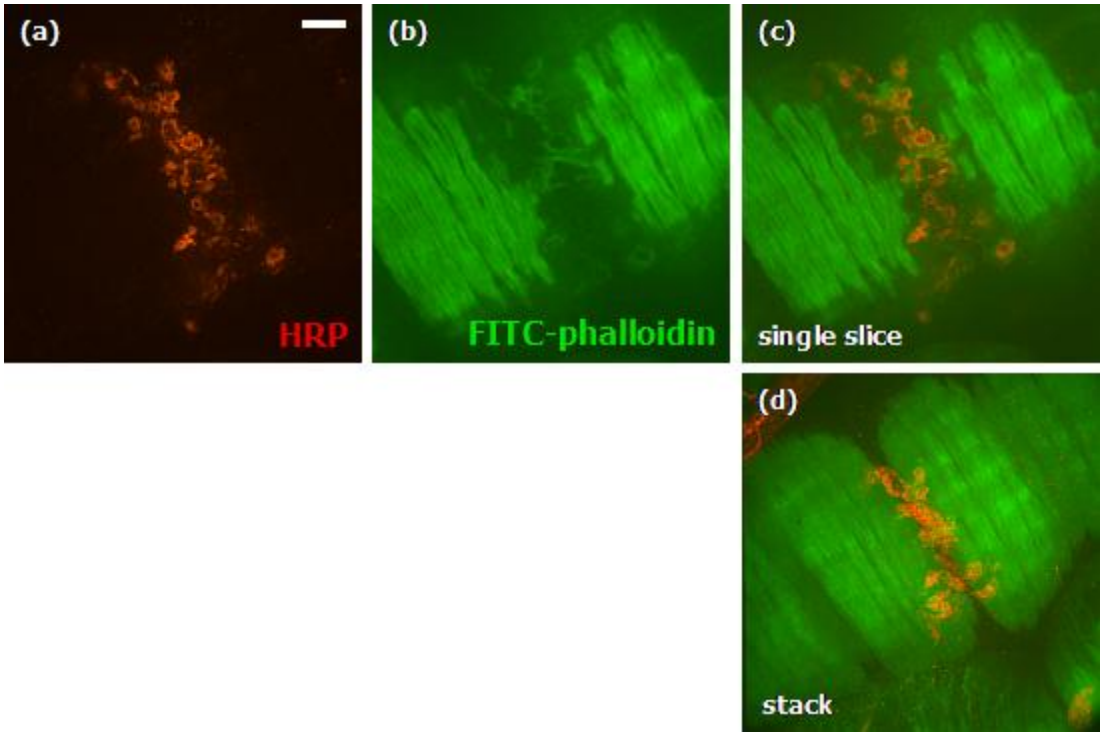

Figure 3.4 FITC-conjugated phalloidin staining of a muscle 12/13 NMJ

(a-c) Images from a single confocal slice of a muscle 12/13 NMJ shows distinct fluorescence surrounding boutons, indicating the presence of actin at the postsynaptic NMJ.
(d) Maximum intensity projection (confocal stack) of the same NMJ. The high degree of overlap between the fluorescence from postsynaptic actin and muscular actomyosin prevented objective analysis of the postsynaptic actin levels.
Scale bar, 10μm.

3.4 *hts* null mutant NMJ exhibit decreased levels of the active zone marker Bruchpilot

As described in the introduction, Fas2 is a homodimeric CAM that contributes to synaptic adhesion, which in turn affects the stability and plasticity of synapses. The same studies have also demonstrated the effects of an unknown retrograde feedback mechanism that ensures proper muscle depolarization despite NMJ under- or overdevelopment. This modulation is accomplished by changing either the probability of presynaptic neurotransmitter release, or the density of active zones (Schuster *et al.*, 1996a; b).

Despite Hts immunoreactivity showing a predominantly postsynaptic distribution pattern at the NMJ, previous findings that Hts regulates the level and distribution of postsynaptic Fas2 and Dlg (Wang *et al.*, submitted) suggest that Hts may also affect presynaptic development. This may be accomplished by modulation of synaptic adhesion strength through Fas2, which is in turn partially regulated by Dlg (Thomas *et al.*, 1997). Thus the disruption of postsynaptic Fas2 and Dlg seen when Hts is lost or overexpressed may also have presynaptic phenotypes. In addition to examining roles Hts may have postsynaptically, its potential effects on development of the presynaptic active zone were also examined.

Active zones represent the specific domains within each bouton at which signal transmission across the synapse occurs. Neurotransmitters are stored in synaptic vesicles near the active zone until exocytosis is triggered by an action potential. The controlled release of neurotransmitter is mediated by various protein complexes, comprising the molecular machinery that facilitate and regulate the rate of synaptic vesicle fusion and reformation (Burns and Augustine, 1995). During embryogenesis, the

development of a nascent presynaptic terminal into a fully functional one requires certain retrograde inputs from the postsynaptic muscle cell, and defects in muscle formation or differentiation can lead to the failure of synapse maturation (Prokop *et al.*, 1996). As described in the introduction, perturbations in *hts* expression lead to changes in NMJ morphology and distribution of postsynaptic proteins (Yang, 2008). While the synapses remain functional, there may be differences in presynaptic active zone assembly or organization in relation to these changes.

In order to investigate potential roles for Hts in this process, NMJ were examined using immunostaining against Bruchpilot (Brp), which is a structural component of the active zone commonly used as a presynaptic active zone marker (Wagh *et al.*, 2006). Brp immunoreactivity shows up as discrete puncta localized at the boutons in wildtype NMJ, but is absent from the axonal process (Figure 3.5a-c). *hts* null mutant NMJ show decreased levels of Brp immunoreactivity, and when taking NMJ size difference into account, still exhibit 33% (±13%, n=22, $p<0.01$) less Brp immunoreactivity compared to controls (Figure 3.5d-g). In addition, Brp puncta density at *hts* null mutant NMJ was 24% (±30%, n=22, $p<0.05$) lower, and individual Brp puncta were on average 30% (±23%, n=22, $p<0.05$) smaller (Figure 3.5g) compared to wildtype NMJ. Surprisingly, overexpression of either phosphomimetic or non-phosphorylable Hts in the muscle appeared to produce no significant changes in Brp immunoreactivity (Figure 3.6). While the mechanism remains unknown, these results suggest that Hts may influence the development or stability of the presynaptic active zone. Muscle-specific overexpression of the endogenous *hts* gene using $hts^{GS13858}$ (described below) was also attempted, however, the overwhelming level of GFP fluorescence in the muscle tissue precluded analysis of presynaptic Brp immunoreactivity levels.

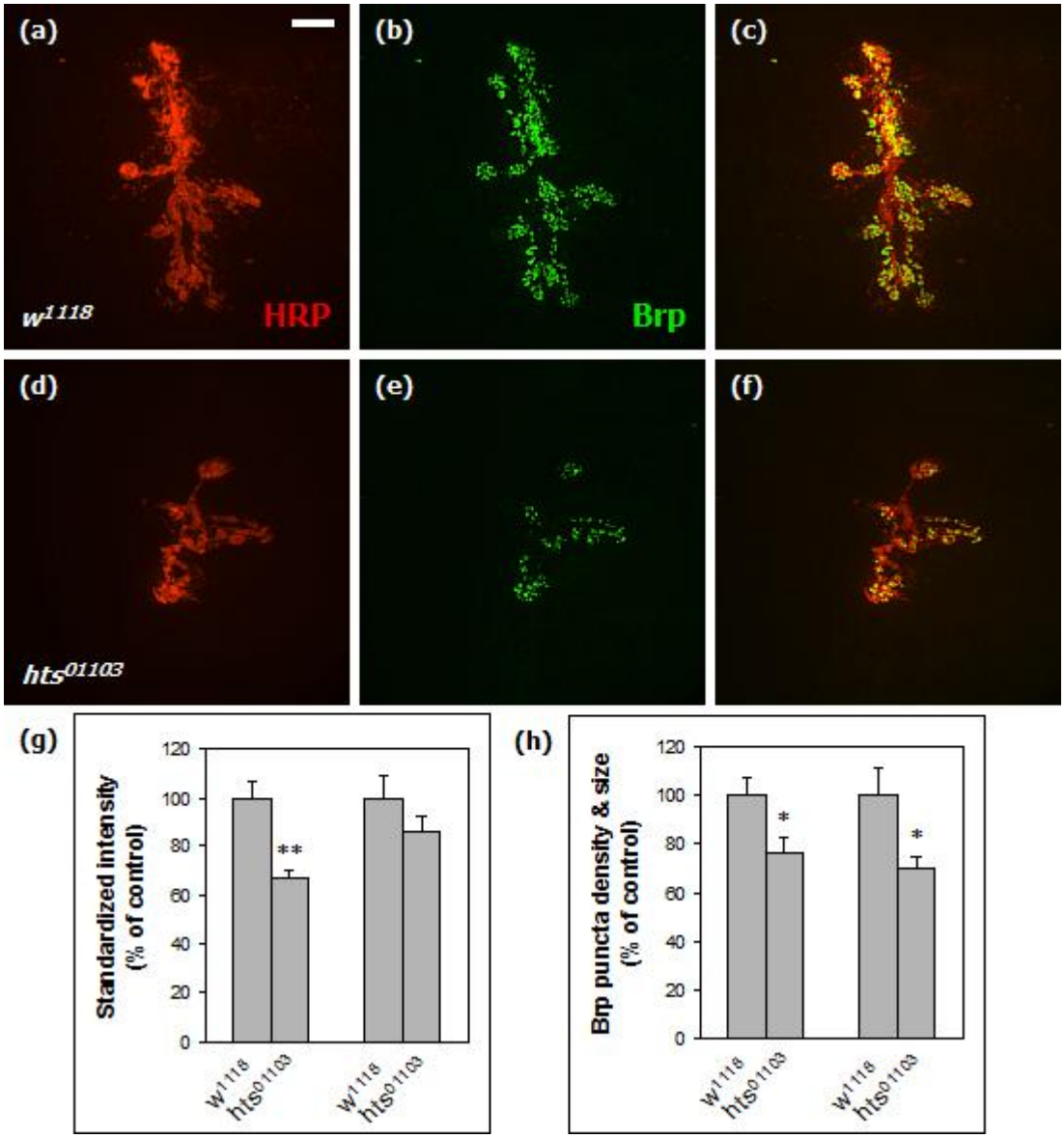

Figure 3.5 *hts* null mutant NMJ exhibit fewer and smaller Brp puncta

(a-c) Wildtype NMJ show discrete Brp puncta localized to boutons but is absent from the axonal process.
(d-f) *hts* null mutant NMJ show diminished levels of Brp immunoreactivity for their size.
(g) *hts* null mutant NMJ show a 33% (±13%, n=22, $p<0.01$) decrease in Brp immunoreactivity compared to wildtype NMJ, when standardized based on NMJ volume.
(h) *hts* null mutant NMJ show a 24% (±30%, n=22, $p<0.05$) decrease in Brp puncta density, and a 30% (±23%, n=22, $p<0.05$) decrease in puncta size compared wildtype NMJ.
Scale bar, 10μm.

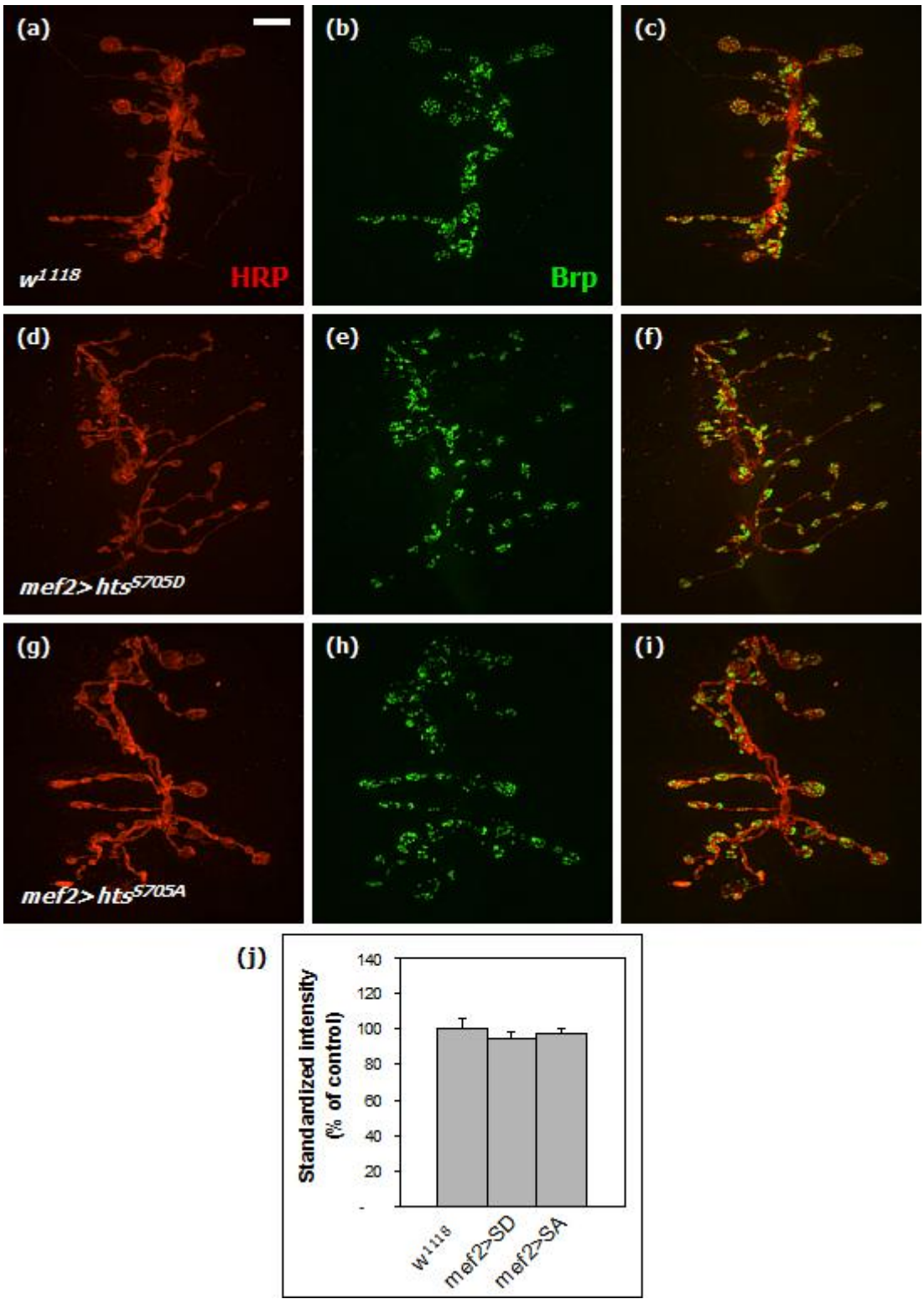
(a)
(b)
(c)
w1118
HRP
Brp
(d)
(e)
(f)
mef2>hts S705D
(g)
(h)
(i)
mef2>hts S705A
(j)
Standardized intensity (% of control)
140
120
100
80
60
40
20
-
w1118
mef2>SD
mef2>SA

Figure 3.6 Overexpression of Hts in muscle does not affect Brp immunoreactivity

(a-c) Wildtype NMJ show discrete Brp puncta localized to boutons but is absent from axonal processes.
(d-i) Muscle-specific overexpression of phosphomimetic or non-phosphorylable *hts* give similar patterns of Brp puncta localization.
(j) Quantification of Brp immunoreactivity showed no statistically significant differences between NMJ from wildtype and *hts* mutant overexpression.
Scale bar, 10μm.

3.5 GFP reporter complication in *hts*^{GS13858}

Since the beginning of the Hts project, the standard method to induce overexpression of endogenous Hts gene products was using *hts*^{GS13858}, a line generated from the *Drosophila* Gene Search Project by random genomic insertion of a GSV6 vector, which contains two UAS sequences. This vector is embedded in an intron near the 5' end of *hts* in *hts*^{GS13858} (Figure 1.5a). Overexpression of this allele in the muscle seemingly led to a very dramatic increase in muscle-specific immunofluorescence for many proteins that were being examined by immunostaining (Yang, 2008; Wang *et al.*, submitted; this manuscript). Among these was the presynaptic protein Brp, which should not have been present in muscle at all, leading to the suspicion that the immunofluorescence was spurious. It was later uncovered by Simon Wang that this particular version of the vector used to generate this *hts*^{GS13858} allele contained a GFP reporter, and hence background fluorescence would show up whenever the FITC/GFP channel was used for immunostaining. Future immunohistochemistry studies with this allele will require the use of fluorescent secondary antibodies that do not overlap in spectrum with GFP.

3.6 Generation of *hts* & *dlg1* transgenic lines

3.6.1 *UAS-hts*^{S705S} and *UAS-hts*^{S705A}

Since the *hts*^{GS13858} allele uses the endogenous *hts* promoter, all Hts isoforms could be expressed during GAL4 induction, which could complicate analysis of experimental results with respect to differentiating between the actions of the different Hts isoforms. To avoid the complication with the GFP reporter in *hts*^{GS13858}, and to allow specific overexpression of a single Hts isoform, new UAS lines for *hts* were created. A

UAS-hts^{S705D} transgenic line had previously been generated based on cDNA for Add1 (formerly called Hts-R1; Yang, 2008); however, the original pUAST vector containing the wildtype clone could no longer be located. Therefore, the *hts*^{S705D} transgene was back-mutated to recreate wildtype *hts*^{S705S}, and also mutated to create non-phosphorylable *hts*^{S705A}. pUAST vectors containing these transgenes were sent for injection by BestGene Inc. The returned transgenic lines (Appendix B) were then tested by Amy Tsai for relative protein expression levels by Western blotting, and the most comparable lines, (7F) *hts*^{S705S} and (7M) *hts*^{S705A}, were selected for use in further studies.

3.6.2 *UAS-eGFP-dlg1*^{S48A,S797A}

One of the broader goals of the Hts project is to examine its effects on Dlg phosphorylation and localization. Single-site non-phosphorylable mutants for *dlg1* at Ser-48 and Ser-797 were previously generated by the Vivian Budnik (Koh *et al.*, 1999) and BingWei Liu (Zhang *et al.*, 2007) labs, respectively. The S48A mutation blocks Dlg phosphorylation by CaMKII, whereas the S797A mutation blocks Dlg phosphorylation by PAR-1. However, work with existing mutants cannot rule out whether this is mediated by CaMKII, PAR-1, both cooperatively, or through other potential signalling routes. As such, a GFP-tagged doubly non-phosphorylable mutant of *dlg1* was created by site-directed mutagenesis based on the *pUAST-eGFP-dlg1*^{S797A} construct (Zhang *et al.*, 2007). Targeted genomic insertions for the 3rd, 2nd and X chromosomes (at cytological locations 86Fb, 22A and 2A) are currently being carried out by BestGene Inc. These transgenic lines can be used to establish or rule out the possibility that Dlg localization is linked to its phosphorylation by CaMKII or PAR-1.

3.7 The phospholipid PI(4,5)P_2 is detected at the NMJ

In an effort to investigate further possible interactions between Hts and other synaptic molecules, the phospholipid PI(4,5)P_2 was selected as a candidate due its role in negatively regulating NMJ development, as well as its relation to mammalian MARCKS protein (Khuong *et al.*, 2010). The sequestration of PI(4,5)P_2 by MARCKS protein is an important mechanism for regulating the levels of available PI(4,5)P_2 (Arbuzova *et al.*, 2002). While peptides corresponding to adducin MHD can bind to PI(4,5)P_2-containing vesicles *in vitro* (Wang *et al.*, 2002), it is unknown whether Hts is capable of binding to PI(4,5)P_2 by electrostatic interactions through the conserved polybasic residues at its MHD. Such an interaction would present a whole new avenue through which Hts might influence synaptic signalling and NMJ development.

To address this possibility, both immunostaining using a PI(4,5)P_2-specific antibody and the expression of an *in vivo* reporter were used to first determine whether there is PI(4,5)P_2 present at the NMJ. The anti-PI(4,5)P_2 antibody was previously used for immunostaining of *Drosophila* spermatid cysts, and its specificity was confirmed by manipulating the expression of known PIP kinases and phosphatases (Fabian *et al.*, 2010). Since the antibody has not been tested on body wall tissue before, immunostaining on *Sac1* mutants was performed as a control to confirm the effectiveness and specificity of the antibody. Sac1 is a homologue of yeast Sac1p, which is a phosphoinositide phosphatase that can generate PI(4,5)P_2 by dephosphorylating PI(3,4,5)P_3, and *Sac1p* mutants in yeast show as low as only 20% PI(4,5)P_2 levels compared to controls in *in vitro* assays (Hughes *et al.*, 2000).

Immunostaining against PI(4,5)P_2 in wildtype NMJ showed enriched presynaptic signal (in colocalization with HRP immunoreactivity) compared to the background seen

in muscle, and was also found concentrated at large globular structures in the muscle, presumed to be their nuclei (Figure 3.7a-c). The uncharacterized *EY02269* allele of Sac1 contains a P-element insertion situated the 5' exon where gene expression or protein function may be disrupted. In $Sac1^{EY02269}$ mutant NMJ, decreased levels of presynaptic PI(4,5)P_2 immunoreactivity that were colocalized with HRP immunoreactivity were observed (Figure 3.7d-f). Quantification of the levels of presynaptic PI(4,5)P_2 immunoreactivity showed a 32% (±14%, n=10, $p<0.01$) decrease in $Sac1^{EY02269}$ mutant NMJ compared to wildtype NMJ, which is in line with our expectations of decreased PI(4,5)P_2 levels in these mutants (Figure 3.7g). Due to the amount of background staining seen in the muscle, it was difficult to identify any specific postsynaptic localization that resembled a distinct pattern around the NMJ.

On rare occasions when observing at higher magnification, PI(4,5)P_2 puncta appeared to interdigitate perfectly with gaps in HRP immunoreactivity (Figure 3.8). Most confocal stacks that were taken were not sharp enough to resolve this pattern, therefore this was only observed clearly in a few instances. This finding suggests that PI(4,5)P_2 may be localized to distinct lipid microdomains on the presynaptic NMJ membrane, or that it may be sequestered by PI(4,5)P_2-binding proteins.

Immunostaining of *hts* null mutant NMJ was also attempted, however, perhaps due to the inconsistency in sensitivity of this antibody, the levels of immunoreactivity occasionally varied wildly within the same sample set, and sometimes even within the same body wall. Despite trying antibodies from different production lots, this variability persisted, and the results from several attempts at *hts* null mutant immunostainings were not replicable.

In order to evaluate PI(4,5)P_2 levels at the NMJ in a more consistent and reliable manner, a transgenic line containing an *in vivo* GFP reporter, $PH_{PLC\delta}$-GFP, that specifically binds to PI(4,5)P_2 was used to analyze endogenous PI(4,5)P_2 distribution. The specificity of this reporter has previously been demonstrated by manipulating the expression of PI(4,5)P_2 kinases and phosphatases in *Drosophila* adult spermatocytes and larval muscles (Wong *et al.*, 2005; Khuong *et al.*, 2010). Expression of this reporter using a neuronal driver revealed GFP fluorescence at axonal processes (Figure 3.9, arrows) and in faint puncta at the NMJ where it colocalized with HRP immunoreactivity (Figure 3.9a-c). Compared with the anti-PI(4,5)P_2 immunostaining, the GFP puncta were less distinct and therefore clear signs of interdigitation between GFP reporter puncta and HRP immunoreactivity were not observed.

Expression of the reporter in muscle tissue indicated strong localization to the postsynaptic NMJ, where the GFP fluorescence was observed to be surrounding HRP immunoreactivity (Figure 3.9d-f). In contrast to the distribution of anti-PI(4,5)P_2 immunoreactivity, the reporter appeared to be specifically excluded from the muscle nuclei. Expression of the PI(4,5)P_2 reporter in muscle together with Hts immunostaining showed colocalization of GFP fluorescence with Hts immunoreactivity (Figure 3.9g-h), suggesting that PI(4,5)P_2 and Hts share the same postsynaptic distribution pattern, where interactions between the two could be occurring. Future studies to examine this possibility will help shed light on how Hts regulates NMJ development.

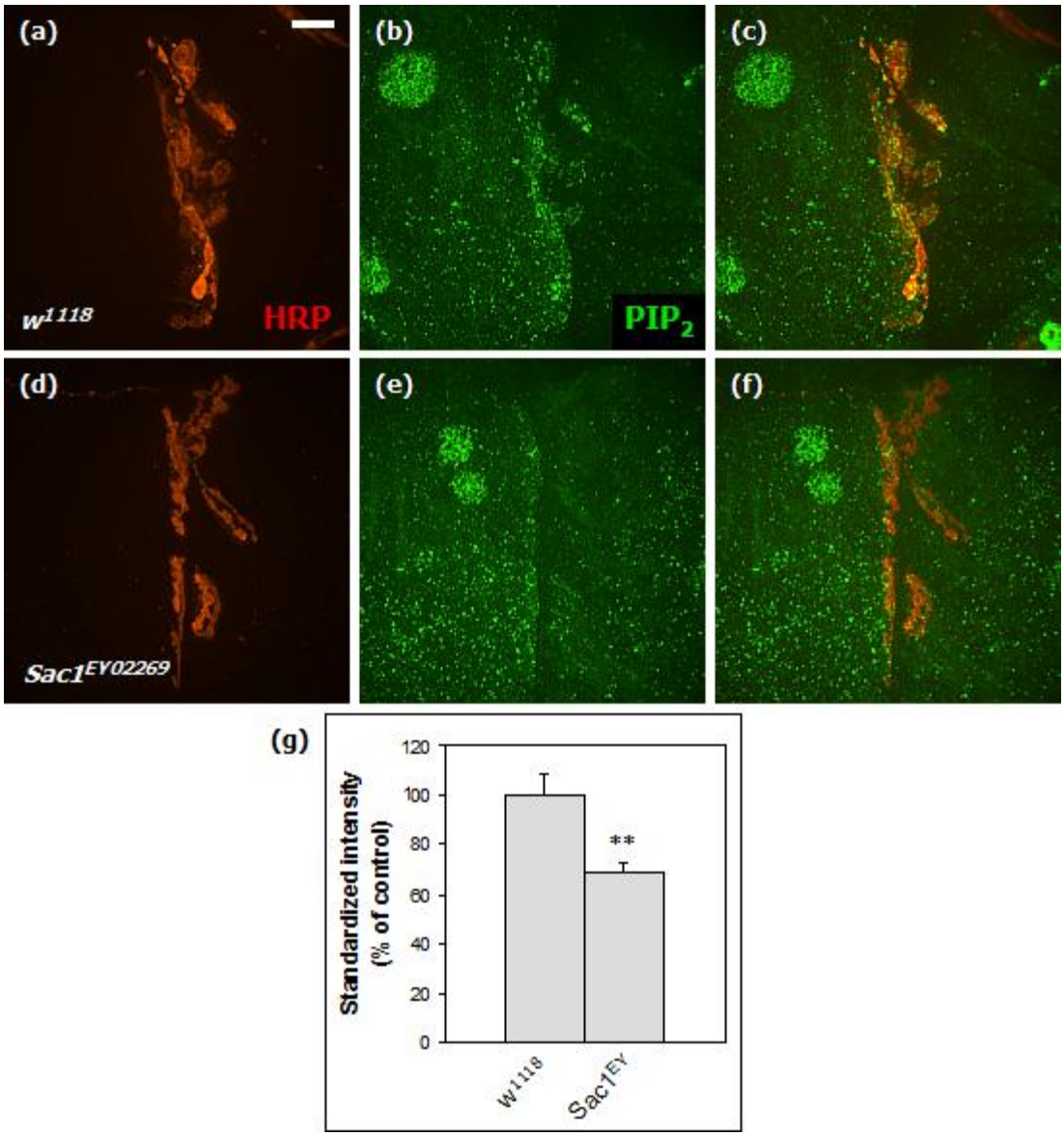

Figure 3.7 Anti-PI(4,5)P_2 antibody detects PI(4,5)P_2 at the presynaptic NMJ, and *Sac1*^{EY02269} mutant NMJ exhibit lower presynaptic PI(4,5)P_2 immunoreactivity

(a-c) Wildtype NMJ showed enrichment of PI(4,5)P_2 immunoreactivity at the NMJ in colocalization with HRP immunoreactivity. Large spherical regions of concentrated signal were also observed in the muscle, which may be the muscle nuclei.
(d-f) *Sac1* mutant NMJ show decreased levels of PI(4,5)P_2 immunoreactivity at the NMJ compared to wildtype NMJ.
(g) Quantification of presynaptic PI(4,5)P_2 immunoreactivity showed a 32% (±14%, n=10, $p<0.01$) decrease in *Sac1* mutant NMJ compared to wildtype NMJ.
Scale bar, 10μm.

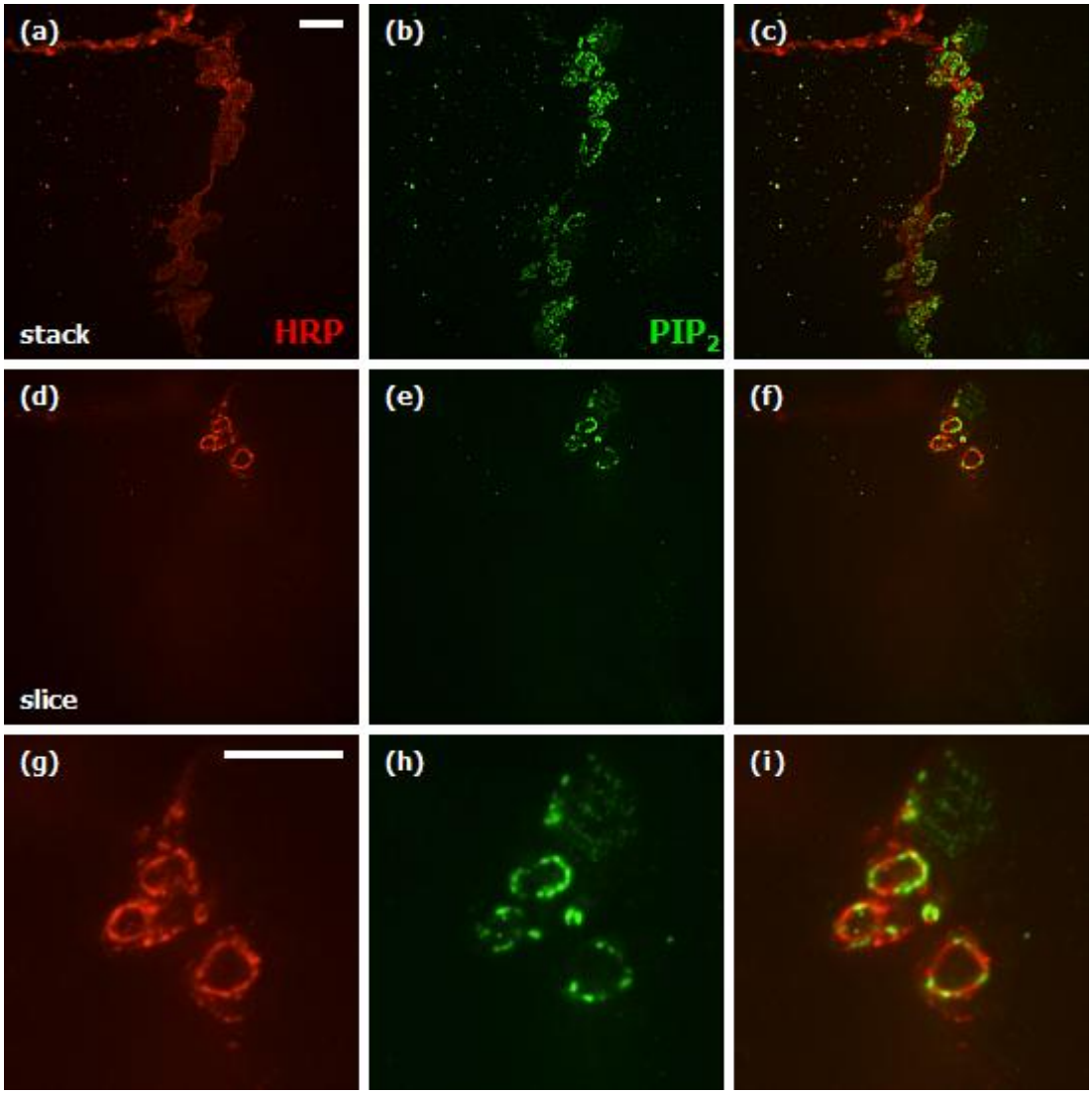

Figure 3.8 $PI(4,5)P_2$ immunoreactive puncta interdigitates with gaps in HRP immunoreactivity at the NMJ

(a-c) Confocal stack of a muscle 6/7 NMJ showing localization of $PI(4,5)P_2$ immunoreactivity to the presynaptic NMJ.
(d-f) Single confocal slice of the same NMJ.
(g-i) Zoomed images from the single confocal slice, showing interdigitation between $PI(4,5)P_2$ and HRP immunoreactivity.
Scale bar, 10μm.

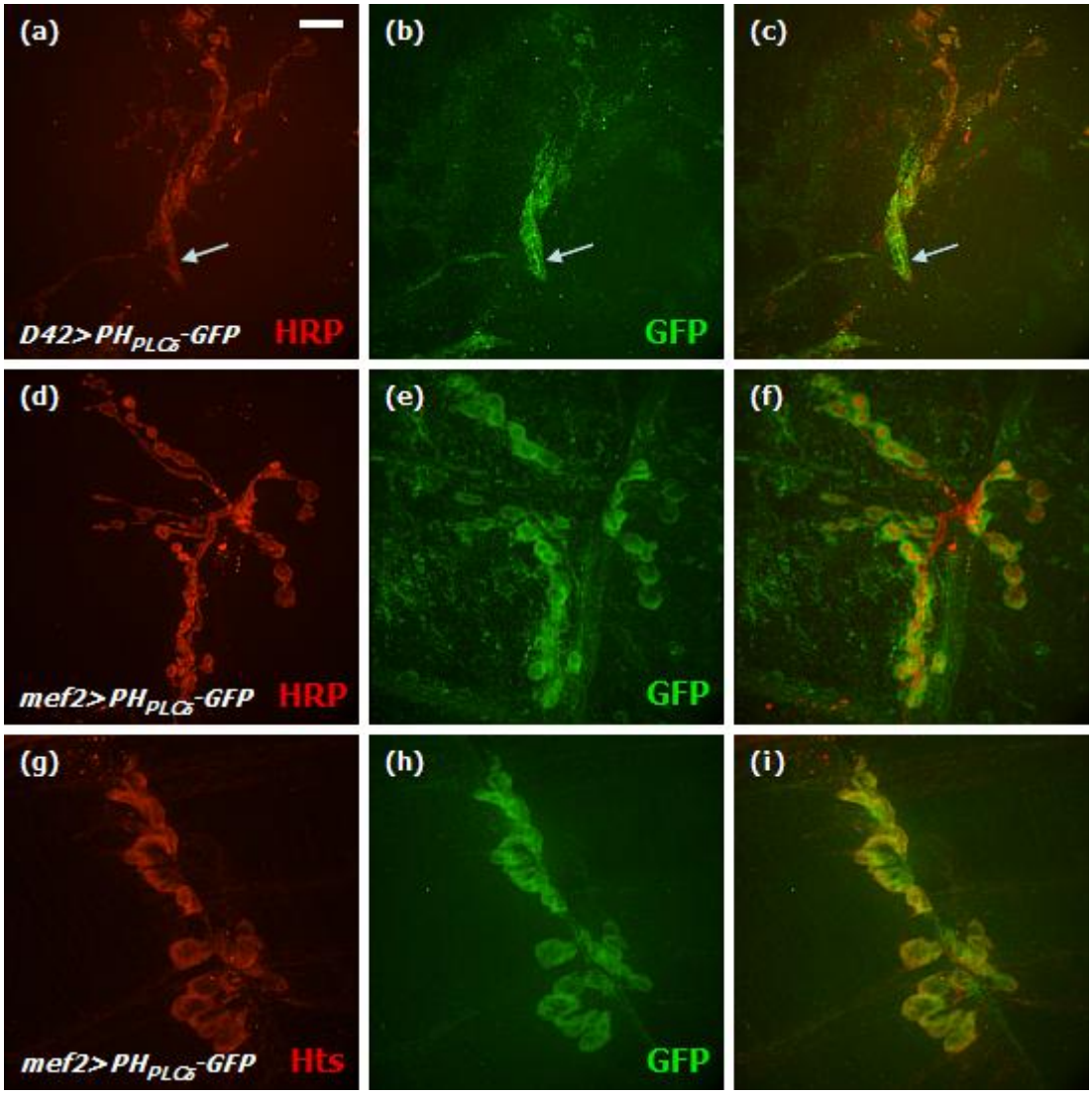

Figure 3.9 GFP-tagged *in vivo* PI(4,5)P_2 reporter localizes to the NMJ and colocalizes with HRP and Hts immunoreactivity

(a-c) An *in vivo* GFP-tagged PI(4,5)P_2-binding reporter, when expressed in neurons, showed localization to axonal processes (arrow) and faint puncta at the presynaptic NMJ, colocalizing with HRP immunoreactivity.
(d-f) The PI(4,5)P_2 reporter, when expressed in muscle, strongly localized to the postsynaptic NMJ, surrounding the presynaptic terminal as indicated by HRP immunoreactivity.
(g-i) The PI(4,5)P_2 reporter, when expressed in muscle, colocalized with Hts immunoreactivity, suggesting that PI(4,5)P_2 and Hts share the same postsynaptic distribution pattern.
Scale bar, 10μm.

3.8 The transmembrane engulfment receptor gene *draper* interacts with *hts*

During development and throughout the lifetime of higher order organisms, neural networks undergo continuous remodeling and refinement of their connectivity, and modulation of synaptic strength. In addition to the expansion of synaptic terminals and strengthening of synapses mentioned in the introduction, another aspect is the selective elimination of neuronal connections. This involves local disassembly of synapses and the retraction of axonal processes. This process is essential to the development of the mammalian CNS, as the excessive number of neuronal connections formed during initial network establishment mean that a target cell may be innervated by multiple neurons, and many of these connections must be pruned back until a proper level of control is achieved (Luo and O'Leary, 2005). This selective elimination of synapses and axons is partially mediated by glial cell engulfment of degenerating axons and cellular debris (Bishop *et al.*, 2004; Awasaki and Ito, 2004).

In *C. elegans*, the CED-1/CED-6 signalling pathway is critical to the engulfment process. CED-1 encodes a transmembrane receptor, whereas CED-6 encodes an adaptor protein, and disruption of either gene impairs the cell engulfment ability (Zhou *et al.*, 2001; Liu and Hengartner, 1998). The *Drosophila* gene homologues *draper (drpr)* and *ced-6* have been implicated in axonal pruning by glial cells in mushroom bodies during metamorphosis (Awasaki *et al.*, 2006). Drpr antibody staining shows postsynaptic immunoreactivity in a punctate pattern surrounding boutons at *Drosophila* NMJ, in partial colocalization with the postsynaptic protein Dlg. Larvae homozygous for $drpr^{\Delta 5}$, a putative null allele, have fewer boutons compared to wildtype (Fuentes-Medel *et al.*, 2009), suggesting a role in synaptic growth. Furthermore, a previous two-hybrid based

screen of the *Drosophila* proteome had identified Hts and Drpr as putative binding partners (Giot *et al.*, 2003). Given the morphological similarities between *hts* and *drpr* mutant NMJ, their common postsynaptic distribution, and the possibility of protein interaction, *drpr* mutants were examined to look for interactions with *hts*.

Due to stock contamination issues, it took over five months before the $drpr^{\Delta 5}$ putative null allele requested from Dr. Marc Freeman (Freeman *et al.*, 2003) was sent, and the stock is currently being rebalanced. In lieu of an available null allele, preliminary interaction studies were carried out using two uncharacterized alleles of *drpr*, $drpr^{MB06916}$ and $drpr^{HP37013}$. Each alleles contain a P-element insertion in an intron of *drpr*. Each was independently examined for changes in Hts or pAdd levels by immunostaining. NMJ from larvae homozygous for *drpr* mutant alleles showed similar Hts localization patterns compared to wildtype, but had mild decreases in Hts immunoreactivity by 17% (±22%, n=22, $p<0.01$) for $drpr^{MB06916}$, and by 17% (±12%, n=23, $p<0.001$) for $drpr^{HP37013}$ (Figure 3.10). Localization patterns for pAdd immunoreactivity were also similar to wildtype, but a small portion of $drpr^{HP37013}$ NMJ had barely detectable levels of pAdd immunoreactivity at the NMJ. Overall decreases in intensity were quantified, with $drpr^{MB06916}$ NMJ showing a 22% (±24%, n=22, $p<0.01$) decrease, and $drpr^{HP37013}$ NMJ showing a 32% (±21%, n=20, $p<0.001$) decrease (Figure 3.11). No significant differences in the size of NMJ were observed. These results indicate that proper expression of Drpr influences Hts levels and phosphorylation, however, how this is accomplished remains to be established.

In order to see whether changes in *hts* expression may affect Drpr expression or localization, attempts to examine *hts* null mutant NMJ by anti-Drpr immunostaining have been carried out. Unfortunately, there have been repeated difficulties in getting

consistent staining results with the antibody even among the wildtype samples. An alternative fixing and staining protocol will be used to troubleshoot this problem in the future.

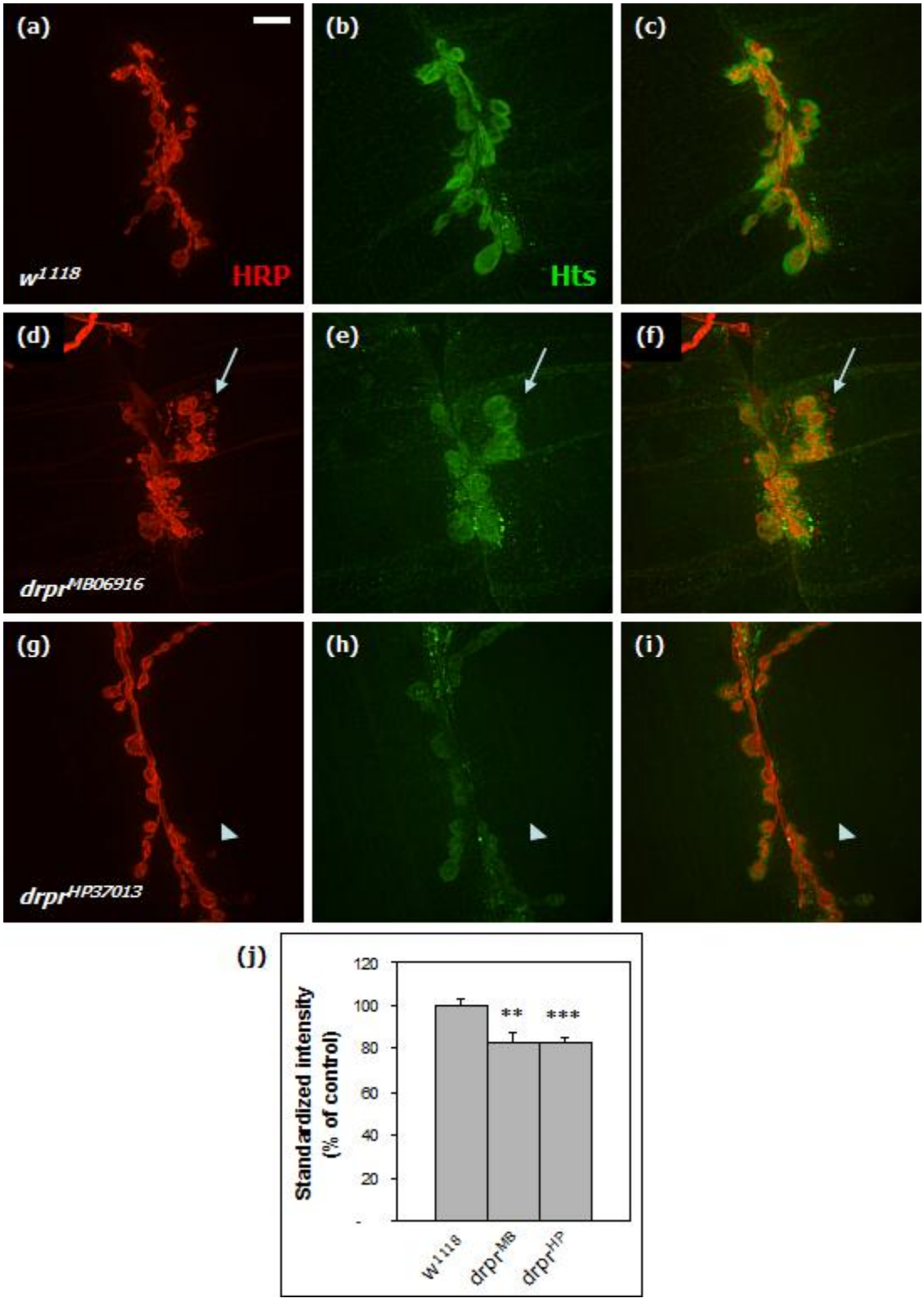
(a)
(b)
(c)
w1118
HRP
Hts
(d)
(e)
(f)
drprMB06916
(g)
(h)
(i)
drprHP37013
(j)
Standardized intensity (% of control)
120
100
80
60
40
20
-
**
***
w1118
drprMB
drprHP

Figure 3.10 *drpr* mutant NMJ show mildly decreased Hts immunoreactivity

(a-c) Wildtype NMJ show Hts immunoreactivity surrounding neuronal HRP immunoreactivity at the NMJ.
(d-i) Homozygous *drpr* mutant NMJs display similar distribution patterns, but intensity of Hts immunoreactivity is decreased. Presynaptic debris (arrow) and ghost boutons (arrowhead) in the muscle can be seen in these mutants.
(j) Quantification of Hts immunoreactivity at the NMJ shows decreases by 17% (±22%, n=22, $p<0.01$) for $drpr^{MB06916}$, and by 17% (±12%, n=23, $p<0.001$) for $drpr^{HP37013}$.
Scale bar, 10μm.

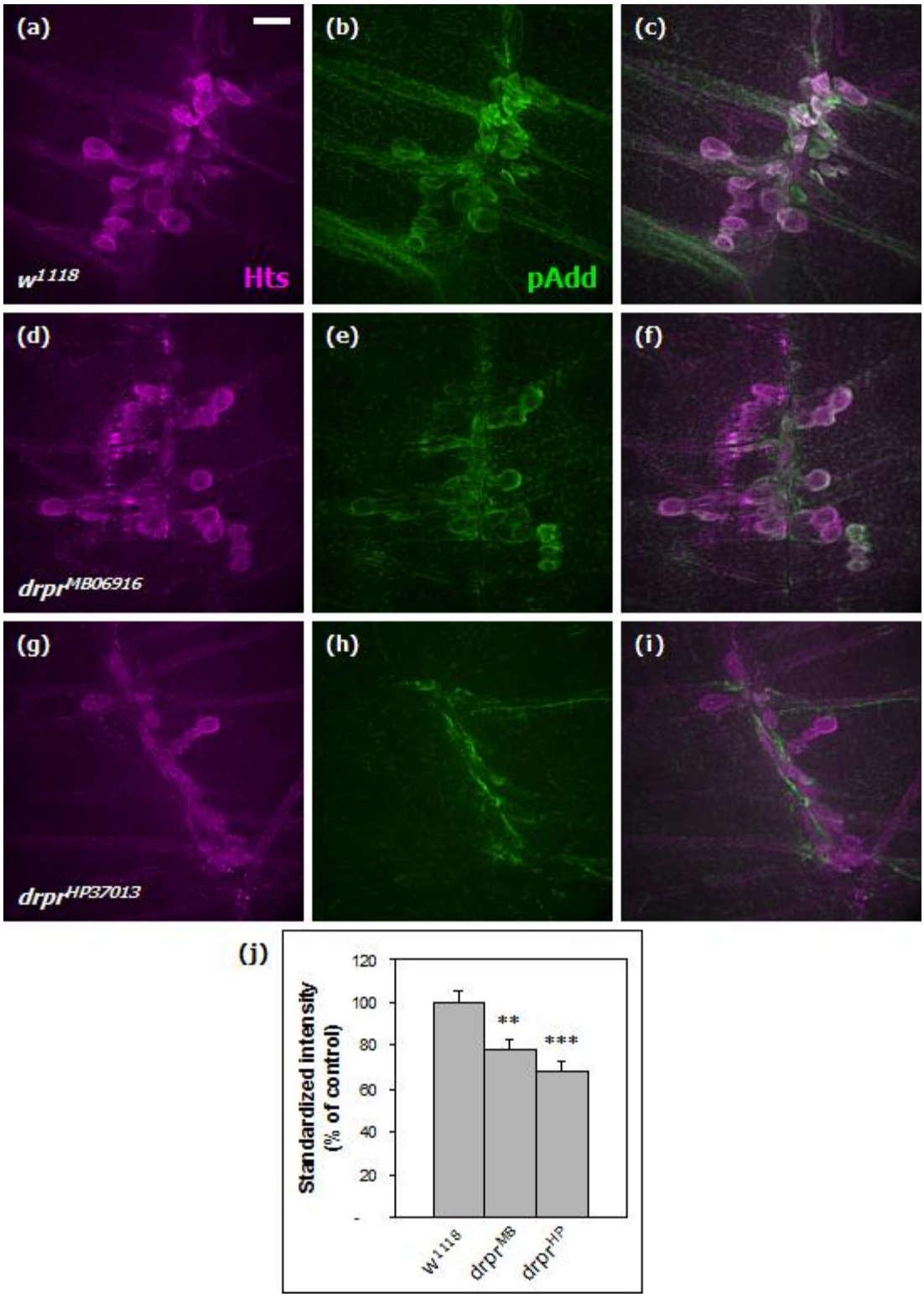
(a)
(b)
(c)
w1118
Hts
pAdd
(d)
(e)
(f)
drprMB06916
(g)
(h)
(i)
drprHP37013
(j)
Standardized intensity (% of control)
120
100
80
60
40
20
-
**
***
w1118
drprMB
drprHP

Figure 3.11 *drpr* mutant NMJ show moderate decrease in pAdd immunoreactivity

(a-c) Wildtype NMJ show colocalization of immunoreactivity against Hts and pAdd at the NMJ.
(d-i) Homozygous *drpr* mutant NMJs display similar distribution patterns, but intensity of pAdd immunoreactivity is decreased. Some $drpr^{HP37013}$ NMJ had barely detectable levels of pAdd immunoreactivity at the NMJ.
(j) Quantification of pAdd immunoreactivity at the NMJ shows decreases by 22% (±24%, n=22, $p<0.01$) for $drpr^{MB06916}$, and by 32% (±21%, n=20, $p<0.001$) for $drpr^{HP37013}$.
Scale bar, 10μm.

One of the hallmark phenotypes of the *drpr*$^{\Delta 5}$ NMJ are higher than normal levels of ghost boutons and presynaptic debris, which are neuronally derived membrane and cell fragments. In addition to debris from axonal degeneration, debris also results from shed presynaptic membrane during the course of normal synaptic growth. Ghost boutons are immature boutons that fail to become established, detach from the synaptic terminal and are subsequently degraded. Since these boutons never matured, no postsynaptic markers are seen surrounding them. Both presynaptic debris and ghost boutons are normally cleared via phagocytosis by glial and muscle cells, but loss of either Drpr or Ced-6 leads to unusually high number of ghost boutons and significant accumulation of debris around the NMJ in a halo-like pattern (Fuentes-Medel *et al.*, 2009). Traces of presynaptic debris and detached boutons, visualized by HRP immunostaining, were observed in the *drpr*^{MB06916} and *drpr*^{HP37013} mutant NMJ (Figure 3.10, arrow and arrowhead), similar to what has been previously reported for *drpr*$^{\Delta 5}$ null mutant NMJ (Fuentes-Medel *et al.*, 2009). No signs of debris or ghost boutons were seen in the wildtype NMJ. This suggests that *drpr* expression is indeed disrupted in these two *drpr* mutant alleles.

4: Discussion

4.1 A note on variability in NMJ development

Despite the rigidly defined structural layout of the neuromuscular system in *Drosophila*, the development of NMJ will naturally have a certain degree of variability even between larvae of the same genotype due to experience-dependent growth. These could be influenced by various factors such as differences in condition of the fly media and population density. As a measure to limit the external factors that could skew results, samples and controls were started at the same time using the same batch of fly media, raised at the same temperature, and only actively crawling third-instar larvae were selected for dissection. A significant number of experiments in this study were based on immunohistochemistry. To control for possible differences in fixation or immunostaining, samples and controls were processed concurrently using common master mix solutions. Based on these preventative measures, larger error bars seen in the quantifications for some of the data should reflect natural variations in development that are not caused by externally controllable factors, and should be considered reliable. All quantifications were tested for statistical significance using the Student's *t*-test.

4.2 Regulation of Hts by phosphorylation

One of the primary goals of this study was to identify factors that directly regulate Hts activity or function by altering its phosphorylation state. Based on homology to mammalian adducins, PKC and PKA were prime candidates for this role. As the immunostaining has shown, muscle-specific RNAi knockdown of *Pkc53E* was capable

of causing a very dramatic loss of pAdd immunoreactivity at the NMJ. This should only be possible if Pkc53E itself or a downstream kinase is responsible for Hts phosphorylation. As the phosphorylation levels of Hts could not be compensated by other protein kinases in the absence of Pkc53E, this suggests that Pkc53E may be a primary source of Hts S705 phosphorylation at *Drosophila* larval NMJ.

Muscle-specific RNAi knockdown of the PKA regulatory subunit gene *Pka-R2*, which should lead to an increase in PKA activity, showed increased pAdd immunoreactivity at the NMJ. This suggests that Hts could be a potential kinase target of PKA, however, it is unclear from this whether the increase in Hts S705 phosphorylation is caused by PKA or one of its downstream effectors. Collectively, these results implicate Pkc53E and PKA in the phosphorylation of Hts at its MHD (Figure 4.1).

Two additional concerns regarding these two results are as follows: (1) no verification of the effectiveness of the RNAi knockdown, (2) no evidence of direct phosphorylation by the kinases in question. Further experiments should be able to address these issues. To assess the effectiveness of the RNAi knockdown, *in situ* hybridization can be performed to examine mRNA levels, and immunoblotting against Pkc53E and Pka-R2 can be performed on larval lysates to look for decreases in protein levels. This should clarify that the observed changes in phosphorylation are specifically caused by changes in PKC/PKA gene expression. Future studies examining known mutants of *Pkc53E* and *Pka-R2* will be able to support the findings here. To examine direct phosphorylation, *in vitro* kinase assays can be carried out by expression of *hts*, *Pkc53E* and PKA catalytic subunit cDNA, and subsequent testing for phosphorylation in gel-shift assays.

The other *Drosophila* PKC genes that were tested by muscle-specific RNAi knockdown were *Pkc98E, aPKC* and *inaC*. The lack of observable changes in Hts or pAdd immunoreactivity in these cases does not conclusively mean that these genes are not involved in Hts regulation. Since the RNAi constructs were constitutively expressed in muscle, protein stability should not be an issue, however other factors such as variability in the production of siRNA can impinge on the efficacy of gene silencing. Alternative splicing of target genes may also means that some isoforms will not be affected by the siRNA. Given these limitation, the three PKC genes mentioned would have to be tested by other means, such as interaction studies using mutants, before being ruled out as upstream regulators of Hts. Note that an additional PKC gene *PKCδ* did not have available RNAi lines specific for it and therefore was not examined in this study.

The phosphorylation of mammalian adducin delocalizes it from the membrane and prevents its interaction with actin and spectrin (Gilligan *et al.*, 2002; Barkalow *et al.*, 2003). While phosphorylated Hts has a different distribution pattern from Hts (Wang *et al.*, submitted), it is yet unclear how this change in localization affects the function of phosphorylated Hts. Future studies on Hts will include examining how its phosphorylation state affects its interactions with other synaptic proteins, and how this has an impact on NMJ morphology. The creation of the wildtype and non-phosphorylable Hts transgenic lines should prove to be valuable tools in this regard. Together with the previously created phosphomimetic Hts line, comparative observations can be made to examine NMJ morphology and synaptic protein localization, such that any noted differences can be attributed to specific Hts phosphorylation states. This should provide insight into how regulation of Hts in turn affects NMJ development.

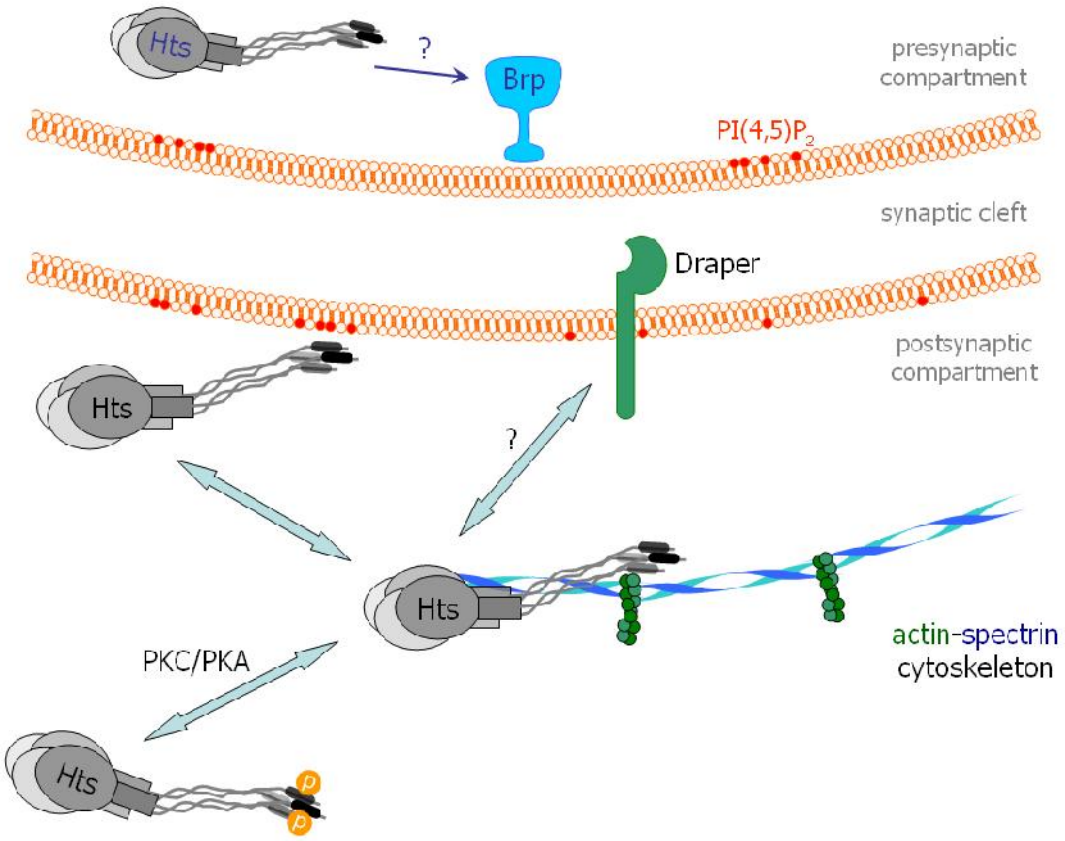

Figure 4.1 Proposed model of Hts regulation and function at the *Drosophila* larval NMJ

Add1/2 isoforms of Hts are present at the NMJ, and are required for the proper organization of the postsynaptic spectrin cytoskeleton, possibly by a spectrin-recruiting activity similar to that of mammalian adducin. Hts may also sequester the membrane phospholipid PI(4,5)P_2 by electrostatic interactions via its MHD, shielding it from other binding proteins such as Wsp, which normally restricts synaptic growth. Hts activity is regulated by phosphorylation at the MHD directly or indirectly through Pkc53E and PKA; this blocks all other interactions that require the MHD, and alters Hts interactions with postsynaptic proteins such as Dlg. The membrane receptor protein Drpr regulates postsynaptic Hts levels and phosphorylation through an unknown mechanism. Presynaptic Hts regulates the formation or stability of active zones (as detected by changes in Brp immunoreactivity) through an unknown mechanism.

4.3 Hts regulates postsynaptic spectrin organization

In mammalian cells, adducin facilitates the formation and stability of the actin-spectrin cytoskeletal network beneath the plasma membrane (Gardner and Bennett, 1987; Bennett *et al.*, 1988). The results from *hts* null mutants and overexpression suggest that Hts, the *Drosophila* homolog of adducin, may have a similar function. Loss of Hts significantly decreases α-Spectrin immunoreactivity at the NMJ, suggesting that Hts may be required for the initial recruitment of α-Spectrin to the NMJ. A few *hts* null mutant NMJ appeared to have a typical α-Spectrin distribution, albeit at lower levels than in wildtype; since NMJ formation occurs in the early embryo (Ritzenthaler *et al.*, 2000), trace amounts of maternally contributed Hts may have been sufficient for formation of the actin-spectrin cytoskeleton in these rare instances.

Overexpression of either phosphomimetic or non-phosphorylable *hts* in muscle has been shown to increase bouton number, branch number and branch length (Wang *et al.*, submitted). A similar phenotype was seen here, and the overexpression of mutant *hts* also led to a disruption of α-Spectrin localization at the NMJ; the diffuse appearance of the signal could potentially be related to a number of situations: (a) disruption or expansion of SSR organization, (b) disruption or expansion of the actin-spectrin cytoskeleton, and (c) delocalization of other scaffolding proteins.

That some boutons have partial or full coverage by α-Spectrin suggests that the NMJ may have previously had a properly developed actin-spectrin cytoskeleton that was subsequently lost or not properly maintained. Since Hts normally interacts with Spectrin, it is possible that ectopic levels of Hts in the muscle could disrupt the organization of the actin-spectrin cytoskeleton at the NMJ, leading to loss of integrity in some areas.

This diffuse appearance of α-Spectrin is reminiscent of Dlg immunoreactivity in NMJ of the same genotype (Wang *et al.*, submitted), albeit the disruption appears more severe in this case. As Dlg is a scaffolding protein, it could be the case that disruption of the actin-spectrin cytoskeleton interferes with anchoring of Dlg at the postsynaptic NMJ. Since Dlg is necessary for proper SSR development (Budnik *et al.*, 1996; Guan *et al.*, 1996), any changes to Dlg distribution may also affect SSR structure. While the specific mechanism is yet unknown, it is clear that Hts plays an important role in the maintenance of spectrin organization at the postsynaptic NMJ (Figure 4.1).

4.4 Hts regulates active zone stability

Previous studies by Schuster *et al*. involving genetically altering the level of muscle innervation showed that the neuromuscular system is capable of compensating for an abnormal number of synaptic contacts by modulating the synaptic strength, thereby giving rise to normal depolarization patterns (1996a; b). This homeostasis is accomplished by an increase in the number of active zones per bouton for hypo-innervated muscles, and a decrease in presynaptic transmitter release for hyper-innervated muscles (Stewart *et al.*, 1996; Davis and Goodman, 1998).

The gene *bruchpilot (brp)* encodes an active zone cytoskeletal matrix protein involved in the assembly and function of active zones, and is present in most if not all synapses in *Drosophila* (Kittel *et al.*, 2006; Wagh *et al.*, 2006). The decreased density and size of Brp-immunoreactive puncta detected in *hts* null mutant NMJ suggests that they may have fewer and smaller active zones (Figure 4.1), however, this would have to be verified by ultrastructural analysis. Whether this difference has an impact on synaptic

transmission characteristics would require further examination using electrophysiological measurements.

Given the effect that loss of *hts* has on Brp immunoreactivity, one might expect overexpression of Hts to produce an effect as well. Surprisingly, despite the overdeveloped NMJ that result when either phosphomimetic or non-phosphorylable Hts is overexpressed in muscle (Yang, 2008; Wang *et al.*, submitted), no difference was seen in Brp immunoreactivity in this case. Two possibilities could explain this result: (1) the point mutations in these transgenic Hts proteins may be interfering with its normal function, or (2) the effect on Brp immunoreactivity may be due to loss of presynaptic Hts, therefore postsynaptic overexpression would have no effect.

The most straightforward way to address the first point would be to examine overexpression of unmodified Hts in muscle to determine if the effect is dependent upon having S705 present. This was originally attempted using the $hts^{GS13858}$ line, prior to knowing about the endogenous GFP reporter; however, the overwhelming background in the muscle tissue made the Brp signals unquantifiable. To further examine this possibility, the new hts^{S705S} transgene can be used instead.

In regards to the second possibility, the presynaptic spectrin cytoskeleton is also critical for preserving synapse stability, and presynaptic RNAi knockdown of either α- or β-spectrin can lead to loss of synaptic proteins and neuronal retraction (Pielage *et al.*, 2005). While the effects observed here were not nearly as severe, it is plausible that loss of Hts in the null mutant partially disrupted presynaptic spectrin localization, leading to a small reduction in Brp levels. Indeed, this idea would be consistent with recent reports that the retracting boutons found in presynaptic *hts* knockdown or *hts* mutants no longer contain Brp immunoreactivity (Pielage *et al.*, 2011). To test this hypothesis, other

active zone and presynaptic proteins can be examined in *hts* null mutants to verify if there is disruption to the organization of synapses. Presynaptic overexpression of *hts* transgenes using neuron-specific drivers can also be attempted to look for changes in presynaptic protein levels or distribution.

4.5 Hts may have a role in the sequestration of $PI(4,5)P_2$

Another potential interaction partner for Hts is the phospholipid $PI(4,5)P_2$, which has recently been reported to act as a negative regulator of NMJ growth, via the activation of Wiscott-Aldrich Syndrome protein (WASP; *wsp*) and Arp2/3 complex. Neuronal expression of the PH domain in a similar *in vivo* reporter has also been shown to sequester $PI(4,5)P_2$ and de-repress NMJ development (Khuong *et al.*, 2010). No obvious differences in NMJ development were observed with reporter expression in this study, possibly due to the weaker neuronal driver that is being used here. Since *hts* null mutants also exhibit underdeveloped NMJ, if Hts is truly capable of binding to $PI(4,5)P_2$, this could be a signalling mechanism through which it is acting (Figure 4.1). Genetic interaction studies between *hts* and *wsp*, which functions downstream of $PI(4,5)P_2$ in the signalling cascade (Khuong *et al.*, 2010), will help shed light on how Hts exerts its effect on NMJ development.

In this study, $PI(4,5)P_2$ immunoreactivity was observed along the presynaptic NMJ membrane as punctate domains exclusive of the presynaptic epitope that cross-reacts with anti-HRP antibody, suggesting that $PI(4,5)P_2$ may be localized to specific lipid microdomains. This is consistent with previous reports that a portion of cellular $PI(4,5)P_2$ is indeed compartmentalized in lipid rafts (Pike and Miller, 1998), and that $PI(4,5)P_2$ is enriched at mouse neuron nerve terminals where it regulates synaptic

vesicle endocytosis (Cremona *et al.*, 1999). An alternative (although not conflicting) explanation is that the PI(4,5)P_2 may be clustered via interactions with PI(4,5)P_2-binding proteins, as is the case with MARCKS and related proteins in mammalian neurons (Ouimet *et al.*, 1990; Yamaguchi *et al.*, 2009). Whether this is the case at *Drosophila* NMJ with Hts or other proteins is not yet clear.

Studies *in vitro* suggests that MHDs with sufficient polybasic residues should be capable of binding to PI(4,5)P_2 via electrostatic interactions (Wang *et al.*, 2002). Other proteins such as Neuralized have also been shown to bind to membrane phospholipids through a polybasic region (Skwarek *et al.*, 2007). While direct binding to PI(4,5)P_2 by Hts has not been demonstrated in this work, sequence alignment shows that polybasic residues are conserved in Hts (Figure 1.4B), and the evidence from the *in vivo* reporter indicates that PI(4,5)P_2 and Hts at least physically share the same postsynaptic distribution, where such an interaction could occur. Previous studies have used commercially available PIP Strips (Echelon Biosciences Inc) to assess the phospholipid binding ability of proteins (Skwarek *et al.*, 2007). These membrane strips are pre-spotted with a variety of common lipid and phospholipid species (*e.g.* PI(3,5)P_2, PI(4,5)P_2, PI(3,4,5)P_3 *etc.*), such that binding ability can be determine in a very species-specific manner. A separate PIP Assay strip contains a series of spots with diminishing concentration for each phospholipid, such that specific binding affinity for a phospholipid can be calculated. These tools will be used to directly examine the ability of Hts to bind to PI(4,5)P_2 *in vitro*.

The binding of mammalian MARCKS protein to PI(4,5)P_2, along with the insertion of its myristoylated N-terminus into the lipid bilayer, physically anchor MARCKS protein to the membrane. Disruption of either one of these interactions strongly diminishes

membrane association of MARCKS protein (McLaughlin and Aderem, 1995). It is still unknown whether a PI(4,5)P_2 interaction with Hts, should it exist, would help to anchor Hts near the postsynaptic NMJ; however, such an interaction would likely be exclusive of other Hts cellular functions, since research on MARCKS protein shows that phosphorylation by PKC or binding to calmodulin antagonizes its ability to bind to PI(4,5)P_2, either by changing the net charge of the binding sequence or by occluding it altogether (Swierczynski and Blackshear, 1996). This is consistent with the displacement of phosphorylated adducin away from the membrane into the cytosol (Gilligan *et al.*, 2002; Barkalow *et al.*, 2003); however, a significant portion of phosphorylated Hts appears to remain at the postsynaptic NMJ, which suggests that there may be other factors or interacting partners that keep it localized in that area.

An interesting difference between the PI(4,5)P_2 antibody and *in vivo* reporter is that postsynaptic signal is observed with the reporter but not in the immunostainings. PI(4,5)P_2 is a relatively small molecule, and the only specific distinction between PI(4,5)P_2 and related phosphoinositide species is the number and location of phosphate groups in the inositol ring at its polar head. The anti-PI(4,5)P_2 antibody used is very specific to this phospholipid species; however, under cellular conditions, it will only be able to bind the polar head of an exposed PI(4,5)P_2 molecule. If PI(4,5)P_2 is being shielded by bound proteins in the fixed samples, the antibody would not able to bind; however, since the reporter is expressed in live tissue, it should be able to competitively bind to PI(4,5)P_2 if other protein interactions are transient. No postsynaptic immunoreactivity was observed while the reporter indicates that PI(4,5)P_2 is indeed present at the postsynaptic NMJ. This suggests that under normal circumstances,

without the ectopic expression of a reporter, postsynaptic PI(4,5)P_2 is bound to proteins. Whether Hts is one of these proteins is not yet certain.

Further experiments to examine this possibility include testing whether overexpression of the reporter can compensate for loss of *hts* in a null mutant background. If the *hts* null mutant phenotypes are partly due to loss of occlusion of PI(4,5)P_2, overexpression of the PI(4,5)P_2 reporter in the same background should be able to result in a partial rescue. For this purpose, recombination between the *hts* null allele and PI(4,5)P_2 reporter has already been carried out, however the putative recombinants require validation to confirm the presence of both elements.

It is also of interest to see whether overexpression of the reporter would be able to compete with native Hts for PI(4,5)P_2-binding, and whether this has any effect on Hts localization at the NMJ. Comparative analysis of Hts immunostainings in wildtype, reporter overexpression, and reporter expression in *hts* null background would be able to address this issue.

4.6 Interaction between *hts* and *drpr*

The final candidate as an interaction partner for Hts that was examined is Draper, which is the *Drosophila* homolog of nematode CED-1, a transmembrane receptor required for the engulfment activity of glia and muscle cells. Previous reports have shown that $drpr^{\Delta 5}$ null mutant NMJ display ghost boutons and high levels of presynaptic debris that are not normally seen around the NMJ (Fuentes-Medel *et al.*, 2009). In this study, signs of presynaptic debris and ghost boutons were observed at the NMJ from larvae homozygous for either of two uncharacterized *drpr* alleles. This confirms that these *drpr* alleles indeed have decreased function, as these engulfment

defects are almost never seen at wildtype NMJ. *drpr*$^{\Delta 5}$ null mutants also have underdeveloped NMJ (Fuentes-Medel *et al.*, 2009), but the lack of any significant difference in NMJ size observed here suggests that these uncharacterized *drpr* alleles are only hypomorphs, and may still have residual expression and function.

The preliminary search for an interaction between *hts* and *drpr* showed small but statistically significant decreases in both Hts and pAdd immunoreactivity at the NMJ in larvae homozygous for either of two *drpr* hypomorphic alleles. This suggests that the expression levels or stability of Hts and phosphorylated Hts may partially depend upon Drpr (Figure 4.1), which was previously shown to be localized that the postsynaptic NMJ (Fuentes-Medel *et al.*, 2009). Since these *drpr* alleles have not been fully characterized, it cannot be concluded whether the changes observed here are due to decreased *drpr* expression levels, or the expression of either truncated or incorrectly spliced forms of Drpr. Once the *drpr*$^{\Delta 5}$ null allele stock is available for use, immunostainings against Hts and pAdd can be done to confirm these results, and resolve the uncertainty as to whether the observed changes are due to loss of *drpr*.

In further support of an interaction between *hts* and *drpr*, *hts* null mutant NMJ were also observed to have signs of increased presynaptic debris compared to wildtype NMJ, suggesting a disruption to cell engulfment abilities in *hts* null mutants; however, the degree of difference in debris amounts compared to *drpr*$^{\Delta 5}$ null mutants has not yet been quantified (Mannan Wang, personal communication). Testing for changes in Drpr immunoreactivity in *hts* null mutants will help establish if the interaction is bidirectional, and the increased presynaptic debris observed in *hts* null mutants supports this idea.

Since the *in vitro* data suggests that Hts and Drpr may be binding partners (Giot *et al.*, 2003), and both proteins localize to the postsynaptic NMJ (Yang, 2008; Fuentes-

Medel *et al.*, 2009), future studies will also be aimed at examining whether a physical interaction occurs between the two proteins by using coimmunoprecipitation assays.

4.7 Calpain as a speculative regulator of synaptic protein levels at the NMJ

Calpains are calcium-dependent cysteine endopeptidases that are expressed in many cell types including neurons and glia. Mammalian studies have demonstrated that calpains cleave many cellular target substrates, among which are PSD-95 (mammalian homolog of Dlg), N-CAM (mammalian homolog of Fas2), CaMKII, PKC and α-Spec. The activation of calpain disrupts the integrity of the actin-spectrin cytoskeleton and postsynaptic assemblies, and is proposed to facilitate membrane insertion of glutamate receptors and dendritic spine reorganization, which are critical for LTP induction and memory formation. Calpains require Ca^{2+} for self-activation, but prior to that, autolysis causes conformational changes that primes the protein for Ca^{2+} binding (Zadran *et al.*, 2010).

Of note is that the Ca^{2+} concentrations required for calpain-2 activation are beyond what is normally seen in the cell. As such, it has been previously proposed that association with $PI(4,5)P_2$, either via intrinsically unstructured domains on calpain or through another binding protein, positions calpain in closer proximity to calcium channels at the membrane, allowing for a greater likelihood of activation (Shao *et al.*, 2006; Sprague *et al.*, 2008).

Previous immunohistochemistry studies at the NMJ involving muscle-specific overexpression of *hts* have shown that immunoreactivity against several proteins are strongly increased in muscle: Fas2, CaMKII, PAR-1, pAdd and pDlg, and some of these changes have since been verified by immunoblotting (Wang *et al.*, submitted). Notably,

many of these are known cleavage substrates of mammalian calpains. In fact, one of the most commonly used assays for detecting and measuring calpain activity is testing for the presence of α-Spectrin breakdown products (SBDP), two protein fragments of 150 and 145 kDa that result from calpain cleavage (Siman and Noszek, 1988).

The two functional *Drosophila* calpains, CalpA and CalpB, are both expressed in stage L3 larvae, and CalpB (homolog of calpain-2) has been shown to be expressed in the larval CNS (Chintapalli *et al.*, 2007). Together with the hypothesis that $PI(4,5)P_2$-binding enhances calpain activation, a speculative model is presented in Figure 4.2 where Hts could be sequestering free $PI(4,5)P_2$, thereby inhibiting calpain activation. The resultant decrease in calpain proteolytic activity thus could lead to the observed increase in the levels of calpain substrates.

Future studies to test this model will involve looking for a correlation between Hts levels and calpain activation. Extracts from larvae of *hts* null mutants or with overexpressed Hts transgenes can be examined for calpain activity by assaying for the presence and levels of SBDP. As the $PH_{PLC\delta}$-GFP reporter should also be capable of secluding $PI(4,5)P_2$, it may also be used as a control for comparison.

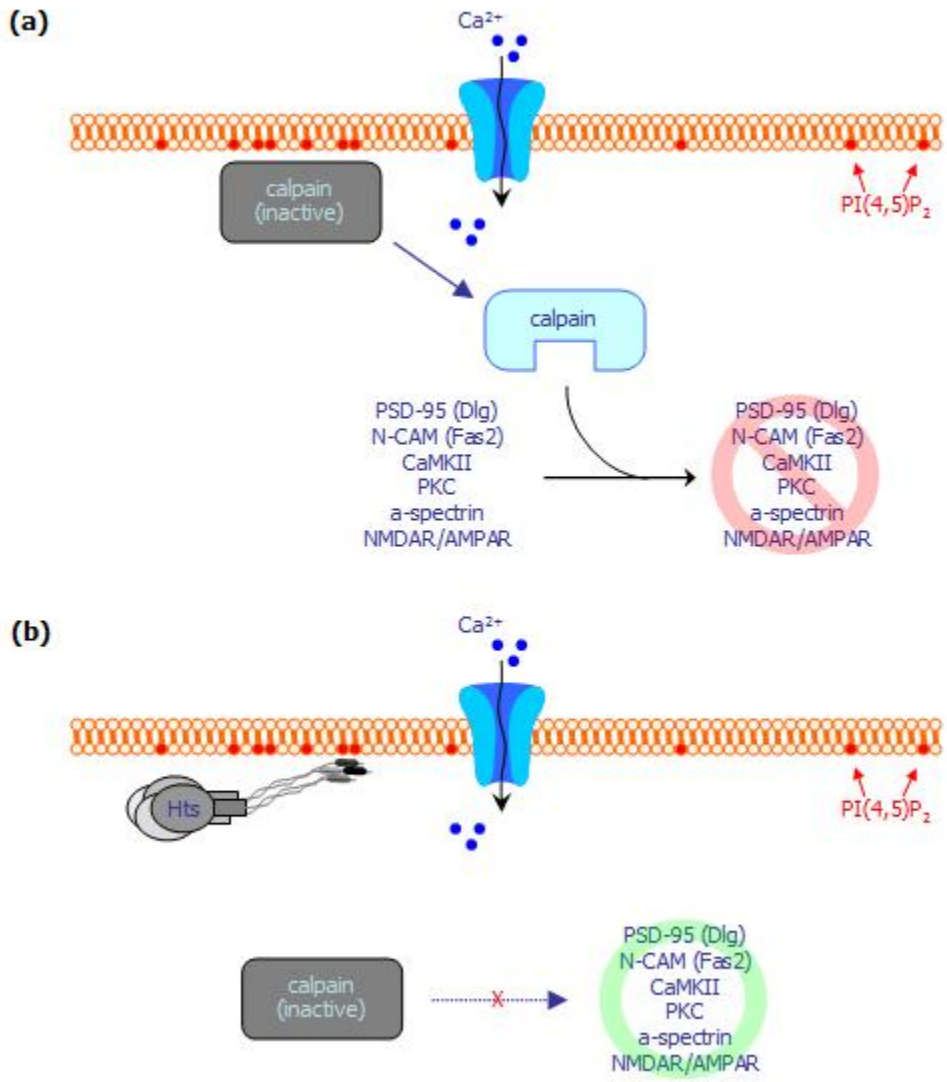

Figure 4.2 Speculative Model: Hts inhibits Calpain activation by sequestering $PI(4,5)P_2$

(a) Inactive calpain associates with membrane $PI(4,5)P_2$; the closer proximity to Ca^{2+} channels raises Ca^{2+} exposure, which enhances calpain activation; active calpain degrades many synaptic proteins.
(b) Hts sequesters $PI(4,5)P_2$ by binding via its MARCKS-homology domain, shielding $PI(4,5)P_2$ from calpain; inactive calpain cannot degrade target proteins, leading to increased protein levels.

5: Concluding remarks

In an effort to better understand the regulation of Hts expression and activity at the NMJ, an examination of potential interaction partners by muscle-specific gene silencing has uncovered two genes that alter postsynaptic Hts phosphorylation levels: the conventional PKC gene *Pkc53E* and the PKA regulatory subunit gene *Pka-R2*. Hts was found to be required for proper organization of postsynaptic α-spectrin and the presynaptic active zone. An *in vivo* reporter has demonstrated the presence of the phospholipid PI(4,5)P_2 at the postsynaptic NMJ where it could potentially interact with Hts. Finally, the membrane receptor gene *draper* was shown to genetically interact with *hts* (Figure 4.1).

Previous characterizations of Hts function at the NMJ have established a role for it in NMJ development (Yang, 2008; Wang *et al.*, submitted), however, what regulates Hts activity or how it brings about these changes at the NMJ were not entirely clear. The results from this study identify two putative kinases that could restrict Hts activity, and several promising interaction partners that all have previously demonstrated roles at the NMJ, through which Hts could be influencing NMJ development. This opens up possibilities for many follow-up studies to validate these results, and to further probe the signalling mechanisms involved therein.

Since adducin misregulation has been implicated in the neurodegenerative disease ALS, it would be of interest to see whether overexpression of phosphomimetic *hts* in either neurons or muscles could lead to motor defects in older adult flies, which

could be assessed by flight and crawling assays. Given the high degree of sequence conservation between Hts and mammalian adducin, and the findings here suggesting that Hts may function in a manner similar to adducin, it is likely that at least part of our understanding into Hts regulation and function at the NMJ may be extrapolated to help shed light on the role of adducin in mammalian neuronal development and disease.

Appendices

Appendix A: Primers used for mutagenesis, PCR and sequencing

Primer Name	Sequence	Purpose	Notes
HtsR1-D835S-F	gaagggtctgcgcacaccaagcttttgaaaaagaagaagg	Create wildtype *hts* transgene	Nucleotides corresponding to S705 underlined
HtsR1-D835S-R	ccttcttctttttcaaaaagcttggtgtgcgcagacccttc		
HtsR1-D835A-F	gggtctgcgcacaccagcctttttgaaaaagaagaa	Create non-phosphorylable *hts* transgene	
HtsR1-D835A-R	ttcttctttttcaaaaaggctggtgtgcgcagaccc		
HtsPI-528-F	gcaaggacagattgtggagca	Sequencing primers for *pUAST-hts* constructs	Hts-PI cDNA from Flybase
HtsPI-1238-F	cagctgtttcatcactgggct		
pUAST-259-F	gcgcagctgaacaagctaaac		145 bp from EcoRI
pUAST-640-R	ccaccactgctcccattcatc		175 bp from XhoI
dlg1-S48A-F	gagcgcggcaacgccggattgggct	Create doubly non-phosphorylable *dlg* transgene	Nucleotides corresponding to S48 underlined
dlg1-S48A-R	agcccaatccggcgttgccgcgctc		
eGFP-614-F	gacaaccactacctgagcacc	Sequencing primers for *eGFP-dlg* constructs	
dlg1B-728-F	cctccatctacatcaccaag		
dlg1B-2339-R	gtgtagttgatggacaaacg		
4-EagI-GFPdlg-F	taagcggccggaatagggaattgggaatc	PCR primers for subcloning	added EagI site underlined
GFPdlg-R	cgactcactatagggcgaat		

Appendix B: Transgenic stocks received from BestGene Inc

Completed vectors were sent out to BestGene Inc. for embryo injection service. Lists of returned transgenic stocks are shown below, along with the chromosome where insertion occurred. The exact cytological locations for the doubly non-phosphorylable Dlg1 stocks will be known due to the targeted insertion method (see Section 2.2.2); however, the injection and balancing is still in progress, and these transgenic stocks have not yet been received.

Vector	**BestGene Inc Order/Ref #**	**Line # and sex of G_1 adult**	**Chromosome: cytological loc.**
pUAST-HtsR1-WT-A (hts^{S705S})	5881-1	1M	2nd
		2M	2nd
		3M	3rd
		4M	2nd
		5M	2nd
		6M	2nd
		7F	2nd
		8F	3rd
pUAST-HtsR1-DA-B (hts^{S705A})	5881-2	1M	3rd
		2M	2nd
		3M	2nd
		4M	2nd
		5M	3rd
		6M	2nd
		7M	3rd
		8M	2nd
		9M	3rd
pUAST.attB-eGFP-dlg1^{S48A,S797A}	7920-1	Not yet received	3rd: 86Fb
	7920-2	Not yet received	2nd: 22A
	7920-3	Not yet received	X: 2A

Appendix C: Summary of results for RNAi knockdown studies

Expression of a *UAS-RNAi* construct directed against each target gene was induced by using a muscle-specific driver (*mef2-GAL4*) at 29°C. Third-instar larvae were dissected and body walls were immunostained with anti-1B1 (Hts) and anti-pAdd. NMJ were then examined by confocal microscopy. Changes in immunoreactivity levels were recorded and are shown below, denoted by positive and negative signs, or n.c. for no change.

Gene	**Stock number**	**Change in Hts immunoreactivity**	**Change in pAdd immunoreactivity**
Pkc53E	CG6622R-2 ; 27696	n.c.	----
Pkc98E	33434	n.c.	n.c.
	108151	n.c.	n.c.
aPKC	105624	n.c.	n.c.
InaC (eye-PKC)	2894	n.c.	n.c.
	101719	n.c.	n.c.
Pka-C1	101524	n.c.	n.c.
Pka-R2	39436	n.c.	n.c.
	101763	n.c.	++
rok (Rho-kinase)	104675	n.c.	n.c.
Cam (calmodulin)	28242	n.c.	n.c.
	109037	n.c.	n.c.
PIP5K59B	47027	n.c.	n.c.
	47029	n.c.	n.c.
	108104	n.c.	n.c.
fab1 (PI3P5K)	27591	n.c.	n.c.

Reference List

Adams, M D, S E Celniker, R A Holt, C A Evans, J D Gocayne, P G Amanatides*, et al.* (2000). "The genome sequence of Drosophila melanogaster." Science **287**(5461): 2185-2195.

Anong, W A, T Franco, H Chu, T L Weis, E E Devlin, D M Bodine*, et al.* (2009). "Adducin forms a bridge between the erythrocyte membrane and its cytoskeleton and regulates membrane cohesion." Blood **114**(9): 1904-1912.

Arbuzova, A, A A Schmitz and G Vergeres (2002). "Cross-talk unfolded: MARCKS proteins." Biochem J **362**(Pt 1): 1-12.

Atwood, H L, C K Govind and C F Wu (1993). "Differential ultrastructure of synaptic terminals on ventral longitudinal abdominal muscles in Drosophila larvae." J Neurobiol **24**(8): 1008-1024.

Awasaki, T and K Ito (2004). "Engulfing action of glial cells is required for programmed axon pruning during Drosophila metamorphosis." Curr Biol **14**(8): 668-677.

Awasaki, T, R Tatsumi, K Takahashi, K Arai, Y Nakanishi, R Ueda*, et al.* (2006). "Essential role of the apoptotic cell engulfment genes draper and ced-6 in programmed axon pruning during Drosophila metamorphosis." Neuron **50**(6): 855-867.

Baines, A J and J C Pinder (2005). "The spectrin-associated cytoskeleton in mammalian heart." Front Biosci **10**: 3020-3033.

Barkalow, K L, J E Italiano, Jr., D E Chou, Y Matsuoka, V Bennett and J H Hartwig (2003). "Alpha-adducin dissociates from F-actin and spectrin during platelet activation." J Cell Biol **161**(3): 557-570.

Bate, M (1990). "The embryonic development of larval muscles in Drosophila." Development **110**(3): 791-804.

Bateman, J R, A M Lee and C T Wu (2006). "Site-specific transformation of Drosophila via phiC31 integrase-mediated cassette exchange." Genetics **173**(2): 769-777.

Bayat, V, M Jaiswal and H J Bellen (2011). "The BMP signaling pathway at the Drosophila neuromuscular junction and its links to neurodegenerative diseases." Curr Opin Neurobiol **21**(1): 182-188.

Bellen, H J and V Budnik (2000). The neuromuscular junction. Drosophila Protocols. W Sullivan, M Ashburner and R S Hawley. Cold Spring Harbor, New York, Cold Spring Harbor Library Press.

Bennett, V and A J Baines (2001). "Spectrin and ankyrin-based pathways: metazoan inventions for integrating cells into tissues." Physiol Rev **81**(3): 1353-1392.

Bennett, V, K Gardner and J P Steiner (1988). "Brain adducin: a protein kinase C substrate that may mediate site-directed assembly at the spectrin-actin junction." J Biol Chem **263**(12): 5860-5869.

Bennett, V and D M Gilligan (1993). "The spectrin-based membrane skeleton and micron-scale organization of the plasma membrane." Annu Rev Cell Biol **9**: 27-66.

Berridge, M J and R F Irvine (1984). "Inositol trisphosphate, a novel second messenger in cellular signal transduction." Nature **312**(5992): 315-321.

Bischof, J, R K Maeda, M Hediger, F Karch and K Basler (2007). "An optimized transgenesis system for Drosophila using germ-line-specific phiC31 integrases." Proc Natl Acad Sci U S A **104**(9): 3312-3317.

Bishop, D L, T Misgeld, M K Walsh, W B Gan and J W Lichtman (2004). "Axon branch removal at developing synapses by axosome shedding." Neuron **44**(4): 651-661.

Blackshear, P J (1993). "The MARCKS family of cellular protein kinase C substrates." J Biol Chem **268**(3): 1501-1504.

Boillee, S, C Vande Velde and D W Cleveland (2006). "ALS: a disease of motor neurons and their nonneuronal neighbors." Neuron **52**(1): 39-59.

Broadie, K and M Bate (1993a). "Innervation directs receptor synthesis and localization in Drosophila embryo synaptogenesis." Nature **361**(6410): 350-353.

Broadie, K S and M Bate (1993b). "Development of the embryonic neuromuscular synapse of Drosophila melanogaster." J Neurosci **13**(1): 144-166.

Budnik, V (1996). "Synapse maturation and structural plasticity at Drosophila neuromuscular junctions." Curr Opin Neurobiol **6**(6): 858-867.

Budnik, V, Y H Koh, B Guan, B Hartmann, C Hough, D Woods*, et al.* (1996). "Regulation of synapse structure and function by the Drosophila tumor suppressor gene dlg." Neuron **17**(4): 627-640.

Burns, M E and G J Augustine (1995). "Synaptic structure and function: dynamic organization yields architectural precision." Cell **83**(2): 187-194.

Byers, T J and D Branton (1985). "Visualization of the protein associations in the erythrocyte membrane skeleton." Proc Natl Acad Sci U S A **82**(18): 6153-6157.

Cantera, R and D R Nassel (1992). "Segmental peptidergic innervation of abdominal targets in larval and adult dipteran insects revealed with an antiserum against leucokinin I." Cell Tissue Res **269**(3): 459-471.

Chakravarthy, B, P Morley and J Whitfield (1999). "Ca2+-calmodulin and protein kinase Cs: a hypothetical synthesis of their conflicting convergences on shared substrate domains." Trends Neurosci **22**(1): 12-16.

Chang, H C, D N Dimlich, T Yokokura, A Mukherjee, M W Kankel, A Sen*, et al.* (2008). "Modeling spinal muscular atrophy in Drosophila." PLoS One **3**(9): e3209.

Chen, K and D E Featherstone (2005). "Discs-large (DLG) is clustered by presynaptic innervation and regulates postsynaptic glutamate receptor subunit composition in Drosophila." BMC Biol **3**: 1.

Chen, K, C Merino, S J Sigrist and D E Featherstone (2005). "The 4.1 protein coracle mediates subunit-selective anchoring of Drosophila glutamate receptors to the postsynaptic actin cytoskeleton." J Neurosci **25**(28): 6667-6675.

Chiba, A, P Snow, H Keshishian and Y Hotta (1995). "Fasciclin III as a synaptic target recognition molecule in Drosophila." Nature **374**(6518): 166-168.

Chintapalli, V R, J Wang and J A Dow (2007). "Using FlyAtlas to identify better Drosophila melanogaster models of human disease." Nat Genet **39**(6): 715-720.

Citterio, L, C Lanzani, P Manunta and G Bianchi (2010). "Genetics of primary hypertension: the clinical impact of adducin polymorphisms." Biochim Biophys Acta **1802**(12): 1285-1298.

Consortium, I H G S (2004). "Finishing the euchromatic sequence of the human genome." Nature **431**(7011): 931-945.

Cremona, O, G Di Paolo, M R Wenk, A Luthi, W T Kim, K Takei*, et al.* (1999). "Essential role of phosphoinositide metabolism in synaptic vesicle recycling." Cell **99**(2): 179-188.

Davis, G W and C S Goodman (1998). "Synapse-specific control of synaptic efficacy at the terminals of a single neuron." Nature **392**(6671): 82-86.

de Bivort, B L, H F Guo and Y Zhong (2009). "Notch signaling is required for activity-dependent synaptic plasticity at the Drosophila neuromuscular junction." J Neurogenet **23**(4): 395-404.

de Cuevas, M, J K Lee and A C Spradling (1996). "alpha-spectrin is required for germline cell division and differentiation in the Drosophila ovary." Development **122**(12): 3959-3968.

Dietzl, G, D Chen, F Schnorrer, K C Su, Y Barinova, M Fellner*, et al.* (2007). "A genome-wide transgenic RNAi library for conditional gene inactivation in Drosophila." Nature **448**(7150): 151-156.

Ding, D, S M Parkhurst and H D Lipshitz (1993). "Different genetic requirements for anterior RNA localization revealed by the distribution of Adducin-like transcripts during Drosophila oogenesis." Proc Natl Acad Sci U S A **90**(6): 2512-2516.

Dong, L, C Chapline, B Mousseau, L Fowler, K Ramsay, J L Stevens*, et al.* (1995). "35H, a sequence isolated as a protein kinase C binding protein, is a novel member of the adducin family." J Biol Chem **270**(43): 25534-25540.

Fabian, L, H C Wei, J Rollins, T Noguchi, J T Blankenship, K Bellamkonda*, et al.* (2010). "Phosphatidylinositol 4,5-bisphosphate directs spermatid cell polarity and exocyst localization in Drosophila." Molecular Biology of the Cell **21**(9): 1546-1555.

Foster, J L, J J Guttman, L M Hall and O M Rosen (1984). "Drosophila cAMP-dependent protein kinase." J Biol Chem **259**(21): 13049-13055.

Fowler, L, J Everitt, J L Stevens and S Jaken (1998). "Redistribution and enhanced protein kinase C-mediated phosphorylation of alpha- and gamma-adducin during renal tumor progression." Cell Growth Differ **9**(5): 405-413.

Frasch, M (1999). "Controls in patterning and diversification of somatic muscles during Drosophila embryogenesis." Curr Opin Genet Dev **9**(5): 522-529.

Freeman, M R, J Delrow, J Kim, E Johnson and C Q Doe (2003). "Unwrapping glial biology: Gcm target genes regulating glial development, diversification, and function." Neuron **38**(4): 567-580.

Fuentes-Medel, Y, M A Logan, J Ashley, B Ataman, V Budnik and M R Freeman (2009). "Glia and muscle sculpt neuromuscular arbors by engulfing destabilized synaptic boutons and shed presynaptic debris." PLoS Biol **7**(8): e1000184.

Gaidarov, I and J H Keen (1999). "Phosphoinositide-AP-2 interactions required for targeting to plasma membrane clathrin-coated pits." J Cell Biol **146**(4): 755-764.

Gardner, K and V Bennett (1987). "Modulation of spectrin-actin assembly by erythrocyte adducin." Nature **328**(6128): 359-362.

Gilligan, D M, R Sarid and J Weese (2002). "Adducin in platelets: activation-induced phosphorylation by PKC and proteolysis by calpain." Blood **99**(7): 2418-2426.

Giot, L, J S Bader, C Brouwer, A Chaudhuri, B Kuang, Y Li*, et al.* (2003). "A protein interaction map of Drosophila melanogaster." Science **302**(5651): 1727-1736.

Glaser, M, S Wanaski, C A Buser, V Boguslavsky, W Rashidzada, A Morris*, et al.* (1996). "Myristoylated alanine-rich C kinase substrate (MARCKS) produces reversible inhibition of phospholipase C by sequestering phosphatidylinositol 4,5-bisphosphate in lateral domains." J Biol Chem **271**(42): 26187-26193.

Gorczyca, M, C Augart and V Budnik (1993). "Insulin-like receptor and insulin-like peptide are localized at neuromuscular junctions in Drosophila." J Neurosci **13**(9): 3692-3704.

Gorczyca, M and V Budnik (2006). "Appendix: Anatomy of the larval body wall muscles and NMJs in the third larval stage." Int Rev Neurobiol **75**: 367-373.

Guan, B, B Hartmann, Y H Kho, M Gorczyca and V Budnik (1996). "The Drosophila tumor suppressor gene, dlg, is involved in structural plasticity at a glutamatergic synapse." Curr Biol **6**(6): 695-706.

Harlan, D M, J M Graff, D J Stumpo, R L Eddy, Jr., T B Shows, J M Boyle*, et al.* (1991). "The human myristoylated alanine-rich C kinase substrate (MARCKS) gene (MACS). Analysis of its gene product, promoter, and chromosomal localization." J Biol Chem **266**(22): 14399-14405.

Hartwig, J H, G M Bokoch, C L Carpenter, P A Janmey, L A Taylor, A Toker*, et al.* (1995). "Thrombin receptor ligation and activated Rac uncap actin filament barbed ends through phosphoinositide synthesis in permeabilized human platelets." Cell **82**(4): 643-653.

Herget, T, S A Oehrlein, D J Pappin, E Rozengurt and P J Parker (1995). "The myristoylated alanine-rich C-kinase substrate (MARCKS) is sequentially phosphorylated by conventional, novel and atypical isotypes of protein kinase C." Eur J Biochem **233**(2): 448-457.

Hoang, B and A Chiba (2001). "Single-cell analysis of Drosophila larval neuromuscular synapses." Dev Biol **229**(1): 55-70.

Hoy, R R. (2006, 2007). "Project Fruitfly: Genetic Dissection of Neural Systems and Behaviour." from http://hoylab.cornell.edu/fruitfly/shaker/physiology/.

Hu, J H, H Zhang, R Wagey, C Krieger and S L Pelech (2003). "Protein kinase and protein phosphatase expression in amyotrophic lateral sclerosis spinal cord." J Neurochem **85**(2): 432-442.

Huang, F L and K P Huang (1991). "Interaction of protein kinase C isozymes with phosphatidylinositol 4,5-bisphosphate." J Biol Chem **266**(14): 8727-8733.

Hughes, W E, R Woscholski, F T Cooke, R S Patrick, S K Dove, N Q McDonald*, et al.* (2000). "SAC1 encodes a regulated lipid phosphoinositide phosphatase, defects in which can be suppressed by the homologous Inp52p and Inp53p phosphatases." J Biol Chem **275**(2): 801-808.

Jan, L Y and Y N Jan (1976). "L-glutamate as an excitatory transmitter at the Drosophila larval neuromuscular junction." J Physiol **262**(1): 215-236.

Jan, L Y and Y N Jan (1982). "Antibodies to horseradish peroxidase as specific neuronal markers in Drosophila and in grasshopper embryos." Proc Natl Acad Sci U S A **79**(8): 2700-2704.

Jia, X X, M Gorczyca and V Budnik (1993). "Ultrastructure of neuromuscular junctions in Drosophila: comparison of wild type and mutants with increased excitability." J Neurobiol **24**(8): 1025-1044.

Johansen, J, M E Halpern, K M Johansen and H Keshishian (1989a). "Stereotypic morphology of glutamatergic synapses on identified muscle cells of Drosophila larvae." J Neurosci **9**(2): 710-725.

Johansen, J, M E Halpern and H Keshishian (1989b). "Axonal guidance and the development of muscle fiber-specific innervation in Drosophila embryos." J Neurosci **9**(12): 4318-4332.

Joshi, R, D M Gilligan, E Otto, T McLaughlin and V Bennett (1991). "Primary structure and domain organization of human alpha and beta adducin." J Cell Biol **115**(3): 665-675.

Keleman, K and B J Dickson (2001). "Short- and long-range repulsion by the Drosophila Unc5 netrin receptor." Neuron **32**(4): 605-617.

Keshishian, H and A Chiba (1993). "Neuromuscular development in Drosophila: insights from single neurons and single genes." Trends Neurosci **16**(7): 278-283.

Keshishian, H and Y S Kim (2004). "Orchestrating development and function: retrograde BMP signaling in the Drosophila nervous system." Trends Neurosci **27**(3): 143-147.

Khuong, T M, R L Habets, J R Slabbaert and P Verstreken (2010). "WASP is activated by phosphatidylinositol-4,5-bisphosphate to restrict synapse growth in a pathway parallel to bone morphogenetic protein signaling." Proc Natl Acad Sci U S A **107**(40): 17379-17384.

Kimura, K, Y Fukata, Y Matsuoka, V Bennett, Y Matsuura, K Okawa*, et al.* (1998). "Regulation of the association of adducin with actin filaments by Rho-associated kinase (Rho-kinase) and myosin phosphatase." J Biol Chem **273**(10): 5542-5548.

Kittel, R J, C Wichmann, T M Rasse, W Fouquet, M Schmidt, A Schmid*, et al.* (2006). "Bruchpilot promotes active zone assembly, Ca2+ channel clustering, and vesicle release." Science **312**(5776): 1051-1054.

Knight, D, K Iliadi, M P Charlton, H L Atwood and G L Boulianne (2007). "Presynaptic plasticity and associative learning are impaired in a Drosophila presenilin null mutant." Dev Neurobiol **67**(12): 1598-1613.

Koh, Y H, E Popova, U Thomas, L C Griffith and V Budnik (1999). "Regulation of DLG localization at synapses by CaMKII-dependent phosphorylation." Cell **98**(3): 353-363.

Kohsaka, H, E Takasu and A Nose (2007). "In vivo induction of postsynaptic molecular assembly by the cell adhesion molecule Fasciclin2." J Cell Biol **179**(6): 1289-1300.

Kolodkin, A L, D J Matthes and C S Goodman (1993). "The semaphorin genes encode a family of transmembrane and secreted growth cone guidance molecules." Cell **75**(7): 1389-1399.

Kordeli, E (2000). "The spectrin-based skeleton at the postsynaptic membrane of the neuromuscular junction." Microsc Res Tech **49**(1): 101-107.

Kuhlman, P A, C A Hughes, V Bennett and V M Fowler (1996). "A new function for adducin. Calcium/calmodulin-regulated capping of the barbed ends of actin filaments." J Biol Chem **271**(14): 7986-7991.

Lahey, T, M Gorczyca, X X Jia and V Budnik (1994). "The Drosophila tumor suppressor gene dlg is required for normal synaptic bouton structure." Neuron **13**(4): 823-835.

Landgraf, M, M Baylies and M Bate (1999). "Muscle founder cells regulate defasciculation and targeting of motor axons in the Drosophila embryo." Curr Biol **9**(11): 589-592.

Landgraf, M and S Thor (2006). "Development of Drosophila motoneurons: specification and morphology." Semin Cell Dev Biol **17**(1): 3-11.

Li, X, Y Matsuoka and V Bennett (1998). "Adducin preferentially recruits spectrin to the fast growing ends of actin filaments in a complex requiring the MARCKS-related domain and a newly defined oligomerization domain." J Biol Chem **273**(30): 19329-19338.

Lin, H and A C Spradling (1995). "Fusome asymmetry and oocyte determination in Drosophila." Dev Genet **16**(1): 6-12.

Lin, H, L Yue and A C Spradling (1994). "The Drosophila fusome, a germline-specific organelle, contains membrane skeletal proteins and functions in cyst formation." Development **120**(4): 947-956.

Liu, Q A and M O Hengartner (1998). "Candidate adaptor protein CED-6 promotes the engulfment of apoptotic cells in C. elegans." Cell **93**(6): 961-972.

Liu, S C, L H Derick and J Palek (1987). "Visualization of the hexagonal lattice in the erythrocyte membrane skeleton." J Cell Biol **104**(3): 527-536.

Loyet, K M, J A Kowalchyk, A Chaudhary, J Chen, G D Prestwich and T F Martin (1998). "Specific binding of phosphatidylinositol 4,5-bisphosphate to calcium-dependent activator protein for secretion (CAPS), a potential phosphoinositide effector protein for regulated exocytosis." J Biol Chem **273**(14): 8337-8343.

Luo, L and D D O'Leary (2005). "Axon retraction and degeneration in development and disease." Annu Rev Neurosci **28**: 127-156.

Marques, G (2005). "Morphogens and synaptogenesis in Drosophila." J Neurobiol **64**(4): 417-434.

Marrus, S B and A DiAntonio (2004). "Preferential localization of glutamate receptors opposite sites of high presynaptic release." Curr Biol **14**(11): 924-931.

Matsuoka, Y, C A Hughes and V Bennett (1996). "Adducin regulation. Definition of the calmodulin-binding domain and sites of phosphorylation by protein kinases A and C." J Biol Chem **271**(41): 25157-25166.

Matsuoka, Y, X Li and V Bennett (2000). "Adducin: structure, function and regulation." Cell Mol Life Sci **57**(6): 884-895.

McLaughlin, S and A Aderem (1995). "The myristoyl-electrostatic switch: a modulator of reversible protein-membrane interactions." Trends Biochem Sci **20**(7): 272-276.

Monastirioti, M, M Gorczyca, J Rapus, M Eckert, K White and V Budnik (1995). "Octopamine immunoreactivity in the fruit fly Drosophila melanogaster." J Comp Neurol **356**(2): 275-287.

Naydenov, N G and A I Ivanov (2010). "Adducins regulate remodeling of apical junctions in human epithelial cells." Molecular Biology of the Cell **21**(20): 3506-3517.

Nguyen, H T, R Bodmer, S M Abmayr, J C McDermott and N A Spoerel (1994). "D-mef2: a Drosophila mesoderm-specific MADS box-containing gene with a biphasic expression profile during embryogenesis." Proc Natl Acad Sci U S A **91**(16): 7520-7524.

Ohler, S, S Hakeda-Suzuki and T Suzuki (2011). "Hts, the Drosophila homologue of Adducin, physically interacts with the transmembrane receptor Golden goal to guide photoreceptor axons." Dev Dyn **240**(1): 135-148.

Ouimet, C C, J K Wang, S I Walaas, K A Albert and P Greengard (1990). "Localization of the MARCKS (87 kDa) protein, a major specific substrate for protein kinase C, in rat brain." J Neurosci **10**(5): 1683-1698.

Pariser, H, G Herradon, L Ezquerra, P Perez-Pinera and T F Deuel (2005). "Pleiotrophin regulates serine phosphorylation and the cellular distribution of beta-adducin through activation of protein kinase C." Proc Natl Acad Sci U S A **102**(35): 12407-12412.

Petersen, S A, R D Fetter, J N Noordermeer, C S Goodman and A DiAntonio (1997). "Genetic analysis of glutamate receptors in Drosophila reveals a retrograde signal regulating presynaptic transmitter release." Neuron **19**(6): 1237-1248.

Petrella, L N, T Smith-Leiker and L Cooley (2007). "The Ovhts polyprotein is cleaved to produce fusome and ring canal proteins required for Drosophila oogenesis." Development **134**(4): 703-712.

Pielage, J, V Bulat, J B Zuchero, R D Fetter and G W Davis (2011). "Hts/Adducin controls synaptic elaboration and elimination." Neuron **69**(6): 1114-1131.

Pielage, J, R D Fetter and G W Davis (2005). "Presynaptic spectrin is essential for synapse stabilization." Curr Biol **15**(10): 918-928.

Pielage, J, R D Fetter and G W Davis (2006). "A postsynaptic spectrin scaffold defines active zone size, spacing, and efficacy at the Drosophila neuromuscular junction." J Cell Biol **175**(3): 491-503.

Pike, L J and J M Miller (1998). "Cholesterol depletion delocalizes phosphatidylinositol bisphosphate and inhibits hormone-stimulated phosphatidylinositol turnover." J Biol Chem **273**(35): 22298-22304.

Porro, F, M Rosato-Siri, E Leone, L Costessi, A Iaconcig, E Tongiorgi*, et al.* (2010). "beta-adducin (Add2) KO mice show synaptic plasticity, motor coordination and behavioral deficits accompanied by changes in the expression and phosphorylation levels of the alpha- and gamma-adducin subunits." Genes Brain Behav **9**(1): 84-96.

Porumb, T, A Crivici, P J Blackshear and M Ikura (1997). "Calcium binding and conformational properties of calmodulin complexed with peptides derived from myristoylated alanine-rich C kinase substrate (MARCKS) and MARCKS-related protein (MRP)." Eur Biophys J **25**(4): 239-247.

Prokop, A, M Landgraf, E Rushton, K Broadie and M Bate (1996). "Presynaptic development at the Drosophila neuromuscular junction: assembly and localization of presynaptic active zones." Neuron **17**(4): 617-626.

Rabenstein, R L, N A Addy, B J Caldarone, Y Asaka, L M Gruenbaum, L L Peters*, et al.* (2005). "Impaired synaptic plasticity and learning in mice lacking beta-adducin, an actin-regulating protein." J Neurosci **25**(8): 2138-2145.

Ramachandran, P, R Barria, J Ashley and V Budnik (2009). "A critical step for postsynaptic F-actin organization: regulation of Baz/Par-3 localization by aPKC and PTEN." Dev Neurobiol **69**(9): 583-602.

Raucher, D, T Stauffer, W Chen, K Shen, S Guo, J D York*, et al.* (2000). "Phosphatidylinositol 4,5-bisphosphate functions as a second messenger that regulates cytoskeleton-plasma membrane adhesion." Cell **100**(2): 221-228.

Rinholm, J E, G Slettalokken, P Marcaggi, O Skare, J Storm-Mathisen and L H Bergersen (2007). "Subcellular localization of the glutamate transporters GLAST and GLT at the neuromuscular junction in rodents." Neuroscience **145**(2): 579-591.

Ritzenthaler, S, E Suzuki and A Chiba (2000). "Postsynaptic filopodia in muscle cells interact with innervating motoneuron axons." Nat Neurosci **3**(10): 1012-1017.

Robinson, D N, K Cant and L Cooley (1994). "Morphogenesis of Drosophila ovarian ring canals." Development **120**(7): 2015-2025.

Rose, D, X Zhu, H Kose, B Hoang, J Cho and A Chiba (1997). "Toll, a muscle cell surface molecule, locally inhibits synaptic initiation of the RP3 motoneuron growth cone in Drosophila." Development **124**(8): 1561-1571.

Rosenthal, A, L Rhee, R Yadegari, R Paro, A Ullrich and D V Goeddel (1987). "Structure and nucleotide sequence of a Drosophila melanogaster protein kinase C gene." EMBO J **6**(2): 433-441.

Rossi, E A, Z Li, H Feng and C S Rubin (1999). "Characterization of the targeting, binding, and phosphorylation site domains of an A kinase anchor protein and a myristoylated alanine-rich C kinase substrate-like analog that are encoded by a single gene." J Biol Chem **274**(38): 27201-27210.

Ruiz-Canada, C and V Budnik (2006). "Introduction on the use of the Drosophila embryonic/larval neuromuscular junction as a model system to study synapse development and function, and a brief summary of pathfinding and target recognition." Int Rev Neurobiol **75**: 1-31.

Schmid, A, A Chiba and C Q Doe (1999). "Clonal analysis of Drosophila embryonic neuroblasts: neural cell types, axon projections and muscle targets." Development **126**(21): 4653-4689.

Schuster, C M (2006). "Glutamatergic synapses of Drosophila neuromuscular junctions: a high-resolution model for the analysis of experience-dependent potentiation." Cell Tissue Res **326**(2): 287-299.

Schuster, C M, G W Davis, R D Fetter and C S Goodman (1996a). "Genetic dissection of structural and functional components of synaptic plasticity. I. Fasciclin II controls synaptic stabilization and growth." Neuron **17**(4): 641-654.

Schuster, C M, G W Davis, R D Fetter and C S Goodman (1996b). "Genetic dissection of structural and functional components of synaptic plasticity. II. Fasciclin II controls presynaptic structural plasticity." Neuron **17**(4): 655-667.

Shan, X, J H Hu, F S Cayabyab and C Krieger (2005). "Increased phospho-adducin immunoreactivity in a murine model of amyotrophic lateral sclerosis." Neuroscience **134**(3): 833-846.

Shao, H, J Chou, C J Baty, N A Burke, S C Watkins, D B Stolz*, et al.* (2006). "Spatial localization of m-calpain to the plasma membrane by phosphoinositide biphosphate binding during epidermal growth factor receptor-mediated activation." Mol Cell Biol **26**(14): 5481-5496.

Shidara, Y and P J Hollenbeck (2010). "Defects in mitochondrial axonal transport and membrane potential without increased reactive oxygen species production in a Drosophila model of Friedreich ataxia." J Neurosci **30**(34): 11369-11378.

Shieh, B H, L Parker and D Popescu (2002). "Protein kinase C (PKC) isoforms in Drosophila." J Biochem **132**(4): 523-527.

Sigrist, S J, D F Reiff, P R Thiel, J R Steinert and C M Schuster (2003). "Experience-dependent strengthening of Drosophila neuromuscular junctions." J Neurosci **23**(16): 6546-6556.

Sigrist, S J, P R Thiel, D F Reiff, P E Lachance, P Lasko and C M Schuster (2000). "Postsynaptic translation affects the efficacy and morphology of neuromuscular junctions." Nature **405**(6790): 1062-1065.

Siman, R and J C Noszek (1988). "Excitatory amino acids activate calpain I and induce structural protein breakdown in vivo." Neuron **1**(4): 279-287.

Skwarek, L C, M K Garroni, C Commisso and G L Boulianne (2007). "Neuralized contains a phosphoinositide-binding motif required downstream of ubiquitination for delta endocytosis and notch signaling." Dev Cell **13**(6): 783-795.

Snow, P M, N H Patel, A L Harrelson and C S Goodman (1987). "Neural-specific carbohydrate moiety shared by many surface glycoproteins in Drosophila and grasshopper embryos." J Neurosci **7**(12): 4137-4144.

Sprague, C R, T S Fraley, H S Jang, S Lal and J A Greenwood (2008). "Phosphoinositide binding to the substrate regulates susceptibility to proteolysis by calpain." J Biol Chem **283**(14): 9217-9223.

Steinert, J R, H Kuromi, A Hellwig, M Knirr, A W Wyatt, Y Kidokoro*, et al.* (2006). "Experience-dependent formation and recruitment of large vesicles from reserve pool." Neuron **50**(5): 723-733.

Stewart, B A, C M Schuster, C S Goodman and H L Atwood (1996). "Homeostasis of synaptic transmission in Drosophila with genetically altered nerve terminal morphology." J Neurosci **16**(12): 3877-3886.

Swierczynski, S L and P J Blackshear (1996). "Myristoylation-dependent and electrostatic interactions exert independent effects on the membrane association of the myristoylated alanine-rich protein kinase C substrate protein in intact cells." J Biol Chem **271**(38): 23424-23430.

Tejedor, F J, A Bokhari, O Rogero, M Gorczyca, J Zhang, E Kim*, et al.* (1997). "Essential role for dlg in synaptic clustering of Shaker K+ channels in vivo." J Neurosci **17**(1): 152-159.

Telonis-Scott, M, A Kopp, M L Wayne, S V Nuzhdin and L M McIntyre (2009). "Sex-specific splicing in Drosophila: widespread occurrence, tissue specificity and evolutionary conservation." Genetics **181**(2): 421-434.

Thomas, U, E Kim, S Kuhlendahl, Y H Koh, E D Gundelfinger, M Sheng*, et al.* (1997). "Synaptic clustering of the cell adhesion molecule fasciclin II by discs-large and its role in the regulation of presynaptic structure." Neuron **19**(4): 787-799.

Tixier, V, L Bataille and K Jagla (2010). "Diversification of muscle types: recent insights from Drosophila." Exp Cell Res **316**(18): 3019-3027.

Tomasi, T, S Hakeda-Suzuki, S Ohler, A Schleiffer and T Suzuki (2008). "The transmembrane protein Golden goal regulates R8 photoreceptor axon-axon and axon-target interactions." Neuron **57**(5): 691-704.

Ulrich, A, A A Schmitz, T Braun, T Yuan, H J Vogel and G Vergeres (2000). "Mapping the interface between calmodulin and MARCKS-related protein by fluorescence spectroscopy." Proc Natl Acad Sci U S A **97**(10): 5191-5196.

Wagh, D A, T M Rasse, E Asan, A Hofbauer, I Schwenkert, H Durrbeck*, et al.* (2006). "Bruchpilot, a protein with homology to ELKS/CAST, is required for structural integrity and function of synaptic active zones in Drosophila." Neuron **49**(6): 833-844.

Wang, J, A Gambhir, G Hangyas-Mihalyne, D Murray, U Golebiewska and S McLaughlin (2002). "Lateral sequestration of phosphatidylinositol 4,5-bisphosphate by the basic effector domain of myristoylated alanine-rich C kinase substrate is due to nonspecific electrostatic interactions." J Biol Chem **277**(37): 34401-34412.

Wang, S, J Yang, T Kuca, J Sanny, J Lee, A Tsai*, et al.* (submitted). "Drosophila adducin regulates synaptic growth and the phosphorylation and localization of Dlg."

Whittaker, K L, D Ding, W W Fisher and H D Lipshitz (1999). "Different 3' untranslated regions target alternatively processed hu-li tai shao (hts) transcripts to distinct cytoplasmic locations during Drosophila oogenesis." J Cell Sci **112 (Pt 19)**: 3385-3398.

Winberg, M L, J N Noordermeer, L Tamagnone, P M Comoglio, M K Spriggs, M Tessier-Lavigne*, et al.* (1998). "Plexin A is a neuronal semaphorin receptor that controls axon guidance." Cell **95**(7): 903-916.

Wong, R, I Hadjiyanni, H C Wei, G Polevoy, R McBride, K P Sem*, et al.* (2005). "PIP2 hydrolysis and calcium release are required for cytokinesis in Drosophila spermatocytes." Curr Biol **15**(15): 1401-1406.

Woods, D F and P J Bryant (1991). "The discs-large tumor suppressor gene of Drosophila encodes a guanylate kinase homolog localized at septate junctions." Cell **66**(3): 451-464.

Yamaguchi, H, M Shiraishi, K Fukami, A Tanabe, Y Ikeda-Matsuo, Y Naito*, et al.* (2009). "MARCKS regulates lamellipodia formation induced by IGF-I via association with PIP2 and beta-actin at membrane microdomains." J Cell Physiol **220**(3): 748-755.

Yang, J (2008). "Regulation of neuromuscular synapse development by Hts in Drosophila." M.Sc. Thesis.

Yue, L and A C Spradling (1992). "hu-li tai shao, a gene required for ring canal formation during Drosophila oogenesis, encodes a homolog of adducin." Genes Dev **6**(12B): 2443-2454.

Zaccai, M and H D Lipshitz (1996a). "Differential distributions of two adducin-like protein isoforms in the Drosophila ovary and early embryo." Zygote **4**(2): 159-166.

Zaccai, M and H D Lipshitz (1996b). "Role of Adducin-like (hu-li tai shao) mRNA and protein localization in regulating cytoskeletal structure and function during Drosophila Oogenesis and early embryogenesis." Dev Genet **19**(3): 249-257.

Zadran, S, X Bi and M Baudry (2010). "Regulation of calpain-2 in neurons: implications for synaptic plasticity." Mol Neurobiol **42**(2): 143-150.

Zhang, Y, H Guo, H Kwan, J W Wang, J Kosek and B Lu (2007). "PAR-1 kinase phosphorylates Dlg and regulates its postsynaptic targeting at the Drosophila neuromuscular junction." Neuron **53**(2): 201-215.

Zhou, Z, E Hartwieg and H R Horvitz (2001). "CED-1 is a transmembrane receptor that mediates cell corpse engulfment in C. elegans." Cell **104**(1): 43-56.

Zito, K, R D Fetter, C S Goodman and E Y Isacoff (1997). "Synaptic clustering of Fascilin II and Shaker: essential targeting sequences and role of Dlg." Neuron **19**(5): 1007-1016.

Zito, K, D Parnas, R D Fetter, E Y Isacoff and C S Goodman (1999). "Watching a synapse grow: noninvasive confocal imaging of synaptic growth in Drosophila." Neuron **22**(4): 719-729.